University of Groningen

# Iron(III) spin crossover compounds

van Koningsbruggen, PJ; Maeda, Y; Oshio, H

*Published in:*
SPIN CROSSOVER IN TRANSITION METAL COMPOUNDS I

*DOI:*
10.1007/b95409

**IMPORTANT NOTE: You are advised to consult the publisher's version (publisher's PDF) if you wish to cite from it. Please check the document version below.**

*Document Version*
Publisher's PDF, also known as Version of record

*Publication date:*
2004

Link to publication in University of Groningen/UMCG research database

*Citation for published version (APA):*
van Koningsbruggen, PJ., Maeda, Y., & Oshio, H. (2004). Iron(III) spin crossover compounds. In *SPIN CROSSOVER IN TRANSITION METAL COMPOUNDS I* (pp. 259-324). (TOPICS IN CURRENT CHEMISTRY; Vol. 233). University of Groningen, Stratingh Institute for Chemistry. https://doi.org/10.1007/b95409

**Copyright**
Other than for strictly personal use, it is not permitted to download or to forward/distribute the text or part of it without the consent of the author(s) and/or copyright holder(s), unless the work is under an open content license (like Creative Commons).

The publication may also be distributed here under the terms of Article 25fa of the Dutch Copyright Act, indicated by the "Taverne" license. More information can be found on the University of Groningen website: https://www.rug.nl/library/open-access/self-archiving-pure/taverne-amendment.

**Take-down policy**
If you believe that this document breaches copyright please contact us providing details, and we will remove access to the work immediately and investigate your claim.

*Downloaded from the University of Groningen/UMCG research database (Pure): http://www.rug.nl/research/portal. For technical reasons the number of authors shown on this cover page is limited to 10 maximum.*

Download date: 23-08-2022

Top Curr Chem (2004) 233:259–324
DOI 10.1007/b95409
© Springer-Verlag Berlin Heidelberg 2004

# Iron(III) Spin Crossover Compounds

Petra J. van Koningsbruggen[1] (✉) · Yonezo Maeda[2] · Hiroki Oshio[3]

[1] Stratingh Institute for Chemistry and Chemical Engineering, University of Groningen, Nijenborgh 4, 9747 AG, Groningen, The Netherlands
*P.van.Koningsbruggen@chem.rug.nl*
[2] Department of Chemistry, Kyushu University, 6-10-1 Hakozaki, Higashi-ku, Fukuoka 812-8581, Japan
[3] Department of Chemistry, University of Tsukuba, Tennodai 1-1-1, Tsukuba 305-8571, Japan

**1 Introduction** . . . . . 261
1.1 The Discovery of the Spin Crossover Phenomenon for Iron(III) Compounds 261
1.2 Scope of the Chapter . . . . . 262

**2 Iron(III) Spin Crossover Systems with Chalcogen Donor Atoms** . . . . . 262
2.1 Tris(N,N-Disubstituted-Dithiocarbamato)Iron(III) Compounds . . . . . 262
2.1.1 General Considerations . . . . . 262
2.1.2 Structural Aspects . . . . . 263
2.1.3 Characterisation by Spectroscopic Techniques . . . . . 268
2.2 Tris(N,N-Disubstituted-XY-Carbamato)Iron(III) Compounds (XY=SO, SSe, SeSe) . . . . . 270
2.3 Tris(Substituted-X-Xanthato)Iron(III) Compounds (X=O, S) . . . . . 273
2.4 Tris(Monothio-$\beta$-Diketonato)Iron(III) Compounds . . . . . 274
2.5 Bis(X-Semicarbazone)Iron(III) Compounds (X=S, Se) . . . . . 276
2.6 Other Complexes with Sulfur Donor Atoms . . . . . 282

**3 Iron(III) Spin Crossover Systems of Multidentate Schiff Base-Type Ligands** 285
3.1 Complexes of Tridentate $N_2O$-Donating Ligands . . . . . 286
3.2 Complexes of Tetradentate Ligands . . . . . 295
3.2.1 General Considerations . . . . . 295
3.2.2 Complexes of Tetradentate $N_4$-Donating Ligands . . . . . 296
3.2.3 Five-Coordinate Complexes of Tetradentate $N_2O_2$-Donating Schiff Base Ligands . . . . . 297
3.2.4 Six-Coordinate Complexes of Tetradentate $N_2O_2$-Donating Schiff Base Ligands . . . . . 299
3.3 Complexes of Pentadentate $N_3O_2$-Donating Ligands . . . . . 305
3.4 Complexes of Hexadentate $N_4O_2$-Donating Ligands . . . . . 307
3.4.1 General Considerations . . . . . 307
3.4.2 Hexadentate $N_4O_2$-Donating Ligands Derived from Salicylaldehyde Derivatives and Triethylenetetramine . 308
3.4.3 Hexadentate $N_4O_2$-Donating Ligands Derived from $\beta$-Diketones and Triethylenetetramine . . . . . 312
3.5 Iron(III) Spin Crossover Induced by Irradiation . . . . . 313
3.6 Developments in Materials Science . . . . . 316

**4 Conclusions** . . . . . 317

**References** . . . . . 318

**Abstract** In this chapter, selected results obtained so far on Fe(III) spin crossover compounds are summarized and discussed. Fe(III) spin transition materials of ligands containing chalcogen donor atoms are considered with emphasis on those of *N*,*N*-disubstituted-dithiocarbamates, *N*,*N*-disubstituted-XY-carbamates (XY=SO, SSe, SeSe), X-xanthates (X=O, S), monothio-$\beta$-diketonates and X-semicarbazones (X=S, Se). In addition, attention is directed to Fe(III) spin crossover systems of multidentate Schiff base-type ligands. Examples of spin inter-conversion in Fe(III) compounds induced by light irradiation are given.

**Keywords** Spin crossover · Fe(III) · Dithiocarbamate · Thiosemicarbazone · Schiff base

**List of Abbreviations**

| | |
|---|---|
| $H_2$thsa | Salicylaldehyde thiosemicarbazone |
| $H_2$Phthsa | Salicylaldehyde phenylthiosemicarbazone |
| $H_2$sesa | Salicylaldehyde selenosemicarbazone |
| $H_2$thpu | Pyruvic acid thiosemicarbazone |
| $H_2$sespu | Pyruvic acid selenosemicarbazone |
| $H_2$thpy | Pyridoxal 4-*R*-thiosemicarbazone |
| H-3-OEt-salAPA | Schiff base derived from 3-ethoxysalicylaldehyde and *N*-aminopropylaziridine |
| HsalAEA | Schiff base derived from salicylaldehyde and *N*-(2-aminoethyl)aziridine |
| Hsapa | *N*-Salicylidene-2-pyridylmethylamine |
| Hvapa | *N*-(3-Methoxysalicylidene)-2-pyridylmethylamine |
| H-3-$CH_3$OSPH | Schiff base derived from 3-methoxysalicylaldehyde and 2-pyridylhydrazine |
| H-X-salmeen | Schiff base derived from X-salicylaldehyde and *N*-methylethylenediamine |
| H-X-saleen | Schiff base derived from X-salicylaldehyde and *N*-ethylethylenediamine |
| H-X-salbzen | Schiff base derived from *N*-benzylethylenediamine and X-substituted salicylaldehyde |
| Hacea | Schiff base derived from 2,4-pentanedione and 1,2-diaminoethane |
| Hacpa | *N*-(1-Acetyl-2-propylidene)(2-pyridylmethyl)amine |
| Hbzpa | (1-Benzoylpropen-2-yl)(2-pyridylmethyl)amine |
| Hqsal | *N*-(8-Quinolyl)-salicylaldimine |
| Hpap | 2-Hydroxyphenyl-(2-pyridyl)-methaneimine |
| cyclam | 1,4,8,11-Tetraazacyclotetradecane |
| tcyclam | 1,4,8,11-Tetramethyl-1,4,8,11-tetraazacyclotetradecane |
| $H_2$amben | Schiff base derived from 2-aminobenzaldehyde and ethylenediamine |
| $H_2$salen | *N*,*N*′-Ethylenebis(salicylideneamine) |
| $H_2$salphen | *N*,*N*′-*o*-Phenylenebis(salicylideneamine) |
| Him | Imidazole |
| $H_2$-3-$OCH_3$-salpen | *N*,*N*′-1,2-Propylenebis(3-methoxysalicylideneamine) |

| | |
|---|---|
| $H_2$-3-$OC_2H_5$-sal-$CH_3$-phen | N,N′-3,4-Toluenebis(3-ethoxysalicylideneamine) |
| $H_2$acen | *N,N′*-Ethylenebis(acetylacetonylideneamine) |
| $H_2$bzacen | *N,N′*-Ethylenebis(benzoylacetonylideneamine) |
| $H_2$salacen | Ethylene(*N*-acetylacetonylideneimine) (*N′*-$\alpha$-methylsalicylideneimine) |
| $H_2$salten | *N,N′*-Bis[(2-hydroxy-phenyl)methylene]-4-azaheptane-1,7-diamine |
| $H_2$bpN | *N,N′*-Bis[(2-hydroxy-phenyl)phenylmethylene]-4-azaheptane-1,7-diamine |
| $H_2$mbpN | *N,N′*-Bis[(2-hydroxy-5-methyl-phenyl)phenylmethylene]-4-azaheptane-1,7-diamine |
| $H_2$sal$_2$trien | Schiff base obtained from the 1:2 condensation of triethylenetetramine with salicylaldehyde |
| $H_2$acac$_2$trien | Schiff base obtained from the 1:2 condensation of triethylenetetramine with acetylacetone |
| $H_2$bzac$_2$trien | Schiff base obtained from the 1:2 condensation of triethylenetetramine with benzoylacetone |
| $H_2$tfac$_2$trien | Schiff base obtained from the 1:2 condensation of triethylenetetramine with trifluoroacetylacetone |
| Mepepy | 1-(Pyridin-4-yl)-2-(*N*-methylpyrrol-2-yl)-ethene |

# 1 Introduction

## 1.1 The Discovery of the Spin Crossover Phenomenon for Iron(III) Compounds

Iron(III) occupies a unique position in the development of the spin crossover area since it was for derivatives of this ion that the phenomenon was first discovered. In 1931 Cambi and Szegö reported the unusual temperature dependence of the magnetic susceptibility of various tris(*N,N*-dialkyl-dithiocarbamato)iron(III) compounds [1, 2]. Their initial interpretation of this was in terms of two different magnetic isomers. At higher temperatures, an isomer having five electrons arranged in the d-orbitals according to Hund's rule (S=5/2) was proposed to account for the relatively high magnetic moment. The lower magnetic response observed at lower temperatures was attributed to a second isomer in which the d-orbitals are occupied by nine electrons, five of these originating from the $3d^5$ iron(III) ion supplemented with four electrons from the ligands, resulting in a total spin of S=1/2 [2]. This explanation was based on two different dipole moments present in the isomers, and a thermal equilibrium between these two species with different dipole moments was proposed. Although their assumption of dipole mo-

ments being involved in this phenomenon was later shown to be erroneous, their interesting results certainly attracted the attention of other researchers. This led to the correct description of the Fe(III) spin crossover phenomenon in terms of the two arrangements of the five 3d electrons possible for octahedral complexes depending on the strength of the ligand field. The situation is very similar to that described in Chap. 2 by Hauser for Fe(II) ($3d^6$), the important difference being in the actual spin multiplicity of the low spin and high spin states, for iron(III) these being a doublet $^2T_2$ and a sextet $^6A_1$, respectively [3].

### 1.2
### Scope of the Chapter

In the following sections an overview is given of the progress made in the Fe(III) spin crossover research field. Section 2 deals with Fe(III) spin transition materials containing ligands with chalcogen donor atoms, such as the dithiocarbamates, whereas Sect. 3 focuses on the use of multidentate Schiff base-type ligands to generate Fe(III) spin crossover. Concluding remarks may be found in Sect. 4.

## 2
## Iron(III) Spin Crossover Systems with Chalcogen Donor Atoms

### 2.1
### Tris(N,N-Disubstituted-Dithiocarbamato)Iron(III) Compounds

#### 2.1.1
#### General Considerations

Since the appearance of the first reports by Cambi and Szegö [1, 2], the tris(*N,N*-dialkyl-dithiocarbamato)iron(III) compounds have been extensively studied and the later work has included detailed structural characterisation by X-ray diffraction methods. In addition, new dithiocarbamato-based Fe(III) spin crossover materials have been prepared, those having the alkyl substituents as part of a ring system being of particular note. A schematic representation of the structure of tris(*N,N*-disubstituted-dithiocarbamato)iron(III) is given in Fig. 1, and relevant crystallographic and magnetic data are compiled in Table 1.

These compounds are first characterised by their magnetic behaviour. The spin-only high spin value of Fe(III) is 5.92 B.M., while a normal range for its low spin values in cubic symmetry is 2.0–2.3 B.M. [24–26]. Among the compounds listed in Table 1, these extreme cases are met by the low spin tris(1-pyrrole-dithiocarbamato)iron(III) hemikis(dichloromethane)

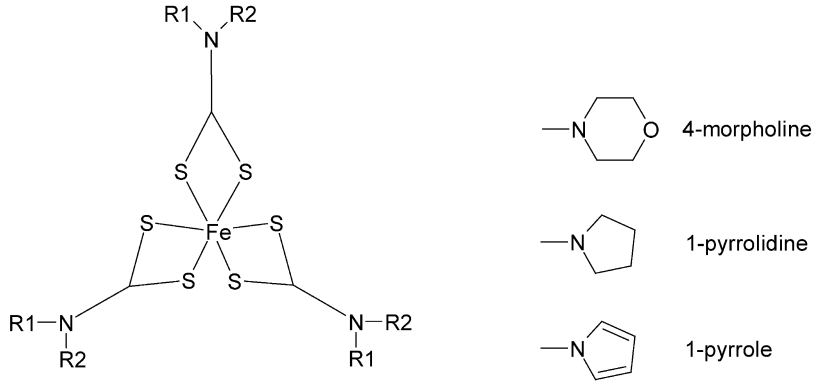


**Fig. 1** Schematic drawing showing the structure of tris(*N,N*-disubstituted-dithiocarbamato)iron(III). Substituents R1 and R2 represent various types of alkyl groups including those being part of the ring systems morpholine, pyrrolidine or pyrrole (Table 1)

($\mu_{eff}$=2.19 B.M.) [23] and the high spin tris(1-pyrrolidine-dithiocarbamato)iron(III) ($\mu_{eff}$=5.9 B.M.) [16].

If the energy difference between the two possible ground terms $^6A_1$ and $^2T_2$ of Fe(III) (assuming $O_h$ symmetry of the $FeS_6$ core) is of the order of $k_BT$, a change in temperature results in a change in the relative occupancy of the sextet and doublet states, and thus a change in the effective magnetic moment. Generally, for this class of materials the change in the magnetic moment as a function of temperature proceeds very smoothly and the transitions are classified as *gradual* (Chap. 1). Therefore, the magnetic moments observed at the temperatures at which the crystal structures have been determined (Table 1) give an indication of the extent to which spin crossover has proceeded in the material.

### 2.1.2 Structural Aspects

The structures of these systems consist of an $FeS_6$ core, which is constrained by the four-membered chelate rings to approximate $D_3$ symmetry, being intermediate between octahedral and trigonal prismatic stereochemistries. Interestingly, this almost perfect threefold-symmetry only becomes evident from the structure (300 K) of the mainly high spin ($\mu_{eff}$=4.72 B.M.) tris(*N*-methyl-*N*-*n*-butyl-dithiocarbamato)iron(III) [13]. This compound crystallises in the space group $P3_1/c$ revealing two crystallographically independent Fe(III) entities, each with $C_3$ symmetry.

The difference between the Fe–S bond lengths in the high spin and low spin states is about 0.15 Å, which is also in line with the Fe–S bond lengths for the low spin tris(1-pyrrole-dithiocarbamato)iron(III) hemikis(dichloro-

**Table 1** Crystallographic and magnetic data of tris(*N,N*-disubstituted-dithiocarbamato)iron(III) compounds

| | | | Crystallographic data | | | | Magnetic data | |
|---|---|---|---|---|---|---|---|---|
| Ligand | Lattice solvent | T (K) | Space group | Fe-S[a] (Å) | S-Fe-S[b] (°) | References | $\mu_{eff}$[c] (B.M.) | References |
| *N,N*-Dimethyl- | | 400 | Pbca | 2.415 | | [4] | 4.83 | [4] |
| | | 295 | Pbca | 2.43 | 73.6 | [5] | 4.2 | [5] |
| | | 150 | Pbca | 2.32 | 74.9 | [5] | 2.4 | [5] |
| | | 25 | Pbca | 2.302 | | [4] | 2.0 | [4] |
| *N,N*-Diethyl- | | 297 | $P2_1/c$ | 2.357 | 74.3 | [6] | 4.3 | [7] |
| | | 79 | C2/n | 2.306 | 75.9 | [6] | 2.2 | [7] |
| *N,N*-Di(2-hydroxyethyl)- | | 295 | P-1 | 2.39 | | [8] | 4.2 | [8] |
| | | 150 | P-1 | 2.33 | | [8] | 2.4 | [8] |
| *N,N*-Dipropionitrile- | | 210 | P-1 | 2.308 | | [9] | 3.19 | [9] |
| | | 295 | P-1 | 2.324 | | [9] | 3.94[d] | [9] |
| *N,N*-Di-*n*-butyl | | 298 | C2/c | 2.416 | 72.8 | [10] | 5.32 | [7, 11] |
| *N,N*-Di-*n*-butyl- | $C_6H_6$ solvate | 295 | Pncn | 2.341 | 74.64 | [12] | 3.6 | [12] |
| *N*-Methyl-*N*-*n*-butyl- | | 300 | $P3_1/c$ | A:2.406[e] | 73.2 | [13] | 4.72 | [13] |
| | | | | B:2.327[e] | 74.6 | | | |
| *N*-Methyl-*N*-phenyl | | 300 | $P2_1/a$ | 2.31 | 75.1 | [14] | 3.0 | [14] |
| *N,N*-Dibenzyl- | | 295 | $P2_1$ | 2.34 | | [15] | 3.45 | [15] |
| | | 150 | $P2_1$ | 2.31 | | [15] | 2.47 | [15] |
| 1-Pyrrolidine[f] | | 300 | $P2_1/n$ | 2.41 | 74.4 | [14] | 5.9 | [14] |
| 1-Pyrrolidine[g] | | 295 | $P2_1/n$[a] | 2.45 | 72.6 | [16] | 5.9[h] | [16] |
| 1-Pyrrolidine | 0.5 $C_6H_6$ solvate | 298 | $P2_1/n$ | 2.434 | 73.3 | [17] | 5.6 | [17] |
| 4-Morpholine | $H_2O$ solvate | 298 | P-1 | 2.443 | 72.7 | [18] | 5.6 | [18] |
| 4-Morpholine | $CH_2Cl_2$ solvate | 298 | P-1 | 2.44 | 72.5 | [19] | 5.1 | [18, 19] |
| | $CH_2Cl_2$ solvate | 293 | P-1 | 2.427 | 72.7 | [20] | 5.60 | [20] |
| | $CH_2Cl_2$ solvate | 178 | P-1 | 2.401 | 73.4 | [20] | 5.05 | [20] |
| | $CH_2Cl_2$ solvate | 110 | P-1 | 2.371 | 74.0 | [20] | 4.45 | [20] |
| | $CH_2Cl_2$ solvate | 20 | P-1 | 2.358 | 74.2 | [20] | 3.80 | [20] |

**Table 1** (continued)

| | | | Crystallographic data | | | | Magnetic data | |
|---|---|---|---|---|---|---|---|---|
| Ligand | Lattice solvent | T (K) | Space group | Fe-S[a] (Å) | S-Fe-S[b] (°) | References | $\mu_{eff}$[c] (B.M.) | References |
| 4-Morpholine | $CHCl_3$ solvate | 298 | P-1 | 2.416 | 73.3 | [18] | 5.45[i] | [18] |
| 4-Morpholine | $2C_6H_6$ solvate | 298 | C2/c | 2.317 | 75.7 | [21] | 3.5 | [21] |
| 4-Morpholine | $C_6H_5NO_2$ solvate | 298 | $P2_1/c$ | 2.353 | 74.5 | [22] | | |
| 1-Pyrrole | 0.5 $CH_2Cl_2$ solvate | 298 | $P2_1/c$ | 2.297 | 75.6 | [23] | 2.19[j] | [23] |

[a] Averaged Fe–S bond distances for the $FeS_6$ core

[b] S–Fe–S bite angle for a chelating dithiocarbamate ligand

[c] The $\mu_{eff}$ value has been determined at the same temperature as the crystal structure determination (unless indicated otherwise)

[d] $\mu_{eff}$ value determined at 297 K

[e] The unit-cell contains two crystallographically independent entities A and B

[f] Phase prepared from ethanol/chloroform solutions

[g] Phase prepared from chloroform/toluene solutions

[h] This compournd remains in the high spin state at all temperatures

[i] $\mu_{eff}$ value determined at 280 K

[j] This compournd remains in the low spin state at all temperatures

methane) (Fe–S=2.297 Å (298 K)) [23] and the high spin tris(1-pyrrolidine-dithiocarbamato)iron(III) (Fe–S=2.45 Å (295 K)) [16]. The contraction in the Fe–S distance accompanying the HS→LS change results from the complete transfer of electrons in the antibonding $e_g$ orbitals to the (almost) non-bonding $t_{2g}$ orbitals. For Fe(III) dithiocarbamates, the spin transition extends over such large temperature intervals that it has not been possible to determine the Fe–S distances for the purely low spin and purely high spin state for the same material by X-ray diffraction methods. Thus data confined within the Fe(III) spin crossover region represent weighted averages for high spin and low spin sites. Only recently, an Fe K-edge XAFS study enabled the direct measurement of the separate Fe–S bond lengths for the high spin and low spin states and the spin state population in spin crossover systems at various temperatures [27]. These simultaneous measurements revealed identical results for tris(4-morpholine-dithiocarbamato)iron(III) and tris(*N*-ethyl-*N*-phenyl-dithiocarbamato)iron(III): in the high spin state the Fe–S distance is 2.44(2) Å, whereas it shortens by 0.14 Å to 2.30(2) Å in the low spin form. An examination of the crystallographic data supports a correlation between an increase in Fe–S distance and a restriction in S–Fe–S ligand bite angle, a common feature in four-membered chelates. Clearly, the Fe(III) spin crossover is accompanied by an important change in molecular volume, which has been confirmed by analyses of the change in the unit-cell volume within the spin crossover temperature range (125–295 K), carried out for tris(*N,N*-dimethyl-dithiocarbamato)iron(III) [5] and tris(*N,N*-dibenzyl-dithio carbamato)iron(III) [15].

Within the dithiocarbamate ligands the $S_2CN$ system is usually conjugated. This is reflected in the generally good planarities of the $S_2CNC_2$ ligand fragments [14]. In this respect, it has been proposed that in the complexes, the partially filled d-orbitals of iron(III) may interact with empty ligand $\pi$-orbitals arising from the d-orbitals of sulfur [28, 29]. This back-donation, together with the inductive strength of the substituent R attached to the nitrogen atom, and the steric constraints involved when the substituent is part of a ring system, should result in partial double-bond character of the S–C and C–N bonds to varying extents [15]. Indeed, the S–C and C–N bonds appear to have partial double-bond character at both low and high values of the effective magnetic moment in all relevant Fe(III) tris(dithiocarbamate) systems investigated [5]. This partial double-bond character of the C–N linkage would normally prevent free rotation about this bond. Although this feature may be crucial, in that it may lead to the formation of different geometric isomers for the Fe(III) entity, it has not been considered in any of the investigations. In addition, there is some degree of Fe–S $\pi$-bonding depending on the spin state of Fe(III), for which further confirmation has been obtained from a $^{13}C$ NMR study indicating that the metal-ligand $\pi$-bonding increases as $\mu_{eff}$ decreases [29].

From the continuous nature of the spin transitions it may be expected that the crossover is not associated with any type of crystallographic phase transition. In the light of this, the structural details for tris(*N,N*-diethyldithiocarbamato)iron(III) appear to be very surprising. The space group of the compound changes from the monoclinic $P2_1/c$ at room temperature, where a significant high spin fraction is present ($\mu_{eff}$=4.3 B.M.), to C2/n at 79 K, where the compound is mainly in the low spin state ($\mu_{eff}$=2.2 B.M.) [6]. Later, differential thermal analysis confirmed that a phase transition indeed takes place at 125 K [30]. It was postulated that this phase transition is not correlated with the spin crossover, but may be attributed to a minor modification of the ligand sphere configuration [30]. It is of note that, although the space group of the present crystal changes on cooling, the crystallographic monoclinic system remains essentially unaltered and the change in lattice constants is very small. The main differences between both structures are that at room temperature the Fe(III) ions are located on a pseudo-twofold axis, which becomes a true twofold axis in the low-temperature structure. Leipoldt and Coppens also proposed that the slight differences in the geometry of the ligand at the two temperatures are compatible with a mechanism by which the effect of the substituent on the crystal field is transmitted through the conjugated system of the ligand [6]. Although electronic and steric effects of substituents have frequently been found to affect the spin crossover behaviour within other classes of materials, their action is not very clear for this family of Fe(III) dithiocarbamates. Apart from the very gradual spin crossover behaviour, and the difficulty in obtaining detailed information on these systems by physical measurement methods (see below), a further complicating feature involves the occurrence of different polymorphs and/or solvates depending on the solvent used in the synthetic procedure [31]. Fe(III) dithiocarbamates are capable of interacting to varying degrees with a wide range of solvents. As a result, solvent molecules may either be incorporated in the crystal lattice by simple inclusion, or they may be involved in stronger hydrogen-bonding interactions. These solvates vary in their stability on exposure to the atmosphere, some persisting for long periods unchanged while others rapidly lose solvent, often crumbling to a powder, yielding a different phase [16]. For instance, $H_2O$ [18], $CH_2Cl_2$ [18–20] or $CHCl_3$ [18] incorporated into tris(4-morpholine-dithiocarbamato)iron(III) favour the high spin state at room temperature [32]. These results have been interpreted in terms of interaction of the solvent molecules through hydrogen-bonding with ligand sulfur atoms, which must weaken the Fe–S bond slightly, and hence reduce the ligand field splitting (10 Dq) significantly ($10Dq \propto (Fe–S)^{-5}$) [22]. Benzene [21] and nitrobenzene [22] do not appear to be involved in any hydrogen-bonding interactions, and in this instance, the existing low spin↔high spin equilibria have been found to be markedly shifted towards the low spin side [32]. Although this explanation appears to be reasonable in this case, the investigation of Albertsson and Os-

karsson, who compared tris(*N,N*-di(2-hydroxyethyl)-dithiocarbamato) iron(III) [8] with tris(*N,N*-dimethyl-dithiocarbamato)iron(III) [5] indicates that the expected effects may not always be observed. Their study may be regarded as an attempt to relate the differences in capability for hydrogen-bonding formation of the two ligands to the magnetic data for these compounds. As expected, the 2-hydroxyethyl-substituted ligand sets up an extensive hydrogen-bonding network [8], whereas the dimethyl-substituted derivative does not. However, the magnetic data recorded over the temperature range 80–300 K are about the same for both compounds. It is also noted that the magnetic behaviour is very similar to that observed for tris(*N,N*-diethyl-dithiocarbamato)iron(III) [7].

The situation may be further complicated by the presence of different polymorphs: for tris(1-pyrrolidine-dithiocarbamato)iron(III) two solvent-free modifications could be characterised. The first one has been crystallised from an ethanol/chloroform solution [14], whereas the second has been isolated from a chloroform/toluene mixture [16]. Both compounds differ in their structural parameters determined at room temperature, where they are both high spin. At lower temperatures the ethanol/chloroform product displays a gradual spin transition [14], whereas the chloroform/toluene form remains high spin down to very low temperature [33].

It was evident even at an early stage in the investigations on Fe(III) dithiocarbamate systems that there exists a correlation between the average Fe–S distance and the magnetic moment of these materials [6]. In their extended study, Ståhl and Ymén [34] attempted to relate ten different mean geometric parameters for 25 accurately determined structures to the effective magnetic moment. However, only the Fe–S distances or S–Fe–S ligand bite angles—both of course highly correlated—revealed a linear dependence on $\mu_{eff}$.

### 2.1.3 Characterisation by Spectroscopic Techniques

Iron(III) dithiocarbamates have been widely studied by a variety of spectroscopic techniques. Unlike the normal situation in iron(II) and also in many other iron(III) systems, $^{57}$Fe Mössbauer spectroscopy generally fails to give clear evidence of the simultaneous existence of the two electronic states. The $^{57}$Fe Mössbauer spectra of the dithiocarbamate systems exhibit only a single quadrupole doublet with broad line widths within the temperature range of the spin crossover [35–50]. The rapid inter-conversion of spin states—faster or comparable to the lifetime of the $^{57}$Fe nucleus ($\tau$=1.4×10$^{-7}$ s)—in those materials prevents the observation of separate lines for high spin and low spin molecules. This feature allowed, on the other hand, the establishment of a linear correlation between the $^{57}$Fe Mössbauer isomer shifts and the magnetic moments of solvated Fe(III) dithiocarbamates [40].

In addition, these Fe(III) spin crossover materials appear to be EPR active. The combined findings of EPR and $^{57}$Fe Mössbauer spectroscopy has allowed the setting of limits for the relaxation times. Thus the relaxation time characteristic of a change from one state to the other is much shorter than the lifetime of the $^{57}$Fe state with nuclear spin I=3/2 ($\tau$=1.4×10$^{-7}$ s) but longer than the Larmor precession time of the electron spin ($\tau \approx 10^{-10}$ s).

The EPR spectra demonstrate two kinds of signals associated with the $^6A_1$ and $^2T_2$ states [51–56], albeit some controversy still exists concerning the reliability of some of these data. This is motivated by the difficulties encountered in, for instance, the preparation of a pure sample, the possibility of sample decomposition and in the definitive assignment of the EPR signals [51, 55]. Hall and Hendrickson reported that it was only possible to observe EPR signals for the magnetically concentrated solids at temperatures approaching 4.2 K. However, the spin crossover could be followed for the complex in a $CH_3Cl$ glass [51]. More accurate spectra could be obtained when doping 1% Fe(III) in tris(*N,N*-dimethyl-dithiocarbamato)cobalt(III), where at about 85 K a signal at g=4.71 attributed to high spin Fe(III) could be observed, while cooling to 12 K yielded additional signals at g=3.27 and 1.66, assigned to low spin Fe(III) [51].

The electronic spectra of these materials recorded in chloroform solution appear to be dominated by intense bands originating from internal ligand transitions, metal-ligand and ligand-metal charge-transfer bands, whose intensities change markedly with changes in the population of the two spin states [7].

Infrared spectroscopy has also been applied to monitor the Fe(III) spin crossover behaviour [30, 49–51, 57, 58]. For instance, for tris(*N,N*-diethyl-dithiocarbamato)iron(III) the temperature dependence (104–300 K) of the IR spectrum suggested that a band at 552 cm$^{-1}$ might be assigned to a metal-ligand stretching mode in the $^2T_2$ state [30]. The intensity of this band increases with decreasing temperature at the cost of an iron-sulfur band at 355 cm$^{-1}$ arising from the high spin state. This behaviour has been found to be in line with the temperature dependence of the magnetic susceptibility.

The effect of an applied external pressure on these Fe(III) spin crossover materials has not been extensively studied, although early experiments by Ewald et al. [7] indicated that the spin crossover may be induced when the pressure on ferric complexes in solution is increased at constant temperature. Later, the infrared spectrum of tris(*N*-ethyl-*N*-phenyl-dithiocarbamato)iron(III), a spin crossover system, was studied in the metal-ligand stretching region as a function of pressure (up to 35 kbar) and compared with non-spin crossover reference compounds [58]. It appeared that only the spin crossover system exhibits two metal-sulfur bands. The intensity of the band assigned to the low spin state increases relative to the high spin band with increasing pressure. This is in agreement with the normal desta-

bilisation of the more voluminous high spin form upon the application of external pressure.

## 2.2 Tris(N,N-Disubstituted-XY-Carbamato)Iron(III) Compounds (XY=SO, SSe, SeSe)

In the course of the quest for new Fe(III) spin crossover compounds, systems related to *N,N*-disubstituted-dithiocarbamates have been explored. This section deals with oxygen and selenium derivatives of this parent ligand system, as displayed in Fig. 2.

In 1976 Nakajima et al. reported that tris(*N,N*-dimethyl-thiocarbamato)iron(III) contains high spin Fe(III) down to 2 K [59]. This was soon confirmed by an X-ray structure determination carried out at 298 K [60]. The [Fe(*N,N*-dimethyl-thiocarbamato)$_3$] entity has the facial conformation. This isomer possesses an approximate $C_3$ axis, with the plane of the three S atoms being virtually parallel to that of the three O atoms. The mean Fe–S bond distances are 2.413(5) Å, whereas the Fe–O distances are, as expected, considerably shorter, 2.073(7) Å. Shortly afterwards, another study appeared indicating that tris(*N,N*-disubstituted-monothiocarbamato)iron(III) compounds display, in fact, spin crossover behaviour [61]. Compounds with R=methyl, ethyl, *n*-propyl, 1-piperidine exhibit a decrease in magnetic moment with decreasing temperature, whereas the 1-pyrrolidine derivative remains in the high spin state ($\mu_{eff}$=5.33 B.M. at 77 K). The room temperature magnetic moments for all spin crossover derivatives range from 5.73 to 6.04 B.M., thus approximating well the spin-only value for high spin Fe(III). The magnetic moments for compounds with R=methyl, ethyl, *n*-propyl determined at 77 K are 4.04 B.M. (corresponding to approximately 60% low spin Fe(III)), 3.61.B.M. (approximately 70% low spin) and 5.69 B.M. (approximately 10% low spin), severally [61]. These spin transitions are far from being complete at 77 K. This is in sharp contrast with the corresponding Fe(III) dithiocarbamates, which are more than 90% low spin at 77 K [51]. The contradictory findings for tris(*N,N*-dimethyl-thiocarbamato)iron(III) were later clarified by Perry et al. [62], who studied several materials obtained from different preparations. It appeared that two different modifications exist, one displaying spin crossover, whereas the other one is a purely high spin compound.

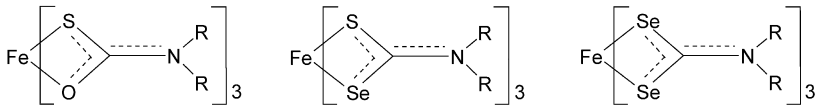


**Fig. 2** Tris(*N,N*-disubstituted-monothiocarbamato)iron(III) (*left*), tris(*N,N*-disubstituted-thioselenocarbamato)iron(III) (*centre*) and tris(*N,N*-disubstituted-diselenocarbamato) iron(III) (*right*)

The increasing quadrupole splitting observed in the $^{57}$Fe Mössbauer spectra for the methyl and ethyl Fe(III) spin crossover derivatives appears to parallel an increase in the low spin isomer population upon cooling [61]. In no case, however, could distinct doublets for the high spin and the low spin state be observed. Compared with the corresponding dithiocarbamates, the Fe(III) monothiocarbamates with an $S_3O_3$ donor atom set produce a significantly more positive isomer shift. A likely explanation for this feature involves increased d-electron shielding in the monothio complex resulting from reduced Fe-to-ligand back $\pi$-bonding.

Interestingly, tris(*N,N*-disubstituted-monothiocarbamato)iron(III) spin crossover compounds show visible thermochromism: their colour changes from red at room temperature to orange at 77 K [61].

The first studies of the magnetism of tris(*N,N*-disubstituted-diselenocarbamato)iron(III) compounds revealed magnetic moments ranging from 1.96 to 2.37 B.M. [63, 64]. Although the close relation with tris(dithiocarbamato)iron(III) spin crossover materials was already evident, these diselenium derivatives were at first wrongly classified as low spin compounds, probably as a result of the occurrence of diamagnetic non-iron-containing golden-yellow oxidation products of the ligands as by-products in the synthesis [65]. In fact, the Fe(III) materials are dark brown and their magnetic and $^{57}$Fe Mössbauer spectroscopic data resemble those of the Fe(III) dithiocarbamates, i.e. both systems exhibit spin crossover [65].

Comparison of the experimental data of the $[Fe(S_2CNR)_3]$ and $[Fe(Se_2CNR)_3]$ series (R=1-piperidine, 1-morpholine, 1-thiomorpholine, dibutyl, diethyl, $(PhCH_2)_2$, $(C_6H_{13})_2$ and methylphenyl) revealed similar magnetic properties, although the spin transition is shifted slightly to higher temperatures in the diselenocarbamates compared to the corresponding dithiocarbamates [65]. This statement appears to be correct although the magnetic data reported for diselenocarbamates may be questionable in some cases, e.g. for the 1-morpholine derivative, the same authors have published three different values for the solid complex, ranging from 1.99 to 4.88 B.M. at about room temperature [65, 66]. The explanation of the usually lower magnetic moments of the diselenocarbamates has focussed on a greater nephelauxetic effect for Se compared to S, i.e. greater $\pi$-backbonding in the diselenocarbamates [66].

In contrast to the extensive literature on Fe(III) dithiocarbamates (Sect. 2.1) and to a lesser extent Fe(III) diselenocarbamates [62, 65, 67–73], the Fe(III) thioselenocarbamates [68–73] have not been widely studied. Certainly, one reason for this is the difficult preparation of the reagent carbon sulfideselenide (CSSe) [74]. This was later circumvented by an improved synthetic method for CSSe [75], allowing Dietzsch et al. [68–73] to report a large range of Fe(III) thioselenocarbamates. Although these studies have been carried out with care, the authors did not address the possibility of formation of different geometric isomers associated with the asymmetric na-

ture of the bidentate ligand. In their comparative study Dietzsch et al. reported various tris(diorganodichalcogencarbamato)iron(III) complexes of formula $[Fe(XYCNR_2)_3]$ (XY=OS, SS, SSe or SeSe; R=organic substituent) [71]. It was concluded that the relative population of the high spin and low spin states depended on the coordinating chalcogen (O, S and/or Se), temperature, pressure, physical state (solution or solid, solvated or unsolvated), and the nature of the organic substituent. The Fe(III) compounds with $FeS_3O_3$ coordination sphere are high spin at room temperature, whereas the ones with $FeS_6$, $FeS_3Se_3$ or $FeSe_6$ environment display different degrees of spin crossover at room temperature depending on the ligand substitution. The substituents, i.e. 1-pyrrolidine, 1-piperidine, 1-morpholine, dicyclohexyl, diethyl and dibenzyl, have been selected such that these cover the range from high spin to low spin Fe(III) compounds at room temperature.

The presence of selenium has been known to cause difficulties in the recording of $^{57}$Fe Mössbauer spectra. Diselenocarbamates prepared with natural iron generally yielded very weak absorption peaks [62, 65, 67]. This feature is associated with the scattering of a large fraction of the incident $\gamma$-rays by the Se atoms. This has been overcome in part by preparing samples enriched up to 90% in $^{57}$Fe [62, 65, 67]. In addition, it also appeared possible to obtain relatively accurate spectra by using collection times of about seven days for the Fe(III) diselenocarbamates and about three days for Fe(III) thioselenocarbamates [71]. The spectra exhibit a single, quadrupole-split absorption, comparable to these observed for Fe(III) dithiocarbamates. While a linear correlation between the $^{57}$Fe Mössbauer isomer shifts and the magnetic moments of solvated Fe(III) dithiocarbamates could be established [40], no such correlation is clearly evident in the limited series of thioseleno- and diselenocarbamates studied by Dietzsch [71]. Although variations are noted for specific organic substituents, the general trend for the average isomer shifts is $^{-}OSCNR_2 < {}^{-}S_2CNR_2 \approx {}^{-}SSeCNR_2 \approx {}^{-}Se_2CNR_2$. On the other hand, the quadrupole splittings tend to increase with selenium substitution: the typical order of the quadrupole splittings for a given ligand system is $^{-}OSCNR_2 < {}^{-}S_2CNR_2 < {}^{-}SSeCNR_2 < {}^{-}Se_2CNR_2$. For the same organic substituent, the magnetic moments usually decrease in the order $^{-}OSCNR_2 > {}^{-}S_2CNR_2 > {}^{-}SSeCNR_2 > {}^{-}Se_2CNR_2$, confirming that the selenium-containing ligands generally exert a slightly stronger ligand field towards Fe(III).

There have been conflicting interpretations of the EPR spectra of these selenium-containing complexes. For example, various X-band EPR spectra of Fe(III) diselenocarbamates recorded in chloroform solutions at 12 K tended to be broad and poorly resolved, except for a series of three resonances centred around g=2 [62]. They also appeared to be very similar to the spectra recorded for Mn(III)-doped Co(III) tris(dithiocarbamate) compounds [76] or Cu(II) di(diselenocarbamate) systems [77]. In another study of EPR spectra recorded for powdered Fe(III) thioselenocarbamates and diselenocarbamates at room temperature [69] broad, poorly resolved lines at $g \approx 4$

and a relatively narrow line around g≈2 were observed. It appears that the relatively narrow signal found in most spectra at g≈2 arises from low spin molecules. On the other hand, the broader lines at g≈4 (which narrow with decreasing temperature) and at g≈2 (that in some cases acquire a fine structure with decreasing temperature) may originate from high spin molecules [69]. The same authors later used information obtained from EPR spectra to propose a new resonance structure for the bonding of spin crossover Fe(III) dichalcogencarbamates. This low spin structure would involve an unpaired electron on the nitrogen atom of the dichalcogencarbamate and the transfer of an electron from the nitrogen to the Fe(III) ion [73]. Unfortunately, X-ray structures have not been reported for these selenium derivatives.

## 2.3 Tris(Substituted-X-Xanthato)Iron(III) Compounds (X=O, S)

Considerably less research has been directed towards Fe(III) compounds of substituted X-xanthates (X=O, S), as well as of the related dithiophosphates (Fig. 3), which can be thought of as being very closely related to the dithiocarbamates.

Iron(III) dithiophosphates are high spin compounds having magnetic moments of ca. 5.80 B.M. at room temperature [78, 79]. On the other hand, the Fe(III) thioxanthates exhibit thermal and pressure induced spin crossover, though the low spin form predominates for the *O*-xanthates and thioxanthates [80]. The structure of tris(*tert*-butyl-thioxanthato)iron(III) has been determined at room temperature and consists of an approximately octahedral $FeS_6$ entity with an average Fe–S distance of 2.297(7) Å and S–Fe–S bond angles of 75.2(2)° [81]. It was also concluded from the structural data that there is a significant amount (10–30%) of double bond character to the C–X bond for coordinated $^{-}S_2CX$ (X=OR, SR) ligands, although appreciably less than for analogous dithiocarbamate ($X=NR_2$) compounds (40–50%) [81]. This was also confirmed for the predominantly low spin tris(*O*-ethylxanthato)iron(III), where the relatively short $S_2C$–O bond length (1.328(10) Å) is indicative of considerable double bond character [82]. Its structure has been determined at room temperature: the compound crys-

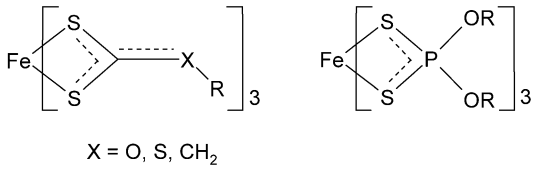


**Fig. 3** Tris(O-substituted-xanthato)iron(III) (*left*; X=O), tris(substituted-thioxanthato) iron(III) (*left*; X=S), tris(substituted-dithioacetato)iron(III) (*left*; $X=CH_2$) and tris(disubstituted-dithiophosphato)iron(III) (*right*)

tallises in the rhombohedral space group R-3, and relevant bond distances and angles for the $FeS_6$ core are Fe–S=2.31 Å and S–Fe-S=75.5(5)°. Tris(*O*-ethyl-xanthato)iron(III) seems to form an exception in the Fe(III) *O*-xanthate series in that it exhibits spin crossover behaviour ($\mu_{eff}$=2.19 B.M. at 108 K and $\mu_{eff}$=2.72 B.M. at 296 K), whereas magnetic measurements recorded for other tris(*O*-xanthato) complexes of Fe(III) suggest that the xanthates are characteristically low spin with magnetic moments of ca. 2.45 B.M. at room temperature [78, 79].

Tris(dithioacetato)iron(III) compounds are purely low spin over the temperature range 93–293 K [83].

Taking the relative favouring of the low spin state for iron(III) as the criterion, the order of field strengths for this type of $S_2$-ligand follows as: $^{-}S_2P(OR)_2 < ^{-}S_2CNR_2 < ^{-}S_2CSR < ^{-}S_2COR < ^{-}S_2CCR$ (R=alkyl).

## 2.4 Tris(Monothio-$\beta$-Diketonato)Iron(III) Compounds

In 1968 the first reports of spin crossover in iron(III) monothio-$\beta$-diketonates appeared [84, 85] and reviews on metal complexes of monothio-$\beta$-diketones were published shortly afterwards [86, 87]. The monothio-$\beta$-diketones can be considered as a ligand system intermediate between acetylacetone and dithioacetylacetone (Fig. 4).

The X-ray structure of [Fe(acetylacetonato)$_3$] has been known for almost 50 years and consists of an Fe(III) ion in a fairly regular octahedral environment of oxygen atoms with Fe–O=1.95 Å [88]. For the unsubstituted complex and for various complexes in which the ligand is substituted at the 2-position (X=Cl, Br, I, $CH_3$, $C_6H_5$, $NO_2$) $^{57}$Fe Mössbauer spectra and the magnetism indicate that they are purely high spin [89–92]. However, for the complex derived from 4,4,4-trifluoro-1-(3-pyridyl)-1,3-butane-dione the temperature dependence of the magnetic moment (3.69 B.M. at 293 K and 2.35 B.M. at 87 K) has been taken as evidence for spin crossover. This is the only system containing an Fe(III)$O_6$ chromophore known to show spin crossover behaviour [93]. On the other hand, tris(dithioacetylacetonato)iron(III) is purely low spin [94] with a mean Fe–S distance of 2.25 Å, typical for low spin Fe(III) [95].

Monothio-$\beta$-diketones generate a ligand field strength intermediate between those exerted by acetylacetone and dithioacetylacetone, and yield

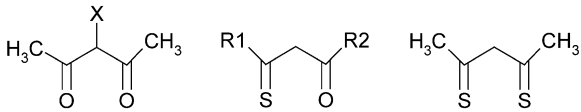


**Fig. 4** 2-Substituted-acetylacetone (*left*), 1,3-disubstituted-monothio-$\beta$-diketone (*middle*) and dithioacetylacetone (*right*)

Fe(III) compounds exhibiting spin crossover behaviour, its extent depending on the nature of the substituents R1 and R2 indicated in Fig. 4.

The structures of two of these mononuclear Fe(III) systems have been determined at room temperature. For the first compound R1=R2=$C_6H_5$, and for the second R1=$C_6H_5$ and R2=$CF_3$ [96]. [Fe($C_6H_5CS$=CHCO$C_6H_5$)$_3$] is high spin at room temperature ($\mu_{eff}$=5.50 B.M.), whereas [Fe($C_6H_5CS$=CHCO$CF_3$)$_3$] is essentially low spin at this temperature ($\mu_{eff}$=2.31 B.M.). Both compounds have a facial, distorted octahedral $FeS_3O_3$ geometry. The sulfur atoms lie at the corners of an almost equilateral triangle, which is parallel to a similar triangle formed by the oxygen atoms. The mean Fe–S distances are 2.368 and 2.239 Å, whereas the Fe–O distances are 1.988 and 1.942 Å for the high spin [Fe($C_6H_5CS$=CHCO$C_6H_5$)$_3$] and the low spin [Fe($C_6H_5CS$=CHCO$CF_3$)$_3$], respectively. Although a comparison of these high spin and low spin $FeS_3O_3$ coordination spheres belonging to different compounds may not be entirely valid in deriving the effects of the spin change on the metal-donor atom distances, it does appear that the Fe–S bond lengths are considerably more affected by the spin crossover than the Fe–O distances, the shortening being approximately 0.13 Å for the former and about 0.05 Å for the latter.

The magnetic data indicate that in all tris(monothio-$\beta$-diketonato)iron(III) systems investigated the spin crossover is gradual [84, 85, 87, 97–99], except for the complex with R1=R2=$CH_3$ which displays a rather abrupt spin transition at about 150 K [97]. Electron-withdrawing groups such as $CF_3$, phenyl and 4-substituted phenyl appear to be the most effective in increasing the population of the low spin configuration [84, 85]. Therefore a systematic study of the magnetic properties of nine iron(III) chelates of fluorinated monothio-$\beta$-ketones (R1C(SH)=CHCO$CF_3$ (R1=2-thienyl, $\beta$-naphthyl, phenyl, *p*-Me$C_6H_4$, *p*-F$C_6H_4$, *p*-Cl$C_6H_4$, *m*-Me$C_6H_4$, *m*-Cl$C_6H_4$, *m*-Br$C_6H_4$)) [99] contributed towards understanding the factors influencing the spin crossover behaviour. The magnetic moments vary from 5.49 to 2.16 B.M. at room temperature and are temperature dependent, falling as low as 1.82 B.M. at 83 K. The room temperature magnetic moments indicate that the order of the effective ligand fields is 2-thienyl<$\beta$-naphthyl<*p*-X$C_6H_4$<phenyl<*m*-X$C_6H_4$ (X=$CH_3$, F, Cl or Br), i.e. the 2-thienyl substituent yields a predominantly high spin complex at room temperature, whereas the ligands with phenyl substituents yield essentially low spin materials [99]. The $^{57}$Fe Mössbauer spectra of these Fe(III) compounds containing fluorinated monothio-$\beta$-ketones show only one doublet. The temperature dependence of the quadrupole splitting reflects the temperature dependence of the magnetic moment: $\mu_{eff}$ values lower than 2.5 B.M. correspond to quadrupole splitting values of ca. 1.75 mm s$^{-1}$, whereas $\mu_{eff}$ values larger than 4.9 B.M. correspond to quadrupole splittings of ca. 0.7 mm s$^{-1}$ [99].

It is noteworthy that these iron(III) chelates of fluorinated monothio-$\beta$-ketones are the only ones of this general family which show only a single

doublet in the $^{57}$Fe Mössbauer spectra. All other studies reported well-resolved $^{57}$Fe Mössbauer spectra for these spin crossover tris(monothio-$\beta$-diketonato)iron(III) compounds, in which contributions from both spin-isomers, with distinct quadrupole splittings, could be observed separately. In these cases, the quadrupole splittings are similar to those generally observed for low spin and high spin Fe(III) compounds [97, 98].

## 2.5 Bis(X-Semicarbazone)Iron(III) Compounds (X=S, Se)

In solution thiosemicarbazones or selenocarbazones probably consist of an equilibrium mixture of thione and thiol tautomers (Fig. 5) [100].

They may be condensed with suitable carbonyl compounds to yield tridentate chelating groups which generally coordinate in the anionic thiolate form. When the carbonyl compound is salicylaldehyde or a substituted salicylaldehyde, the tridentates coordinate as the di-anionic groups shown in Fig. 6. The salts of the (anionic) bis(ligand) iron(III) complexes of this class of Schiff base anion (typically (cation$^+$)[Fe(ligand$^{2-}$)$_2$]·n$H_2O$) frequently show spin crossover behaviour. A series of ligand systems of the X-semicarbazone type (X=S, Se) have been tested with the objective of determining the criteria for the occurrence of spin crossover in the Fe(III) derivatives.

The Fe(III) complexes of R-substituted salicylaldehyde thiosemicarbazone (R-thsa$^{2-}$; Fig. 6) are among the most studied spin crossover materials of this family. The crystal structures of several of them have been determined at various temperatures. The iron-donor atom distances are compiled in Table 2. The Fe(III) ion is in a distorted $FeS_2N_2O_2$ octahedron formed by two thiosemicarbazone ligands, which are geometrically arranged in such a way that the S and O atoms are located in *cis* positions, whereas the N atoms occupy *trans* positions, i.e. each tridentate molecule coordinates in an equatorial plane [101].

The compound $NH_4$[Fe(5-Br-thsa)$_2$] could be crystallised in two forms, one existing as mica-like crystals and the other as tabular plates [102]. The

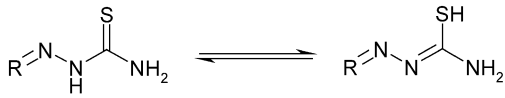


**Fig. 5** Proposed equilibrium in solution for thiosemicarbazones between the thione (*left*) and thiol (*right*) tautomers

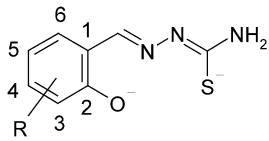


**Fig. 6** The dianion of R-salicylaldehyde thiosemicarbazone (R-thsa$^{2-}$)

**Table 2** Fe–donor atom bond lengths for various (cation$^+$)[Fe(ligand$^{2-}$)$_2$]·n$H_2O$ compounds of *R*-salicylaldehyde thiosemicarbazone (R-thsa$^{2-}$) [101]

| Compound | T (K) | Fe–S | Fe–N | Fe–O (Å) | Spin state[b] |
|---|---|---|---|---|---|
| Cs[Fe(thsa)$_2$] | 298 | 2.44 | 2.12 | 1.96 | HS |
| | 103 | 2.44 | 2.15 | 1.96 | HS |
| $NH_4$[Fe(5-Cl-thsa)$_2$] | 298 | 2.24 | 1.95 | 1.93 | LS |
| | 135 | 2.23 | 1.96 | 1.94 | LS |
| $NH_4$[Fe(5-Br-thsa)$_2$][a] | 298 | 2.23 | 1.93 | 1.95 | LS |
| $NH_4$[Fe(3,5-Cl-thsa)$_2$]·1.5$H_2O$ | 298 | 2.26 | 1.95 | 1.93 (site FeA) | LS |
| | 298 | 2.40 | 2.06 | 1.97 (site FeB) | HS (sco) |
| | 103 | 2.25 | 1.95 | 1.93 (site FeA) | LS |
| | 103 | 2.31 | 1.95 | 1.94 (site FeB) | LS (sco) |
| K[Fe(3,5-Cl-thsa)$_2$]·1.5$H_2O$ | 298 | 2.34 | 2.00 | 1.94 (site FeA) | LS/HS (sco) |
| | 298 | 2.42 | 2.05 | 1.94 (site FeB) | HS (sco) |
| | 103 | 2.25 | 1.88 | 1.93 (site FeA) | LS (sco) |
| | 103 | 2.30 | 1.92 | 1.93 (site FeB) | LS/HS (sco) |

[a] Determined for crystals of tabular form

[b] Predominant spin state (HS or LS) or mixture of both spin states (LS/HS) indicated. In case spin crossover (sco) occurs, this is mentioned in parentheses

mica-like crystals show spin crossover in the region around 200 K. The values for the magnetic moment—$\mu_{eff}$=5.06 B.M at 300 K and 2.29 B.M. at 77 K—indicate that the spin transition is substantially complete at both temperature extremes. The tabular crystalline form also exhibits spin crossover, albeit at a much higher temperature: the effective magnetic moment is 2.16 B.M. at 300 K, but at about 400 K it has almost reached the value for high spin iron(III). The X-ray structure has been determined for this tabular form at room temperature [102], and has been found to be isostructural with $NH_4$[Fe(5-Cl-thsa)$_2$] [103]. The main difference observed in the first coordination sphere of the Fe(III) ion in the Cl and Br derivatives is a slight increase in Fe–N distance and a decrease in Fe–O bond length in the chloro compound. In addition, the introduction of bromine instead of chlorine at the salicylaldehyde residue leads to a slight electronic rearrangement in the ligand.

The structure of $NH_4$[Fe(3,5-Cl-thsa)$_2$]·1.5$H_2O$ has been determined at 298 and 103 K [104]. There seems to be an inconsistency in the report. The authors [104] indicate that the magnetic properties of this material correspond to those reported for a compound without lattice water molecules [105]. Still, the structural features appear to be in line with the magnetic data reported for the solvent-free material, having a magnetic moment of 3.90 B.M. at room temperature, which gradually decreases to reach 2.57 B.M. at 80 K [105]. The asymmetric unit of $NH_4$[Fe(3,5-Cl-thsa)$_2$]·1.5$H_2O$ contains two crystallographically independent Fe(III) entities, denoted as sites FeA and FeB, respectively [104]. At room temperature, the Fe-ligand bond dis-

tances for FeA (Table 2) agree closely with these found for $NH_4$[Fe(5-Cl-thsa)$_2$] [103], and may be considered as the limiting values for the low spin Fe(III) configuration for systems such as these. At 103 K the configuration of FeA has not changed significantly. On the other hand, the structure at site FeB shows considerable temperature dependence. Upon spin crossover (298 K to 103 K), the FeB–S and FeB–N bond lengths decrease by about 0.1 Å, whereas the ligand bite angles S–FeB–O and S–FeB–N increase by about 6° and 3°, respectively. The geometry of FeB at 298 K is very close to that found for the iron atom in Cs[Fe(thsa)$_2$] [106], which contains a purely high spin Fe(III) chromophore.

The analysis of the magnetic and structural data reported by Ryabova revealed a linear correlation between the Fe–S bond distance and the effective magnetic moment [106].

Further attempts have been made to correlate the structural features of these systems with the spin state of Fe(III). The low spin $NH_4$[Fe(thsa)$_2$] complex [107] may be considered as the parent compound of this class of compounds. It was soon discovered that significant changes in the magnetic properties of the Fe(III) chelates may arise from (i) the replacement of the associated cation in the complex, (ii) the introduction of substituents into the benzene ring of the salicylaldehyde residue or (iii) the incorporation of substituents into the amido group of the thiosemicarbazide residue. In addition to these factors, the magnetic properties also appear to depend on heating of the solid compounds to 400 K prior to the magnetic measurements [105].

In the following, various Fe(III) compounds of R-substituted salicylaldehyde thiosemicarbazones will be discussed according to the criteria mentioned above, although it should be pointed out that a comparison of these materials may be rendered less meaningful due to the possible occurrence of different polymorphs. Moreover, upon variation of one substitution parameter, several other structural features may also be changed simultaneously. For instance, a change in outer-sphere cation or the introduction of a substituent at the salicylaldehyde moiety is frequently associated with increased hydration of the Fe(III) material.

The variation of the outer-sphere cation in Fe(III) compounds of the unsubstituted ligand yielded the low spin material $NH_4$[Fe(thsa)$_2$] [107], as well as the high spin compound Cs[Fe(thsa)$_2$] [106]. In addition Li[Fe(thsa)$_2$]·2-$H_2O$ is low spin whereas Na[Fe(thsa)$_2$]·3$H_2O$ [108] shows spin crossover, the magnetic moment decreasing from 5.57 B.M. at 300 K to 5.10 B.M. at 80 K [108]. It is likely that the selected cation has an indirect influence on the spin state of Fe(III) by co-determining the crystal packing and/or the degree of hydration of the material. Moreover, $^{57}$Fe Mössbauer spectroscopy results for pyridineH[Fe(thsa)$_2$]·$H_2O$ have revealed spin crossover behaviour, indicating 100% of low spin Fe(III) at 80 K, which decreases gradually to 19.2% at 280 K [109]. In addition, the magnetic susceptibility measurements

recorded on increasing temperature showed a sharp increase of the magnetic moment in the range 260–280 K.

The variation of the associated cation has also been investigated for 5-halo-salicylaldehyde thiosemicarbazone compounds [105]. The favouring of the low spin configuration for both (cation)[Fe(5-Br-thsa)$_2$] and (cation)[Fe(5-Cl-thsa)$_2$] follows the order of the associated cations: $Na^+$>-$Li^+$>$K^+$>$NH_4^+$ even though the effect of variation of the monovalent cation is not very pronounced. Overall the low spin state is favoured to the greater extent in the salts of the 5-chloro derivative. On the other hand, the $Zn^{2+}$ salt of this derivative, which crystallises as a sesqui hydrate, shows a more extended transition in the range 80–300 K [105].

Spin transitions have also been reported for $Al_{0.33}$[Fe(5-Cl-thsa)$_2$] [110] and H[Fe(5-Cl-thsa)$_2$] [109, 110]. For both compounds, a relatively abrupt and almost complete spin crossover occurs with $T_{1/2}$=228 K for the Al derivative, and 226 K for the H derivative. Transition temperatures determined by variable temperature heat capacity measurements are in agreement with those obtained from the magnetic susceptibility measurements.

It has been proposed that the introduction of substituents into the benzene ring of salicylaldehyde alters the ligand field strength, since the transfer of the polar properties of the substituent through the benzene ring is facilitated by the $\pi$-delocalisation in the ring [108]. Zelentsov et al. concluded that introduction of an $NO_2$ group into the benzene ring results in an increase in Dq/B [105]. Thus $NH_4$[Fe(thsa)$_2$] is a purely low spin compound, whereas a slight increase in magnetic moment for $NH_4$[Fe(5-$NO_2$-thsa)$_2$]·0.5$H_2O$ and $NH_4$[Fe(3-$NO_2$-thsa)$_2$] between 80 and 300 K may indicate Fe(III) spin crossover behaviour. A similar effect was observed for a 5-$CH_3$ substituent [105] but a more significant increase in the magnetic moment has been observed on replacement of H by 5-Cl or 5-Br. At 300 K the 5-Cl and 5-Br derivatives have intermediate values for the magnetic moment, i.e. 3.26 B.M. and 4.04 B.M., respectively, but after a heating treatment at 130 °C almost high spin values, i.e. 5.23 B.M. and 5.54 B.M., respectively, are reached at 300 K [105]. For the systems H[Fe(5-Cl-thsa)$_2$] [109, 110] and H[Fe(5-Br-thsa)$_2$]·0.5$H_2O$ [109] there seems to be a more distinct favouring of the low spin state in the chloro than in the bromo derivative. Thus, the substituents studied have been classified in the following sequence according to the extent of favouring the low spin state: $NO_2$>H>$CH_3$>Cl>Br.

Zelentsov et al. also observed that the high spin fraction in virtually all samples increased to varying extents after the samples were heated [105]. The origin of this effect is not clear since the complexes were mostly unsolvated and thus loss of solvate molecules, the most common cause of such a change, was not applicable. Nevertheless, the importance of the inclusion of lattice water molecules in co-determining the spin crossover properties is evident in the different magnetic properties of Li[Fe(5-Br-thsa)$_2$] [105] and Li[Fe(5-Br-thsa)$_2$]·$H_2O$ [111]. For the unsolvated compound $\mu_{eff}$=1.93 B.M.

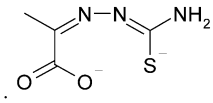

**Fig. 7** The dianion of pyruvic acid thiosemicarbazone ($thpu^{2-}$)

at 80 K and 3.97 B.M. at 300 K [105]. On the other hand the hydrate undergoes a spin transition associated with an asymmetric thermal hysteresis loop of width of 39 K with $T_{1/2}\uparrow$=333 K and $T_{1/2}\downarrow$=294 K [111]. A powder X-ray diffraction study at various temperatures demonstrates the occurrence of a first order crystallographic phase transition in the lattice coupled to the spin transition. This phase transformation might originate from a modification of the extended hydrogen-bonding network [111].

Finally, the effect of substitution of a phenyl group at the thioamido group of the thiosemicarbazide residue has been explored [108]. $NH_4[Fe(Phthsa)_2]\cdot 0.5H_2O$ ($H_2Phthsa$=salicylaldehyde phenylthiosemicarbazone) is low spin [108], like $NH_4[Fe(thsa)_2]$ [107]. Thus it appears that the ligand field and hence the spin state of Fe(III) is relatively insensitive to substitution at the $NH_2$ group, which is assumed to be involved neither in conjugation nor coordination.

The effect of the replacement of the sulfur atom in the ligand by selenium has also been briefly examined. $^{57}Fe$ Mössbauer spectral and magnetic susceptibility measurements show that $NH_4[Fe(sesa)_2]$ ($H_2sesa$ = salicylaldehyde selenosemicarbazone) displays spin crossover behaviour [108, 112]. In this salt there is a slight destabilisation of the doublet state for iron(III), relative to the corresponding derivative of the thiosemicarbazone [107], contrary to the trend observed in the dithio- and diseleno-carbamates. A further, and more significant, difference in the semicarbazone and carbamate series of ligands is seen in the Mössbauer spectra; those of the iron(III) complexes of the thiosemicarbazones and selenosemicarbazones, show separate doublets characteristic of the low spin and high spin forms [108].

The Fe(III) complexes of the dianion of pyruvic acid thiosemicarbazone ($thpu^{2-}$; Fig. 7), $(cation^{+})[Fe(thpu)_2]\cdot nH_2O$, are very similar to those of the salicylaldehyde derivatives (Fig. 6) discussed above. The spin state properties are quite sensitive to changes in the counter-cation (typically an alkali-metal cation or a protonated nitrogenous base) and the lattice water content of the material. The parent compound, $NH_4[Fe(thpu)_2]$, is low spin at room temperature [113]. $Li[Fe(thpu)_2]\cdot 3H_2O$ is also low spin but $K[Fe(thpu)_2]\cdot 2H_2O$ shows almost complete spin crossover between 80 and 300 K [108].

In contrast to the salicylaldehyde X-semicarbazone (X=S, Se) Fe(III) derivatives where replacement of sulfur by selenium results in an apparent slight de-stabilisation of the low spin state, $NH_4[Fe(sespu)_2]$ ($sespu^{2-}$=the dianion of pyruvic acid selenosemicarbazone) is low spin at room temperature [114], like the sulfur derivative $NH_4[Fe(thpu)_2]$ [113].

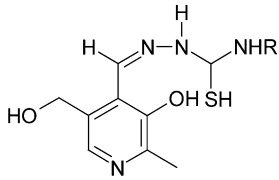


**Fig. 8** Pyridoxal 4-R-thiosemicarbazone (R=alkyl; $H_2$thpy)

Timken et al. have reported the magnetic and spectroscopic characterisation of the spin crossover complex [Fe(Hthpu)(thpu)], where $Hthpu^-$ and $thpu^{2-}$ are the singly and doubly deprotonated forms of pyruvic acid thiosemicarbazone, respectively [115]. This compound shows an abrupt transition with associated thermal hysteresis ($T_{1/2}\downarrow$=225 K and $T_{1/2}\uparrow$=235 K). Sample grinding leads to a more gradual and less complete spin transition. Again for this system distinct $^{57}$Fe Mössbauer spectral features are observed separately for the low spin and high spin states. The structure of [Cr(Hthpu)(thpu)]·$H_2O$ has been determined, which can be considered as a model for the low spin [Fe(Hthpu)(thpu)]·$H_2O$ ($\mu_{eff}$=2.48 B.M. at 299 K) [115]. These structural data, as well as those reported for other thiosemicarbazone Ni(II) [116] and Zn(II) [117] compounds, indicate that intermolecular hydrogen-bonding interactions are significant and result in a relatively strong coupling of the monomeric units in the solid state. It is quite likely, then, that for [Fe(Hthpu)(thpu)] the highly cooperative nature of the spin transition is due to the extended interaction of the complex centres through intermolecular hydrogen bonds.

The singly deprotonated form of pyridoxal 4-*R*-thiosemicarbazone (R= alkyl; $H_2$thpy; Fig. 8) has also been found to generate Fe(III) spin crossover [118, 119]. It has been proposed that the tridentate ligand coordinates to Fe(III) through the mercapto group, the azomethine nitrogen atom and the phenolic oxygen with the loss of a proton. For [Fe(Hthpy)$_2$]Cl [118] an abrupt and essentially complete spin transition ($\mu_{eff}$=5.75 B.M. at 299 K; 2.01 B.M. at 78 K) is associated with thermal hysteresis ($T_{1/2}\uparrow$=256 K; $T_{1/2}\downarrow$=245 K; $\Delta T_{1/2}$=11 K). It is most likely that the cooperative (first order) nature of this spin transition is due to an extended intermolecular hydrogen-bonding network. In fact, there seems to be an analogy with [Fe (Hthpu)(thpu)] [115] mentioned above, which also shows an abrupt transition. In both cases, the monohydrates are purely low spin compounds.

Substitution with R=methyl or ethyl yielded solvent-free compounds, which appeared to be in the low spin state ($\mu_{eff}$=ca. 2.12 B.M. over the temperature range 78–320 K) [119]. However, the phenyl derivative shows an abrupt and almost complete transition, but now centred near room temperature ($T_{1/2}\uparrow$=299 K and $T_{1/2}\downarrow$=290 K) [119].

These complexes of thiosemicarbazones and related systems are of obvious general interest because of the involvement of hydrogen bonding and, in some instances, the association of the transitions with hysteresis. Since the pioneering work of the Russian school they have received relatively little attention but interest in them has been re-kindled [111] and can be expected to grow.

## 2.6 Other Complexes with Sulfur Donor Atoms

Various other Fe(III) systems containing sulfur atoms in the coordination sphere have been reported. Selected examples are discussed in this section.

An $FeN_3S_3$ chromophore is present in (1,4,7-tris(4-*tert*-butyl-2-mercaptobenzyl)-1,4,7-triazacyclononane)iron(III) (Fig. 9 shows the ligand structure) [120, 121]. The complex displays a gradual transition extending over a very broad temperature range, $\mu_{eff}$ increasing from 2.4 B.M. at 77 K to 4.36 B.M. at 500 K [120]. The room temperature structure (where $\mu_{eff}$ is 2.9 B.M.) showed Fe(III) in a pseudooctahedral environment consisting of three nitrogen atoms of the macrocycle and three thiophenolato sulfur atoms in a facial stereochemistry. The average Fe–S and Fe–N distances are 2.28 Å and 2.08 Å, respectively [120]. In the $^{57}$Fe Mössbauer spectra (1.2–450 K) only one quadrupole doublet could be observed, characteristic for compounds where the relaxation time between the high spin and the low spin configurations is shorter than the quadrupole precession time [121]. Interestingly, the temperature dependence of the quadrupole splitting indicates a phase transition at approximately 100 K. This feature has been further investigated by X-ray structure analysis on single-crystals at room temperature, as well as by temperature-dependent EXAFS investigations (30–200 K) on powdered

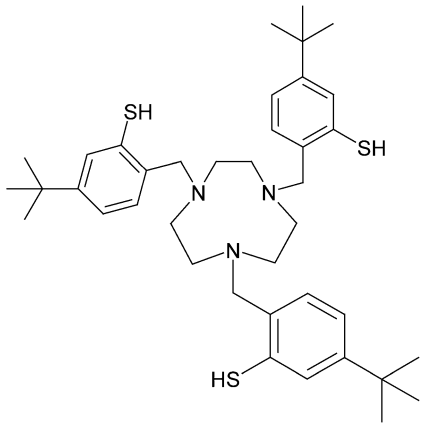


**Fig. 9** 1,4,7-Tris(4-*tert*-butyl-2-mercaptobenzyl)-1,4,7-triazacyclononane

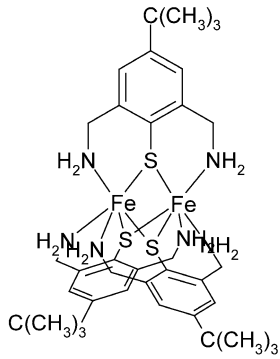


**Fig. 10** Schematic representation of $[Fe_2(2,6\text{-di(aminomethyl)-4-}tert\text{-butyl-thiophenol})_3]^{3+}$

samples, from which it could be concluded that the observed phase transition induces changes of bond angles only, while the spin crossover would additionally be expected to result in changes of metal-donor atom distances [121].

When three 2-mercaptopropyl substituents instead of 4-*tert*-butyl-2-mercaptobenzyl are incorporated into the cyclononane ring shown in Fig. 9, a predominantly high spin material has been obtained [120]. On the other hand, disubstitution of the cyclononane ring by 2-pyridylmethyl groups resulted in [Fe(1,4-bis(2-pyridylmethyl)-1,4,7-triazacyclononane)Cl] $(PF_6)_2$·MeOH containing an $FeN_5Cl$ chromophore [122]. For this material, a gradual transition with $\gamma_{HS}$=0.3 at 77 K and $\gamma_{HS}$=0.5 at 298 K was observed. In this instance, the $^{57}$Fe Mössbauer spectra show three lines, i.e. a singlet attributed to high spin Fe(III) superimposed on an asymmetric quadrupole doublet assigned to low spin Fe(III).

A triply thiolate-bridged dinuclear Fe(III) compound exhibiting spin crossover behaviour has been reported by Kersting et al. [123]. The material has been obtained using the deprotonated form of 2,6-di(aminomethyl)-4-*tert*-butyl-thiophenol as tridentate ligand, yielding two connected $FeN_3S_3$ spin crossover chromophores (Fig. 10). The compound $[Fe_2L_3](ClO_4)_3$ is diamagnetic at room temperature due to the presence of an almost equimolar mixture of low spin-low spin Fe(III) dimers together with strongly antiferromagnetically coupled high spin-high spin species. The $^{57}$Fe Mössbauer spectra show distinctly different features at 293, 180 and 77 K involving well resolved quadrupole doublets for low spin and high spin Fe(III) ions, indicating that both high spin Fe(III) ions within a dinuclear entity undergo a transition to the low spin state with decreasing temperature.

The synergy between magnetic interaction and spin crossover has been explored in five-coordinate Fe(III) complexes containing two bidentate *cis*-1,2-dicyano-1,2-ethylenedithiolates together with a monodentate coordinat-

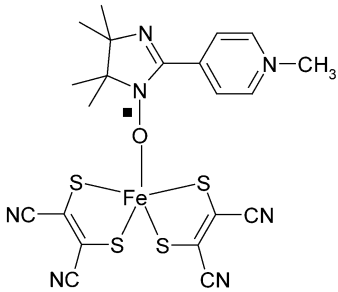


**Fig. 11** Schematic representation of bis(*cis*-1,2-dicyano-1,2-ethylenedithiolato)[2-(para-*N*-methylpyridinium)-4,4,5,5-tetramethylimidazolin-1-oxyl]iron(III) [124]

ed organic radical [124, 125]. The X-ray structure of bis(*cis*-1,2-dicyano-1,2-ethylenedithiolato)[2-(*para-N*-methylpyridinium)-4,4,5,5-tetramethylimidazolin-1-oxyl]iron(III) (Fig. 11) determined at 293 K shows that the two bidentate thiolate ligands form the basal plane of an $OS_4$ square-pyramid about the Fe(III) ion (mean Fe–S=2.24 Å), whereas the radical cation occupies the apical position (Fe–O=2.056(5) Å) [124]. The magnetic data could be interpreted by assuming that the non-exchange-coupled radical spin ($S_{radical=}1/2$) and the quartet spin state of Fe(III) ($S_{Fe}=3/2$) were responsible for the $\chi$T value of 2.33 $cm^3$ K $mol^{-1}$ determined between 100 and 300 K. Below 100 K, the $\chi$T value steadily decreases and tends towards zero at very low temperature. This behaviour may originate from the antiferromagnetic interaction between the radical spin ($S_{radical=}1/2$) and the doublet state of Fe(III) ($S_{Fe}=1/2$), resulting in a higher energetic S=1 molecular state, which is depopulated at decreasing temperature, while the lower lying S=0 molecular state is simultaneously populated. Obviously, this explanation involves an intermediate spin to low spin transition centred on the Fe(III) ion. Unfortunately, this phenomenon has not been further investigated by $^{57}$Fe Mössbauer spectroscopy.

Changing the radical cation yielded the related material bis(*cis*-1,2-dicyano-1,2-ethylenedithiolato)[2-(*p*-pyridyl)-4,4,5,5-tetramethyl-imidazolinium]iron(III)·2DMF [125]. The crystallographic data collected at 293 K again reveal two bidentate thiolate ligands in the basal plane (mean Fe–S=2.23 Å), but in this instance, the apical site is occupied by the N-donor radical cation (Fe–N=2.192(3) Å). The Fe(III) ion has an intermediate spin ($S_{Fe}=3/2$), but below 4 K the $^{57}$Fe Mössbauer spectra show a second doublet with larger quadrupole splitting and a higher isomer shift, which has been ascribed to the low spin state ($S_{Fe}=1/2$).

A low spin↔intermediate spin transition has also been found for a unique Fe(III) compound having an octahedral $FeN_4S_2$ environment [126]. In this compound the Fe(III) ion is surrounded by the tetradentate N-donating macrocycle *N,N′*-dimethyl-2,11-diaza[3.3](2,6)pyridinophane together with

the bidentate S-donating 1,2-benzenedithiolate, which occupies the *cis* positions in the equatorial plane. Magnetic measurements indicate a gradual spin crossover with $\gamma_{HS}$=0.4 at 150 K and $\gamma_{HS}$=0.85 at 298 K. The mean bond distances determined are (at 293 K, 150 K): Fe–N(pyridine)=2.020 Å, 1.979 Å, Fe–N(amine)=2.222 Å, 2.144 Å and Fe–S=2.197 Å, 2.206 Å. It has been proposed that the slight increase in Fe–S bond length may be related to the stronger $\pi$-donor interactions that occur in a compound containing an Fe(III) ion in an intermediate spin state than in one with a low spin Fe(III) ion. It has also been proposed that the highly distorted *cis* octahedral $N_4S_2$ geometry is responsible for the occurrence of this rather unusual intermediate spin state for a six-coordinate Fe(III) ion.

## 3 Iron(III) Spin Crossover Systems of Multidentate Schiff Base-Type Ligands

Schiff base-type systems are the second most widespread class of ligands which have been used to obtain Fe(III) spin crossover materials. These ligands may be classified according to the number of donor atoms available for coordination to the Fe(III) ion. In Sects. 3.1 to 3.4 attention is drawn to tri-, tetra-, penta- and hexadentate Schiff base-type ligands, severally. Section 3.5 focuses on spin crossover in iron(III) induced by light irradiation, whereas Sect. 3.6 is devoted to recent developments in the field of materials science with the objective of incorporation of Fe(III) spin crossover materials in devices.

Section 2 already demonstrated that $^{57}$Fe Mössbauer spectroscopy provides a very powerful experimental technique to assess the spin state of Fe(III). High spin compounds show a quadrupole doublet with isomer shift $\delta$ values in the range 0.25–0.37 mm s$^{-1}$ and quadrupole splitting $\Delta E_Q$ values below 1.3 mm$^{-1}$. On the other hand, low spin Fe(III) compounds have $\delta$ values in the range 0.05–0.20 mm s$^{-1}$ together with relatively large $\Delta E_Q$ values (1.9–3.0 mm s$^{-1}$). It became evident that the spin states of compounds of dithio-, monothio-, and diselenocarbamates interconvert faster than the reciprocal of the lifetime, $\tau_N$, of the $^{57}$Fe Mössbauer nuclear level ($10^{-7}$ s). However, for the complexes of Schiff base ligands the spin-interconversion rates have been found to depend on subtle solid-state effects such as variation in the counter ion and ligand substitution effects. This may give rise to distinctly different $^{57}$Fe Mössbauer spectra even for systems which are chemically very similar. When the spin-interconversion is slower than the reciprocal of $\tau_N$, two sets of quadrupole doublets corresponding to the high spin and low spin states are observed. On the other hand, spin crossover systems with much faster spin-interconversion than $\tau_N^{-1}$ show only one quadrupole doublet with quadrupole splitting and isomer shift parameters related to the fraction of each spin state. In the intermediate case, i.e. the spin-interconver-

sion rate being comparable to $\tau_N^{-1}$, the spectra show broadened quadrupole doublet lines, so-called relaxation spectra or time-averaged spectra. Examples of each type of behaviour can be found in the present section.

### 3.1
### Complexes of Tridentate $N_2O$-Donating Ligands

Among the Schiff base derivatives, the ones providing a tridentate $N_2O$ donor set for Fe(III) have been studied the most extensively. Several ligand systems have been used; these are shown in Fig. 12. The compounds have the general molecular formula $[Fe(ligand^-)_2](anion^-)\cdot solvent$. The anionic nature of the ligand arises from deprotonation of the hydroxy group which is present in all examples. In addition, incorporation of solvent molecules has frequently been observed and this can have a decisive effect on the spin crossover properties. Clearly, a major difference among the ligand systems depicted in Fig. 12 is that these may form chelate rings of different sizes: the coordination involving the N and O atoms of the salicylidene moiety leads in all instances to a six-membered chelate, whereas the N,N coordination yields a six-membered chelate for 3-OEt-salAPA, and a five-membered chelate for all other ligand systems. Moreover, structural studies of these Fe(III) materials containing an $FeN_4O_2$ environment (Table 3), have revealed that the Fe–O distances are always shorter than the Fe–N bond lengths. These features result in a distortion of the $FeN_4O_2$ octahedron. Consequently, the

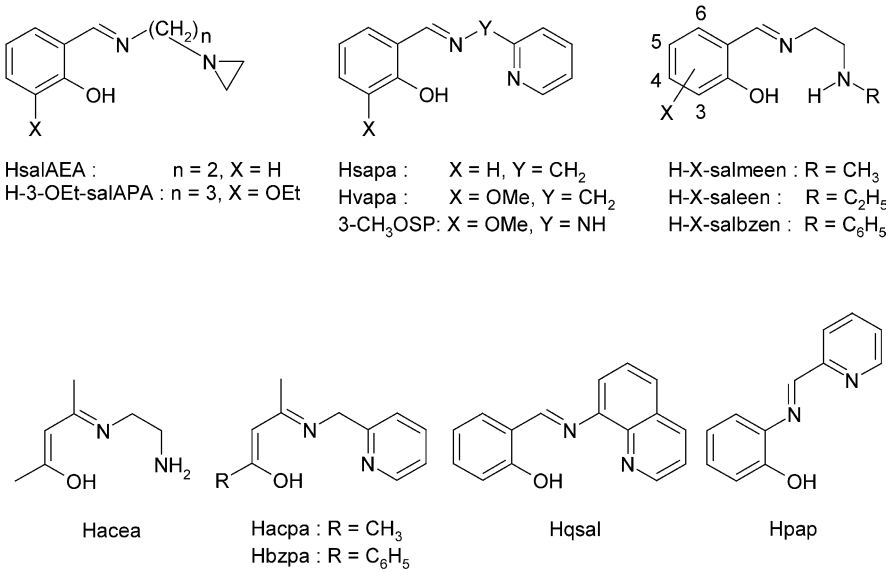


**Fig. 12** Tridentate $N_2O$-donating Schiff base ligands

**Table 3** Average Fe–donor atom bond lengths for Fe(III) compounds of tetradentate $N_2O_2$-donating Schiff base ligands[a,b,c,d]

| Compound | T (K) | Fe—O | Fe–$N_{central}$ | Fe–$N_{outer}$ (Å) | | Spin state | References |
|---|---|---|---|---|---|---|---|
| $[Fe(3\text{-}OEt\text{-}salAPA)_2]ClO_4 \cdot C_6H_6$ | 20 | 1.864 (8) | 1.95 (1) | 2.098 (9) | (Fe1) | LS | [127] |
| | | 1.845 (8) | 1.95 (1) | 2.037 (9) | (Fe2) | LS | |
| | 128 | 1.864 (4) | 1.954 (5) | 2.023 (5) | (Fe1) | LS | |
| | | 1.850 (4) | 1.961 (5) | 2.032 (5) | (Fe2) | LS | |
| | 175 | 1.884 (5) | 1.994 (6) | 2.071 (6) | (Fe1) | LS/HS | |
| | | 1.877 (5) | 2.028 (6) | 2.095 (6) | (Fe2) | LS/HS | |
| | 298 | 1.923 (5) | 2.085 (7) | 2.173 (8) | | HS | |
| | 300 | 1.921 (2) | 2.085 (3) | 2.176 (3) | | HS | |
| $[Fe(3\text{-}OEt\text{-}salAPA)_2]ClO_4 \cdot C_6H_5Cl$ | 158 | 1.860 (5) | 1.968 (6) | 2.040 (6) | (Fe1) | LS | [128] |
| | | 1.866 (5) | 1.969 (6) | 2.046 (6) | (Fe2) | LS | |
| | 296 | 1.914 (6) | 2.095 (6) | 2.185 (6) | | HS | |
| $[Fe(3\text{-}OEt\text{-}salAPA)_2]ClO_4 \cdot C_6H_5Br$ | 163 | 1.900 (7) | 2.027 (8) | 2.115 (7) | (Fe1) | LS | [128] |
| | | 1.882 (7) | 1.974 (7) | 2.060 (7) | (Fe2) | LS | |
| | 296 | 1.917 (10) | 2.091 (11) | 2.179 (9) | | HS | |
| $[Fe(3\text{-}OEt\text{-}salAPA)_2]ClO_4 \cdot C_6H_4Cl_2$ | 296 | 1.925 (3) | 2.081 (4) | 2.198 (6) | | HS | [128] |
| $[Fe(5\text{-}OCH_3\text{-}salmeen)_2]PF_6$ | 292 | 1.913 (2) | 2.092 (3) | 2.224 (3) | | HS | [129] |
| | | 1915 (2) | 2.108 (3) | 2.194 (3) | | | |
| $[Fe(3\text{-}OCH_3\text{-}salmeen)_2]PF_6$ | 292 | 1.880 (2) | 1.933 (3) | 2.053 (3) | | LS[e] | [129] |
| | | 1.877 (2) | 1.934 (3) | 2.067 (3) | | | |
| $[Fe(5\text{-}NO_2\text{-}salmeen)_2]PF_6$ | 292 | 1.886 (1) | 1.944 (1) | 2.046 (1) | | LS[e] | [129] |
| $[Fe(3\text{-}allyl\text{-}salbzen)_2]NO_3$ | 298 | 1.941 (4) | 1.976 (5) | 2.148 (5) | (Fe1) | 67%LS | [130] |
| | | 1.852 (5) | 1.989 (5) | 2.094 (5) | (Fe1) | | |
| | | 1.864 (4) | 1.949 (4) | 2.031 (4) | (Fe2) | LS | |
| | | 1.903 (4) | 1.924 (4) | 2.063 (4) | (Fe2) | | |
| $[Fe(acea)_2]BPh_4$ | 293 | 1.932 (2) | 2.090 (2) | 2.184 (2) | | HS | [131] |
| | | 1.937 (3) | 2.085 (2) | 2.182 (4) | | | |
| $[Fe(acpa)_2]PF_6$ | 120 | 1.889 (2) | 1.941 (2) | 1.989 (2) | | LS | [132] |
| | 205 | 1.914 (2) | 2.010 (2) | 2.070 (2) | | LS/HS | [132] |
| | 290 | 1.939 (2) | 2.081 (2) | 2.153 (2) | | HS | [132] |
| | 298 | 1.939 (2) | 2.081 (2) | 2.153 (2) | | HS | [133] |

**Table 3** (continued)

| Compound | T (K) | Fe—O | Fe–$N_{central}$ | Fe–$N_{outer}$ (Å) | Spin state | References |
|---|---|---|---|---|---|---|
| $[Fe(acpa)_2]BPh_4$ | 120 | 1.902 (3) | 1.937 (3) | 1.976 (3) | LS | [132] |
| | | 1.889 (3) | 1.938 (3) | 1.987 (3) | | |
| | 202 | 1.896 (2) | 1.941 (2) | 1.979 (2) | LS | |
| | | 1.891 (2) | 1.939 (2) | 1.990 (2) | | |
| | 247 | 1.913 (2) | 1.971 (2) | 2.022 (2) | LS/HS | |
| | | 1.873 (2) | 1.969 (2) | 2.001 (2) | | |
| | 311 | 1.920 (2) | 2.027 (2) | 2.082 (2) | LS/HS | |
| | | 1.913 (2) | 2.029 (2) | 2.093 (2) | | |
| $[Fe(bzpa)_2]ClO_4$ | 140 | 1.896 (3) | 1.94 (3) | 1.964 (3) | LS | [134] |
| | | 1.919 (3) | 1.926 (3) | 1.988 (3) | | |
| | 290 | 1.911 (3) | 2.018 (4) | 2.070 (4) | HS | |
| | | 1.930 (3) | 2.015 (4) | 2.078 (4) | | |
| $[Fe(qsal)_2]NCSe{\cdot}MeOH$ | 200 | 1.871 (6) | 1.949 (7) | 1.976 (7) | LS | [135] |
| | | 1.869 (6) | 1.941 (7) | 1.971 (7) | | |
| $[Fe(qsal)_2]NCSe{\cdot}CH_2Cl_2$ | 230 | 1.879 (2) | 1.944 (3) | 1.985 (3) | LS | [135] |
| | | 1.875 (3) | 1.953 (3) | 1.991 (3) | | |
| $[Fe(qsal)_2]NCSe{\cdot}2DMSO$ | 90 | 1.875 (4) | 1.936 (4) | 1.975 (4) | LS | [136] |
| | | 1.874 (3) | 1.938 (4) | 1.961 (4) | | |
| $[Fe(pap)_2]ClO_4{\cdot}H_2O$ | 298 | 1.932 (8) | 2.105 (9) | 2.202 (10) | HS | [137] |
| | | 1.931 (8) | 2.136 (9) | 2.138 (9) | | |
| $[Fe(pap)_2]PF_6{\cdot}MeOH$ | 90 | 1.883 (4) | 1.911 (5) | 1.994 (5) | LS | [138] |
| | | 1.882 (4) | 1.915 (5) | 1.993 (5) | | |

[a] For non-centrosymmetric Fe(III) entities the bond lengths involving the two crystallographically independent tridentate ligands are noted in line 1 and 2, respectively [b] For compounds containing two crystallographically independent Fe(III) cations, the details for sites Fe1 and Fe2 are noted in line 1 and 2, respectively [c] The ligands are shown in Fig. 12. Abbreviations used for the ligands can be found in the list of abbreviations [d] Predominant spin state (HS or LS) or mixture of both spin states (LS/HS) is indicated. All compounds exhibit spin cross-over unless indicated otherwise [e] Purely low spin compound

rigidity and distortion of the Fe(III) coordination octahedron may be varied depending on the ligand.

Iron(III) compounds of 3-OEt-salAPA have been widely studied [127, 128, 139–145]. Both the anion and the incorporated solvent molecule influence the spin crossover behaviour of the complex salts. Thus $T_{1/2}$ for [Fe(3-OEt-salAPA)$_2$]$ClO_4$ is 295 K, whereas that for the dichloromethane solvate is 152 K [140]. The transition in [Fe(3-OEt-salAPA)$_2$]$ClO_4$ and [Fe(3-OEt-salAPA)$_2$]$BPh_4$ is more gradual and occurs at a somewhat higher temperature than that for the benzene solvate [Fe(3-OEt-salAPA)$_2$]$ClO_4$·$C_6H_6$ [141].

Interestingly, various benzene derivatives may be incorporated in the crystal lattice yielding [Fe(3-OEt-salAPA)$_2$]$ClO_4$·solvent [128, 141, 142]. Below about 50 K the six complexes studied (no solvent, $C_6H_6$, $C_6H_5Cl$, $C_6H_5Br$, $C_6H_5I$ or *o*-$C_6H_4Cl_2$) are low spin with a magnetic moment of 2.0 B.M. As the temperature is increased all six compounds exhibit spin crossover, which is the most gradual for the non-solvated material. The $\mu_{eff}$ value for this complex increases gradually from 2.24 B.M. at 99 K to 4.60 B.M. at 300 K. The degree of abruptness varies from one solvate to the other: the transition in the $C_6H_5I$ solvate is the least, and that in the $C_6H_5Cl$ is the most abrupt [128]. The transition temperature for the various [Fe(3-OEt-salAPA)$_2$]$ClO_4$·solvent systems was found to depend linearly on the molecular volume of the monohalogenated benzene derivative [142]. The only exception to this relation is the chlorobenzene analogue.

X-ray structures have been determined at various temperatures for [Fe(3-OEt-salAPA)$_2$]$ClO_4$·solvent containing solvated benzene or its halogenated derivatives (Table 3). Typically, within the $FeN_4O_2$ core the Fe–N(amine) bonds are longest, the Fe–O bonds shortest, and the Fe–N(imine) bonds intermediate. It appears that the Fe–N(amine) distances are most affected by the spin transition. Additional noteworthy structural features have been observed for some of these compounds. The space group determined for [Fe(3-OEt-salAPA)$_2$]$ClO_4$·$C_6H_6$ is $P2_1/c$ at 20 K, 128 K and 175 K and C2/c at room temperature [127]. In the C2/c structures the Fe(III) entity is located on an inversion centre, whereas the perchlorate anion and the benzene molecule are situated on a twofold axis. The transformation to $P2_1/c$ brings about an inequality of the Fe(III) sites: in this instance, two crystallographically independent Fe(III) units are present, each located on a crystallographic inversion centre. However, the gradual, but complete spin crossover at $T_{1/2}$=205 K is not related to this change in space group, which can in fact be considered as an order-disorder transformation taking place at about 180 K [127]. The thermodynamic parameters associated with the phase and spin transitions in [Fe(3-OEt-salAPA)$_2$]$ClO_4$·$C_6H_6$ have been determined from heat capacity measurements (see below) [144].

A change in space group has also been observed for [Fe(3-OEt-salAPA)$_2$]$ClO_4$·$C_6H_5X$ (X=Cl, Br) [128]. The space group for the chlorobenzene derivative is $P2_1/c$ at 296 K and converts to $P2_1/a$ at 158 K. A similar trans-

formation has been observed for the bromobenzene compound: its space group is $P2_1/c$ at 296 K, whereas it is $P2_1/a$ at 163 K. In converting from $P2_1/c$ to $P2_1/a$ the Fe(III) cations and perchlorate anions remain in the same relative positions, however, half of the $C_6H_5X$ solvate molecules experience a re-orientation. These structural phase transitions in $[Fe(3\text{-}OEt\text{-}salAPA)_2]ClO_4 \cdot C_6H_5X$ (X=Cl, Br) have been investigated in detail [143, 145]. For the bromobenzene derivative there is little cooperativity between the structural phase transition at 288.3 K and the spin crossover, since the spin transition progresses essentially as an equilibrium process in the solid state. In contrast, for the chlorobenzene solvate, the 188.4 K phase transition cooperatively involves both the spin crossover and the structural change [143].

While both chelate rings in the complexes of 3-OEt-salAPA are six-membered, for salAEA a six-membered chelate ring involving N and O atoms and a five-membered N,N-chelate ring are formed. Only one compound of this ligand has been reported, $[Fe(salAEA)_2]ClO_4$, which is predominantly high spin; even at 20 K there is probably no more than 20% population of the low spin state [139].

Similar six-membered N,O- and five-membered N,N-chelate rings are formed in Fe(III) compounds of sapa and vapa. $[Fe(vapa)_2]PF_6$ appears to be high spin, whereas $[Fe(sapa)_2]NO_3 \cdot 1.5H_2O$ exhibits a very gradual and incomplete (at low temperature) spin transition [146]. The related $3\text{-}CH_3OSPH$ yielded the low spin compounds $[Fe(3\text{-}CH_3OSPH)_2]X$ ($X=Cl^-$, $NO_3^-$), as well as the spin crossover materials $[Fe(3\text{-}CH_3OSPH)_2]X$ ($X=PF_6^-$, $BPh_4^-$) [147]. Both the latter compounds exhibit gradual spin crossover, with the transition temperature for the $PF_6^-$salt being higher (45% of low spin Fe(III) ions at 298 K) than that of the $BPh_4^-$ salt (fully high spin at 298 K) [147].

Another family of bis(ligand)Fe(III) spin crossover systems with the donor atom set $N_4O_2$ is that derived from Schiff bases obtained from the condensation of X-salicylaldehyde and *N-R*-ethylenediamine (X-salmeen ($R=CH_3$), X-saleen ($R=C_2H_5$), X-salbzen ($R=C_6H_5$); Fig. 12). Within the X-salmeen series crystal structures have been determined at 292 K for high spin $[Fe(5\text{-}OCH_3\text{-}salmeen)_2]PF_6$, as well as for the low spin materials $[Fe(3\text{-}OCH_3\text{-}salmeen)_2]PF_6$ and $[Fe(5\text{-}NO_2\text{-}salmeen)_2]PF_6$ [129] (Table 3). Apart from the observed differences in metal-donor atom bond lengths, the high spin compound is more distorted from octahedral than the low spin compounds [129]. Variation of the substituent X within $[Fe(X\text{-}salmeen)_2]PF_6$ yielded compounds showing substantial differences in their magnetic behaviour, but a general pattern for the influence of the substituent could not be established due to the overlying solid state effects involved [148]. The material containing unsubstituted salmeen (X=H) is purely high spin. Both the $5\text{-}OCH_3$-salmeen and $4\text{-}OCH_3$-salmeen complexes are essentially high spin at room temperature and exhibit gradual and incomplete transitions to low spin at low temperature [148]. The compounds with $X=3\text{-}NO_2$, $3\text{-}OCH_3$ and $5\text{-}NO_2$ show the onset of spin crossover at about 200 K, however, at room

temperature the magnetic moment is still below 3.0 B.M [148]. In acetone solutions, compounds that have been observed to be essentially low spin in the solid state exhibit spin crossover, and moreover, the spin transition becomes more pronounced for compounds that also show spin crossover in the solid state [148]. The percentage of the high spin isomer in acetone solution decreases according to the salicylaldimine ring substituent series: 3-$OCH_3$ (88% at 314 K)>5-$OCH_3$ (82% at 314 K)>H (80% at 314 K)>3-$NO_2$ (36% at 299 K)>5-$NO_2$ (19% at 285 K). The variable-temperature studies confirm this to be the general pattern over the entire 200–300 K temperature range. The same sequence of field strengths, $OCH_3$>H>$NO_2$, has also been observed for [Fe(X-sal$_2$trien)]$PF_6$ (X-sal$_2$trien=hexadentate $N_4O_2$ Schiff base obtained from the 1:2 condensation of triethylenetetramine with salicylaldehyde derivatives; see below) [149], but the actual values appear to be greater in the hexadentate systems [148]. The influence of the solvent on the spin crossover characteristics has been studied for the parent compound [Fe(salmeen)$_2$]$PF_6$ [148], with the order of favouring of the high spin state being acetone >$CH_3CN$>$CH_3OH$>$CH_2Cl_2$>$Me_2SO$. There is no obvious correlation between this sequence and the strength of the [solvent...H–N] hydrogen bonding interaction as deduced from the position of the $\nu_{N-H}$ vibration in the IR spectra [148].

The dependence of the spin state of Fe(III) on the associated anion has been studied for solid-state [Fe(X-saleen)$_2$]Y (Y=$BPh_4^-$, $NO_3^-$, $PF_6^-$) [150]. The tetraphenylborate salts [Fe(saleen)$_2$]$BPh_4$·0.5$H_2O$ [150] and [Fe(3-$OCH_3$-saleen)$_2$]$BPh_4$ [151, 152] are high spin, whereas [Fe(3-$OCH_3$-saleen)$_2$]$NO_3$·0.5$H_2O$ [150–152] and [Fe(5-$OCH_3$-saleen)$_2$]$NO_3$ are predominantly low spin [150, 151]. On the other hand, [Fe(saleen)$_2$]$NO_3$ exhibits an incomplete, gradual spin transition [150–152]. Interestingly, the mixed-anion species [Fe(5-$OCH_3$-saleen)$_2$]$(NO_3)_{0.5}(BPh_4)_{0.5}$ exhibits gradual spin crossover, the transition being complete at low temperature but incomplete at 286 K [150]. The hexafluorophosphate salts give rise to spin crossover in a number of instances [150–154]: [Fe(saleen)$_2$]$PF_6$ undergoes a gradual, but complete spin transition [151]. However, [Fe(3-$OCH_3$-saleen)$_2$]$PF_6$ exhibits an extremely abrupt spin crossover at about 159 K, associated with a thermal hysteresis loop of width 2–4 K [150–152]. The effect of grinding of the sample on the spin crossover characteristics is to render the transition less abrupt and less complete as well as to lower the transition temperature [151, 152]. It was suggested that this results from an increase in defects and stress points in the crystal [151]. Interestingly, a sample of [Fe(3-$OCH_3$-saleen)$_2$]$PF_6$ that had been subjected to an external pressure of about 1.4 kbar for a period of 5 min shows similar features [152]. The effect of grinding has been found to be much greater for a sample doped with Cr(III) ions, [$Fe_{0.5}Cr_{0.5}$(3-$OCH_3$-saleen)$_2$]$PF_6$, which shows a gradual, complete transition. After the sample has been ground in a ball mill, the spin transition has been found to be suppressed [151]. Experiments on [$Fe_xM_{1-x}$(3-$OCH_3$-saleen)$_2$]$PF_6$ doped with

M(III)=Cr or Co show that doping leads not only to more gradual spin transitions but also a displacement of the transition temperature to lower values for Cr(III) and to higher for Co(III) [152]. These features can be related to the difference in ionic radius for high spin Fe(III) (0.65 Å) compared to Cr(III) (0.62 Å) or low spin Co(III) (0.53 Å) [152]. Later the dilution effect of Co(III) on the spin transition of Fe(III) was described in terms of (i) the lattice contraction due to the Co(III) ions, which favours the low spin state of Fe(III) and (ii) the contribution due to the spin transition [154]. The lattice contraction induced by the Co(III) results in the iron centres experiencing an increase in pressure, the so-called "image-pressure" with a concomitant increase in the transition temperature [154]. Since Cr(III) and high spin Fe(III) have comparable ion radii, this lattice contraction is not operative in this instance. Using the model of Sasaki and Kambara [154], the spin transition curves for compounds having varying Co(III) or Cr(III) dopant concentrations could be reproduced.

With X-salbzen the essentially high spin compounds [Fe(3-OEt-salbzen)$_2$]X (X=$Cl^-$, $NO_3^-$) have been obtained [130]. On the other hand, [Fe(3-OEt-salbzen)$_2$]$BPh_4$·$CH_3CN$ shows a gradual, relatively complete spin crossover with a high spin mole fraction of 0.93 at room temperature, which decreases to 0.03 at 10 K [130]. The structure of [Fe(3-allyl-salbzen)$_2$]$NO_3$ has been determined at room temperature [130]. The unit cell contains two centrosymmetric, crystallographically independent cations. The metal-donor atom bond lengths (Table 3) are consistent with Fe2 being in the low spin state, whereas Fe1 may be considered as an average of 67% low spin and 33% high spin Fe1 sites, in agreement with the magnetic data. [Fe(3-allyl-salbzen)$_2$]$NO_3$ exhibits a partial, gradual spin transition, reaching the low spin state ($\mu_{eff}$=1.88 B.M.) at 4.2 K [130].

The complex [Fe(acea)$_2$]$BPh_4$ exhibits a gradual, almost complete spin crossover [131]. The Fe-donor atom bond lengths (Table 3) are consistent with high spin Fe(III) at room temperature.

Complexes of acpa and bzpa have been extensively studied. Crystal structures have been determined for [Fe(acpa)$_2$]$PF_6$ at 120, 290 [132] and 298 K [133] and for [Fe(acpa)$_2$]$BPh_4$ at 120, 202, 247 and 311 K [132]. Both compounds exhibit incomplete, gradual spin crossover behaviour. The transition temperature is higher for the tetraphenylborate salt than for the hexafluorophosphate [132, 133, 155]. The metal-donor atom bond lengths observed for [Fe(acpa)$_2$]$BPh_4$ (Table 3) correspond with the extent to which the spin crossover has progressed at 120 K (low spin Fe(III) percentage=96.7%) and at 311 K (high spin Fe(III) percentage=80.9%). The transition temperature for [Fe(acpa)$_2$]$NO_3$ is higher than that of both the $BPh_4^-$ and $PF_6^-$ derivatives [155].

The $^{57}$Fe Mössbauer spectra for [$Fe_xCo_{1-x}$(acpa)$_2$]$BPh_4$ (x=0.035 and 0.074) show that the transition has been displaced to a higher temperature than that for the pure Fe(III) compound [156]. This may again be related to

the difference in ionic radii for low spin Co(III) compared to high spin Fe(III) (see below). The EPR spectra for these diluted complexes have been measured at various temperatures. Signals attributed to low spin Fe(III) have been observed at g=1.965, 2.219 and 2.291. This observation suggests that the geometry about the Fe(III) ion is more distorted in the diluted complex than in the neat compound. A signal observed at g=4 is characteristic for a high spin ferric complex in a rhombically distorted environment [156].

Fast electronic relaxation within $[Fe(acpa)_2]PF_6$ has been thought to be responsible for the observation of a single doublet in the $^{57}Fe$ Mössbauer spectra throughout the transition with strongly temperature dependent values for the quadrupole splitting and isomer shift [133]. It has been proposed that the spin-interconversion of $[Fe(acpa)_2]BPh_4$ is faster than that of the $PF_6^-$ salt [132]. X-ray crystallographic studies carried out for both compounds at different temperatures revealed smaller changes in metal-donor atom bond length for the $BPh_4^-$ salt. It was therefore concluded that the activation energy for the spin change in the $BPh_4^-$ salt is smaller than that in the $PF_6^-$ salt, which would imply faster spin-interconversion for the former [132].

The thermodynamic parameters associated with the spin transition in $[Fe(acpa)_2]PF_6$ have been determined by calorimetry [157]. The unusual heat capacity anomaly observed for this material was typical for neither a first-order nor a second-order phase transition. It has therefore been assumed that it might originate from a higher order phase transition that is characterised by weak cooperativity [157]. The entropy associated with the low spin→high spin transition in $[Fe(acpa)_2]PF_6$ ($\Delta S$=36.19 J $K^{-1}$ $mol^{-1}$) has been found to be comparable with values for other Fe(III) spin transition materials of tridentate $N_2O$ Schiff base ligands, i.e. $[Fe(3\text{-OMe-saleen})_2]PF_6$ ($\Delta S$=36.74 J $K^{-1}$ $mol^{-1}$) [157], $[Fe(3\text{-OEt-salAPA})_2]ClO_4{\cdot}C_6H_6$ ($\Delta S$=38.4 J $K^{-1}$ $mol^{-1}$) [144] and $[Fe(3\text{-OEt-salAPA})_2]ClO_4{\cdot}C_6H_5Cl$ ($\Delta S$=37.2 J $K^{-1}$ $mol^{-1}$) [145]. It is, however, significantly smaller than the values determined for Fe(II) spin crossover complexes, e.g. $[Fe(1,10\text{-phenanthroline})_2(NCS)_2]$ ($\Delta S$=48.78 J $K^{-1}$ $mol^{-1}$) [158, 159], and $[Fe(2\text{-picolylamine})_3]Cl_2{\cdot}EtOH$ ($\Delta S$=50.59 J $K^{-1}$ $mol^{-1}$) [160]. The observed entropy change associated with the spin crossover of $[Fe(acpa)_2]PF_6$ could be explained by the sum of the contributions due to the change in the spin manifold (9.13 J $K^{-1}$ $mol^{-1}$) and the skeletal vibrational changes accompanying the spin transition (28.56 J $K^{-1}$ $mol^{-1}$). In fact, the temperature dependence of the IR and Raman spectra revealed drastic changes, which could be assigned to skeletal vibration modes of the six-coordinate Fe(III) core [157]. The enthalpy change associated with the low spin→high spin transition in $[Fe(acpa)_2]PF_6$ has been estimated to be 7025 J $mol^{-1}$ [157].

The structure of $[Fe(bzpa)_2]ClO_4$ has been determined for the low spin form at 140 K, as well as for the high spin form at 290 K (Table 3) [134]. The gradual spin transition is complete as has been confirmed by the time-aver-

aged $^{57}$Fe Mössbauer spectra [134]. The transition in $[Fe(bzpa)_2]PF_6$, on the other hand, is incomplete over the range 80–300 K [155, 161].

Both $[Fe(acpa)_2]X$ and $[Fe(bzpa)_2]X$ ($X=PF_6^-$, $BPh_4^-$, $NO_3^-$) show reversible thermochromism in acetone solutions, which is typical for a change in electronic ground state of the Fe(III) ion. The electronic spectra show a temperature dependence of the intensities of the metal-charge transfer bands ascribed to the high spin (550 nm) and low spin state (700 nm) [155].

Early investigations on Fe(III) complexes of qsal provided evidence for spin crossover behaviour, its extent depending on the associated anion and the degree of hydration [162, 163]. The slight change in magnetic moment with change in temperature observed in 1969 for $[Fe(qsal)_2]Cl{\cdot}2H_2O$ [162], was, on the basis of $^{57}$Fe Mössbauer spectral data, later ascribed to a spin transition [163]. The solvent-free iodide salt is purely low spin, whereas the bromide monohydrate is high spin. On the other hand, the solvent-free thiocyanate salt again showed spin crossover behaviour: the magnetic moment gradually decreases from 5.63 B.M. at 299 K to 2.37 B.M. at 24 K [163]. The nature of the transition observed in this instance depends markedly on the temperature at which the material has been synthesised, i.e. either at 298 K or below 280 K [164]. For a sample prepared from a methanolic solution at 298 K the transition is associated with an asymmetric hysteresis loop of width 70 K. There are two steps—at about 220 K and 270 K—in the heating branch, which may suggest the existence of another phase or another isomer with a different transition temperature. In contrast, $[Fe(qsal)_2]NCS$ freshly recrystallised from methanol below 280 K is predominantly low spin. However, the magnetic moment determined at room temperature increases with time. Ten days after preparation the sample shows spin crossover with a pronounced hysteresis loop ($\Delta T_{1/2}$=70 K) centred at 286 K. These interesting spin crossover features prompted the study of the selenocyanate salts [135, 136]. $[Fe(qsal)_2]NCSe{\cdot}MeOH$ [135], $[Fe(qsal)_2]NCSe{\cdot}CH_2Cl_2$ [135] and $[Fe(qsal)_2]NCSe{\cdot}2DMSO$ [136] are low spin at room temperature. However, these all lose solvent molecules on heating, converting to the non-solvated high spin analogues which display spin crossover below room temperature. The non-solvated materials derived from the methanol and dichloromethane compounds show identical magnetic properties involving a reproducible two-step spin crossover. The high spin to low spin transition takes place at $T_{1/2}\downarrow$=212 K, while the low spin to high spin transition exhibits two pronounced steps at 215 K and 282 K, resulting in thermal hysteresis loops of widths 3 K and 70 K for these successive transitions, respectively. This unusual hysteresis loop involving a two-step spin crossover in the warming mode and a one-step transition in the cooling mode could be simulated theoretically [135]. Solvent removal from $[Fe(qsal)_2]NCSe{\cdot}2DMSO$ leads to a transition with an hysteresis loop of width 76 K ($T_{1/2}\uparrow$=285 K, $T_{1/2}\downarrow$=209 K), which is one of the broadest hysteresis effects reported so far for spin crossover compounds [136]. Structures were determined for low spin [Fe

$(qsal)_2]NCSe{\cdot}MeOH$ (200 K) [135], $[Fe(qsal)_2]NCSe{\cdot}CH_2Cl_2$ (230 K) [135] and $[Fe(qsal)_2]NCSe{\cdot}2DMSO$ (90 K) [136] (Table 3). These revealed intermolecular $\pi$-interactions between quinoline and phenyl rings resulting in a two-dimensional network. It is very likely that the cooperativity operating in these selenocyanate systems arises mainly from this structural feature.

Very interesting Fe(III) spin crossover characteristics have been found for compounds of pap. Solvent-free $[Fe(pap)_2]$(anion) compounds have been investigated: the nitrate and tetraphenylborate materials are high spin, whereas the hexafluorophosphate derivative is low spin [164]. The freshly prepared perchlorate compound exhibits spin crossover behaviour associated with an asymmetric thermal hysteresis loop ($T_{1/2}\uparrow$=262 K and $T_{1/2}\downarrow$=242 K) [164]; however, the transition temperature decreases as the compound ages, and reaches 150 K one week after preparation [165]. The authors do not indicate whether the hysteresis is retained. A further notable feature of this "aged" sample is that high spin Fe(III) ions can be frozen in by rapid quenching to 80 K [165]. The monohydrate, $[Fe(pap)_2]ClO_4{\cdot}H_2O$, exhibits abrupt transitions in the heating ($T_{1/2}\uparrow$=180 K) and cooling mode ($T_{1/2}\downarrow$= 165 K) [137]. $[Fe(pap)_2]PF_6{\cdot}MeOH$ also shows a relatively abrupt transition at $T_{1/2}$=288 K, albeit without thermal hysteresis [138]. X-ray structures could be determined for high spin $[Fe(pap)_2]ClO_4{\cdot}H_2O$ (298 K) [137] and low spin $[Fe(pap)_2]PF_6{\cdot}MeOH$ (90 K) [138] (Table 3). Both compounds crystallise in the space group P-1 and their structures are similar. It is noteworthy that the changes in metal-donor atom bond lengths are larger than normally observed in Fe(III) spin crossover compounds. In addition, the changes in the Fe–N bond lengths are much greater than those for the *cis*-arranged Fe–O bonds. Thus the Fe(III) spin crossover is accompanied by an asymmetric stretching of the Fe-ligand bonds involving a scissor-like opening of the pap ligands. Strong intermolecular $\pi$-stacking occurs between the aromatic rings of pap ligands originating from different $[Fe(pap)_2]^+$ units and resulting in the formation of wrapped sheets. This structural feature appears to be responsible for the high cooperativity as well as the occurrence of Light-Induced Excited Spin State Trapping (LIESST) for this system (see below) [137, 138].

## 3.2
## Complexes of Tetradentate Ligands

### 3.2.1
### General Considerations

Spin crossover behaviour generated by Schiff base ligands predominantly occurs when the Fe(III) ion is coordinated by an $N_4O_2$ donor set. This donor set is also found with $N_2O_2$-donating tetradentate Schiff base systems together with two appropriate N-donating heterocyclic bases as co-ligands. In ad-

dition, the N-donating nitrosyl anion may also be incorporated as co-ligand, in this instance resulting in $FeN_3O_2$ spin crossover entities. Interestingly, the use of $N_4$-donating ligands has also lead to the generation of spin transition materials, in this case comprising $FeN_4Br_2$, $FeN_5$ or $FeN_4X$ (X=$Cl^-$, $Br^-$) moieties. These various systems are considered below.

### 3.2.2 Complexes of Tetradentate $N_4$-Donating Ligands

Spin crossover in iron(III) has been generated using the $N_4$-donating macrocyclic ligands 1,4,8,11-tetraazacyclotetradecane (cyclam) and its tetramethylated derivative (tmcyclam), as well as with the Schiff base system $H_2$amben (Fig. 13).

A series of mononuclear Fe(III) cyclam compounds has been reported in which monodentate, monovalent anionic groups occupy the axial positions [166]. The cyclam system acts as a neutral ligand and thus an additional non-coordinating anion is required for charge compensation. Both the magnetism and EPR spectra indicate that $[Fe(cyclam)Cl_2](ClO_4)$ and $[Fe(cyclam)(NCS)_2](NCS)$ are purely low spin compounds, but a transition is observed in $[Fe(cyclam)Br_2](ClO_4)$ for which two sets of EPR signals are observed with relative intensities that are temperature dependent [166].

Using tmcyclam a five-coordinate compound has been obtained [167]. The X-ray structure of $[Fe(tmcyclam)(NO)](BF_4)_2$ has been determined at room temperature, revealing an Fe(III) ion in a distorted tetragonal pyramid consisting of the four nitrogen atoms of the macrocycle (average Fe–N=2.165 Å) together with a nitrosyl anion in the apical position. The Fe–N–O bond angle is essentially linear (177.5(5) °) with Fe–NO and FeN–O interatomic distances of 1.737(6) and 1.137(6) Å, respectively. The axially oriented *N*-methyl groups are all on the same side of the Fe(tmcyclam) moiety as the nitrosyl group. The magnetic moment is 2.66 B.M. at 4.2 K, but gradually increases with increasing temperature, levelling off at about 150 K and remaining virtually constant at 3.62 B.M. to 286 K, characteristic for an S=1/2↔S=3/2 transition, which has also been supported by EPR and $^{57}Fe$ Mössbauer spectral studies. In addition, the change in the appearance of the NO

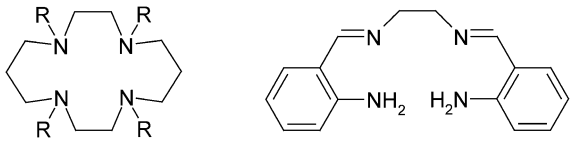


cyclam : R = H
tmcyclam : R = $CH_3$

$H_2$amben

**Fig. 13** Tetradentate $N_4$-donating ligands

stretching vibration in the IR spectra with decreasing temperature is consistent with electrons pairing up in a lower lying molecular orbital that contains a contribution from the $\pi^*$ orbitals of the nitrosyl entity [167]. Related five-coordinate $FeN_3O_2$ spin crossover systems involving the nitrosyl anion and *N,N′*-ethylenebis(salicylideneiminate) have also been described (see below).

Five-coordinate $FeN_4X$ (X=$Cl^-$, $Br^-$) spin transition entities have been obtained using $H_2$amben (Fig. 13) [168]. The magnetic moments of [Fe(amben)Cl] and [Fe(amben)Br]·$H_2O$ are similar (3.85 and 3.62 B.M., respectively at 295 K) and only slightly temperature dependent. However, the occurrence of spin crossover in these compounds has been confirmed by variable temperature $^{57}$Fe Mössbauer spectroscopy, as well as by EPR spectroscopy carried out at 77 K. The $^{57}$Fe Mössbauer spectra recorded at 77 and 295 K for the chloro compound reveal two quadrupole doublets indicating the existence of two different spin components at both temperatures and with relative intensities that are temperature dependent. The EPR spectrum recorded for the bromide material in dilute ethanol solution shows a sharp three line pattern characteristic of low spin Fe(III) at g=2.10, 2.05 and 1.93, and a broader band attributed to the high spin component at g=4.9 [168].

### 3.2.3
### Five-Coordinate Complexes of Tetradentate $N_2O_2$-Donating Schiff Base Ligands

The use of appropriate tetradentate $N_2O_2$-donating Schiff base ligands (Fig. 14) together with the incorporation of the N-donating nitrosyl anion has resulted in the formation of a unique series of five-coordinate Fe(III) spin crossover materials containing $FeN_3O_2$ chromophores.

The first and most extensively studied compound of this class is [Fe(salen)(NO)], which exhibits an abrupt S=1/2↔S=3/2 spin transition with associated hysteresis centred at T=175 K and virtually complete over a temperature interval of a few degrees [169–171]. Such features are relatively uncommon for iron(III). In contrast, [Fe(5-Cl-salen)(NO)] is in the S=3/2 state

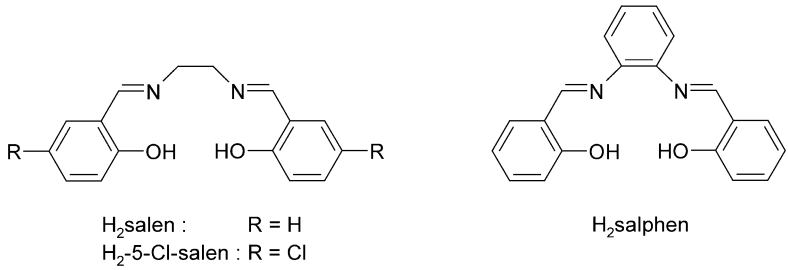


**Fig. 14** Tetradentate $N_2O_2$-donating Schiff base ligands. The use of NO as co-ligand yields $FeN_3O_2$ chromophores

($\mu_{eff}$=3.8 B.M.) at temperatures above 50 K. The magnetic moment decreases at lower temperatures, reaching a value of only 0.5 B.M. at 4.2 K, indicative of antiferromagnetic interactions [169].

The structure of [Fe(salen)(NO)] has been determined at 98 and 296 K [172]. Notwithstanding the abrupt nature of the spin transition and its association with thermal hysteresis, the space group $Pna2_1$ is retained at both temperatures. With decreasing temperature a significant shortening in metal-donor atom bond lengths involving the salen ligand has been observed: the mean Fe–O distance very slightly decreases from 1.908 Å at 296 K to 1.899 Å at 98 K, whereas more substantial changes are detected in the mean Fe–N bond length (2.075 Å at 296 K and 1.974 Å at 98 K). The Fe–N(nitrosyl) distance is 1.783 Å at 296 K, whereas at 98 K, where the NO group is disordered over two sites, an average distance of 1.80 Å was determined. The most important changes occurring with decreasing temperature, i.e. upon the S=3/2→S=1/2 spin crossover are (i) a decrease of almost 0.1 Å in Fe–N(salen) bond lengths, (ii) a smaller displacement of the Fe(III) ion from the salen coordination plane (0.47 Å at 296 K compared to 0.36 Å at 98 K), which is consistent with the smaller volume for the Fe(III) ion in the doublet state, and (iii) a closer approach to coplanarity of the salicylideneiminato moieties of the salen ligand. Interestingly, there are some noteworthy differences with respect to the structure of [Fe(tmcyclam)(NO)]$(BF_4)_2$ (see above) [167]. In the tmcyclam compound the Fe–N–O sequence has been found to be essentially linear, and the coordination geometry about the Fe(III) centre can be regarded as distorted toward a trigonal bipyramid. In contrast, the salen material has a strongly bent Fe–N–O moiety, and the Fe(III) geometry is essentially tetragonal pyramidal at both temperatures [172].

The spin transition in [Fe(salen)(NO)] has been studied by IR [171, 172], $^{57}$Fe Mössbauer [169, 173] and EPR spectroscopy [169]. IR spectra have also been recorded at room temperature for various pressures ranging from ambient up to 37 kbar. At 37 kbar conversion to the S=1/2 state is complete [172]. The quartet state is re-populated on relaxation of the pressure.

A spin transition between the S=1/2 and intermediate S=3/2 spin state has also been observed for [Fe(salphen)(NO)], albeit the spin crossover is gradual in this instance [174, 175]. This material shows $^{57}$Fe Mössbauer parameters comparable to those of the salen derivative. However, the relaxation between the spin states is fast relative to the $^{57}$Fe Mössbauer time scale for the salphen compound, whereas it is slow for the salen compound [175]. Interestingly, the quadrupole splittings obtained from the $^{57}$Fe Mössbauer spectra of [Fe(salphen)(NO)] have been found to decrease linearly with the magnetic susceptibility determined with increasing temperature [175].

### 3.2.4
### Six-Coordinate Complexes of Tetradentate $N_2O_2$-Donating Schiff Base Ligands

Three main families of $N_2O_2$-donating Schiff base ligands have been used to obtain six-coordinate systems: (i) *N,N′*-ethylenebis(salicylideneimine) and its substituted derivatives, (ii) *N,N′*-ethylenebis(acetylacetonylideneimine)-type systems and (iii) ligand systems consisting of a salicylideneimine and an acetylacetonylideneimine moiety (Fig. 15). N-donating heterocyclic bases in axial positions complete the $FeN_4O_2$ coordination environment.

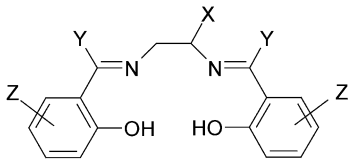


$H_2$salen : X = Y = Z = H
$H_2$dmsalen : X = Z = H, Y = $CH_3$
$H_2$-5-$OCH_3$-salen : X = Y = H, Z = 5-$OCH_3$
$H_2$-3-$OCH_3$-salen : X = Y = H, Z = 3-$OCH_3$
$H_2$-3-$OC_2H_5$-salen : X = Y = H, Z = 3-$OC_2H_5$
$H_2$-3-$OCH_3$-salpen : X = $CH_3$, Y = H, Z = 3-$OCH_3$

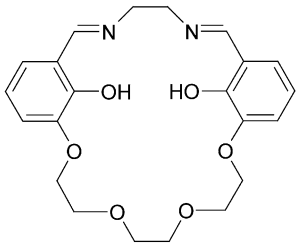


$H_2$cr-salen

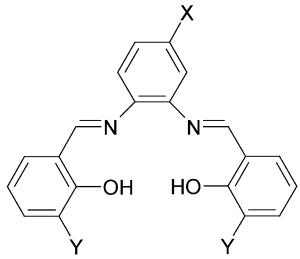


$H_2$salphen : X = Y = H
$H_2$-3-$OC_2H_5$-sal-$CH_3$-phen : X =$CH_3$, Y = $OC_2H_5$

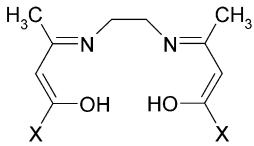


$H_2$acen : X = $CH_3$
$H_2$bzacen : X = $C_6H_5$

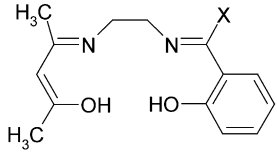


$H_2$salacen : X = H
$H_2$hapacen : X = $CH_3$

**Fig. 15** Tetradentate $N_2O_2$-donating Schiff base ligands

The [Fe(salen)(base)$_2$](anion) systems have been most extensively studied and several X-ray structures have been determined. Table 4 compiles the Fe-donor atom bond lengths, as well as the spin state for these materials. [Fe(salen)(Him)$_2$]$ClO_4$ (Him=imidazole) is the only compound within this series for which the structure has been determined in both the low spin (120 K) and high spin states (295 K) [176, 177]. It appears that the average Fe–O bond distances are rather insensitive to the spin state of the Fe(III) ion (1.903 Å at 120 K and 1.901 Å at 295 K), whereas the mean Fe–N(salen) (1.913 Å at 120 K and 2.067 Å at 295 K) and Fe–N(Him) (1.992 Å at 120 K and 2.146 Å at 295 K) bond distances show a major dependence on the spin state [176, 177]. On the basis of bonding orbital considerations Nishida et al. have rationalised the different sensitivities of these bond lengths to changes in the spin state of the metal atom [178].

The compounds [Fe(salen)(Him)$_2$]$ClO_4$·$H_2O$ [178], [Fe(salen)(Him)$_2$]X (X=$PF_6^-$ [176], $BPh_4^-$ [176, 185]), [Fe(salen)(4-methyl-imidazole)$_2$]Cl [179], [Fe(salen)(base)$_2$]$ClO_4$ (base=*N*-methyl-imidazole [176], 5-Cl-*N*-methyl-imidazole [176]) and [Fe(salen)(pyrazole)$_2$]$BPh_4$·MeOH [176] are purely high spin, whereas Na[Fe(salen)(CN)$_2$]·$CH_3OH$ is purely low spin [185]. On the other hand, [Fe(salen)(Him)$_2$]X (X=$ClO_4^-$, $BF_4^-$) and [Fe(salen)(pyrazole)$_2$]X·$H_2O$ (X=$ClO_4^-$, $BF_4^-$) exhibit gradual spin transitions [176]. Both the magnetism and the $^{57}$Fe Mössbauer spectra indicate that unsolvated [Fe(salen)(Him)$_2$]$ClO_4$ undergoes an almost complete transition between 90 K and 295 K [176], whereas the transitions for [Fe(salen)(Him)$_2$]$BF_4$ and [Fe(salen)(pyrazole)$_2$]X·$H_2O$ (X=$ClO_4^-$, $BF_4^-$) proceed to varying extents over the temperature range 80 K to 295 K [176]. Interestingly, although there are differences in solvation of the materials, the spin crossover behaviour within both the imidazole and pyrazole series reveals a similar anion dependence [176]. In contrast, there does not appear to be a clear dependence of the spin state of Fe(III) on the selected N-donating heterocyclic base: neither their basicity nor position in the spectrochemical series is followed. This suggests that the spin state of Fe(III) in this series depends on the structural features of the particular material.

Comparison of the structures of [Fe(salen)(Him)$_2$]X (X=$ClO_4^-$, $BF_4^-$, $PF_6^-$) revealed subtle structural differences, such as (i) the orientation of the imidazole ligands, (ii) equatorial ligand-imidazole C-H interactions, and (iii) conformations of the $FeN_2C_2$ chelate ring involving the ethylene backbone of salen. It has been proposed that these three parameters contribute to the spin state differences [176]. In particular, the $FeN_2C_2$ conformation has been thought to be substantially related to the spin state of Fe(III). The *envelope* conformation of this entity has been found in the spin crossover perchlorate and tetrafluoroborate salts, whereas it is in the *meso* configuration in the high spin hexafluorophosphate salt. It has been suggested that this *meso* configuration results in constraints of the planar ligand to the extent that it may not be able to adapt to incipient spin state change, i.e. the

**Table 4** Average Fe-donor atom bond lengths for Fe(III) compounds of tetradentate $N_2O_2$-donating Schiff base ligands[a,b]

| Compound | T (K) | Fe–O | Fe–N | Fe–$N_{base}$ (Å) | Spin state[c] | References |
|---|---|---|---|---|---|---|
| $[Fe(salen)(Him)_2]ClO_4$ | 120 | 1.903 | 1.913 | 1.992 | LS (sco) | [176, 177] |
| | 295 | 1.901 | 2.067 | 2.146 | HS (sco) | [176, 177] |
| $[Fe(salen)(Him)_2]BF_4$ | 295 | 1.902 | 2.072 | 2.123 | HS (sco) | [176] |
| $[Fe(salen)(Him)_2]PF_6$ | 295 | 1.904 | 2.136 | 2.153 | HS | [176] |
| $[Fe(salen)(Him)_2]ClO_4 \cdot H_2O$ | 295 | 1.917 | 2.108 | 2.143 | HS | [178] |
| $[Fe(salen)(4\text{-}mim)_2]Cl$[d] | 293 | 1.909 (3) | 2.111 (3) | 2.159 (3) | HS | [179] |
| $[Fe(salen)(tdim)]ClO_4$[e] | 295 | 1.896 | 2.120 | 2.157 | HS (sco) | [180] |
| $[Fe(5\text{-}OCH_3\text{-}salen)(Him)_2]ClO_4$ | 295 | 1.896 | 2.113 | 2.18 | HS | [181] |
| $[Fe(5\text{-}OCH_3\text{-}salen)(Him)_2]Cl$ | 295 | 1.914 | 2.134 | 2.122 | HS | [181] |
| $[Fe(3\text{-}OCH_3\text{-}sapen)(Him)_2]ClO_4$ | 293 | 1.919 | 2.090 | 2.123 | HS (sco) | [182] |
| $[Fe(salphen)(Him)_2]BPh_4$ | 295 | 1.896 | 2.125 | 2.165 | HS | [178] |
| $[Fe(3\text{-}OC_2H_5\text{-}sal\text{-}CH_3\text{-}phen)(Him)_2]ClO_4$ | 293 | 1.899 | 2.105 | 2.148 | HS | [182] |
| $[Fe(acen)(Him)_2]BPh_4$ | 295 | 1.920 | 1.899 | 1.990 | LS | [178] |
| $[Fe(acen)(dmpy)_2]BPh_4$ | 120 | 1.906 | 1.918 | 2.036 | LS (sco) | [183] |
| | 290 | 1.930 | 2.058 | 2.186 | HS (sco) | [183] |
| $[Fe(salacen)(Him)_2]PF_6$ | 293 | 1.895 | 1.924 | 2.017 | 83% LS | [184] |

[a] The ligands are shown in Fig. 15. Abbreviations used for the ligands can be found in the list of abbreviations

[b] Abbreviations used for the monodentate N-donating heterocyclic bases: Him=H-imidazole, 4-min=4-methylimidazole, tdim=1,1′-tetramethylenediimidazole, dmpy=3,4-dimethylpyridine

[c] Spin state (predominant spin state or exact percentage) at the temperature of the crystal structure determination is mentioned. In case spin crossover (sco) occurs, this is mentioned in parentheses

[d] Centrosymmetric

[e] Zigzag chain

complex remains locked in the high spin form [176]. The geometry of the salen ligand was later compared to the environment created by the heme system in metalloproteins; both ligand systems are conformationally flexible and may adopt an overall *stepped*, *umbrella* or *planar* conformation [181]. Analysis of structural data for a large variety of Fe(III) compounds of $N_2O_2$-donating Schiff base ligands—involving most of the materials listed in Table 4—leads to the assumption that the molecule is fixed in a high spin-type *umbrella* or *planar* geometry due to crystal packing effects or intermolecular interactions. It is significant that some of the materials that have been found to be purely high spin in the solid state exhibit spin crossover in solution (see below) where the conformational restraints are relaxed [181]. Another analogy with related porphyrin systems has been considered [178] based on findings that the relative orientation of the imidazole rings is the controlling factor for the spin state of those systems [186]. It is proposed that the relative orientations of the imidazole rings control the metal-to-imidazole $\pi$-back-bonding and consequently the efficiency of stabilisation of the low spin state of Fe(III). Efficient d$\pi$-p$\pi$ overlap—and stabilisation of the low spin state of Fe(III)—is achieved when the two planes defined by the imidazole rings are orthogonal and oriented along the two approximately diagonal N–Fe–O axes of the equatorial coordination frame [182]. However, since other small structural changes—for instance the other parameters mentioned above—may be involved, a dependence of the dihedral angles between the axially coordinated imidazole groups on the spin state could only be established in one comparative study [182].

Spin transitions have also been observed for derivatives of substituted salen-type ligands. $[Fe(dmsalen)(Him)_2]BPh_4 \cdot 2CH_3OH$, in which salen is substituted at the methane C atoms, undergoes a gradual and incomplete transition (experimental range 78–298 K) [187]. The effect of substitution at the 3- or 5-positions of the salicylidene moiety has been more widely investigated. The structures of the purely high spin (in the solid state) $[Fe(5\text{-}OCH_3\text{-salen})(Him)_2]X$ ($X=ClO_4^-$, $Cl^-$) have been determined at 295 K [181]. For both compounds, the five-membered $FeN_2C_2$ ring of the ligand has the *meso* conformation, which further confirms the relation of this constrained form to the high spin state of the Fe(III) ion. However, spin crossover of these compounds in methanolic solutions has been observed by variable temperature EPR spectroscopy [181]. $[Fe(3\text{-}CH_3O\text{-salen})(N\text{-methyl-imidazole})_2]X$ ($X=ClO_4^-$, $BPh_4^-$) and $[Fe(3\text{-}CH_3O\text{-salen})(5\text{-Cl-}N\text{-methyl-imidazole})_2]ClO_4$ are also purely high spin materials in the solid state [176], whereas $[Fe(3\text{-}CH_3O\text{-salen})(Him)_2]BPh_4$ displays gradual spin crossover behaviour [176, 185]. The gradual spin transition in the latter complex involves only half of the Fe(III) ions [176, 185, 188].

While $[Fe(3\text{-}OCH_3\text{-salpen})(Him)_2]BPh_4 \cdot H_2O$ is purely high spin in the solid state, the analogous anhydrous perchlorate salt, which was structurally characterised at 293 K, undergoes gradual spin crossover with $T_{1/2}$=91 K

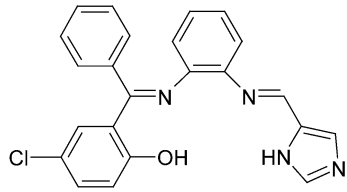


**Fig. 16** 5-*o*-[(5-Chloro-2-hydroxyphenyl)phenylmethyleneamino]phenyliminomethylimidazole

[182]. From an analysis of the magnetic properties according to the model of Slichter and Drickamer the thermodynamic parameters for the spin transition of [Fe(3-$OCH_3$-salpen)$(Him)_2]ClO_4$ were evaluated as $\Delta H$=5.46 kJ $mol^{-1}$ and $\Delta S$=60 J $mol^{-1}$ $K^{-1}$ [182]. These values are close to those found for other iron(III) systems.

The synthesis of dinuclear [189] and linear chain [180] materials based on $[Fe(salen)]^+$ entities has been reported. The structure of dinuclear $[Fe_2(salen)_2$(*trans*-4,4′-vinylenebis(pyridine))$(H_2O)_2](ClO_4)_2\cdot$(*trans*-4,4′-vinylenebis(pyridine))$\cdot H_2O$ has been reported but this compound is purely high spin [189]. On the other hand, [Fe(salen)(1,1′-tetramethylenediimidazole)]$ClO_4$ shows incomplete spin crossover, principally in the temperature range 70–100 K. It is suggested that the large residual high spin fraction (~0.7) may be related to the presence of two different orientations of the imidazole moieties with occupation factors 0.65 and 0.35. The complex has a zigzag chain structure (Table 4) [180].

Two strategies have been applied in order to obtain hetero-dinuclear compounds. In the first example, the incorporation of a spin-inactive cation to modulate the Fe(III) spin crossover has been attempted, exploiting the cyclic ligand cr-salen (Fig. 15) which contains a salen-type $N_2O_2$ cavity together with a polyether cavity [190]. However, both [Fe(cr-salen)(pyridine)$_2$]$ClO_4$ and [BaFe(cr-salen)(pyridine)$_2$]$(ClO_4)_3$ are purely high spin.

In addition, heterodinuclear Fe(III)Ni(II) compounds have been prepared starting from high spin [FeCl(salen)] and NiL with L being the di-anion of the $N_3O$ ligand depicted in Fig. 16 [191]. The imidazole-bridged [FeCl(salen)NiL] [191] and also [FeCl(5-$OCH_3$-salen)NiL] both exhibit Fe(III) spin crossover [192].

The purely high spin nature of [Fe(salphen)$(Him)_2]BPh_4$ [178, 185] and [Fe(3-$OC_2H_5$-sal-$CH_3$-phen)$(Him)_2]ClO_4$ [182] has been confirmed by magnetic measurements and structure determinations. On the other hand, [Fe(acen)$(Him)_2]BPh_4$ [185] is low spin while [Fe(acen)(3,4-dimethylpyridine)$_2$]$BPh_4$ [193] exhibits gradual spin crossover. The structure of the former low spin complex [178] as well as that of the latter in both high spin and low spin states [183] has been determined.

A large variety of heterocyclic bases and anionic groups have been incorporated within the $[Fe(acen)]^+$ system. $[Fe(acen)(Him)_2]BPh_4$ [185] and $[Fe(acen)(4\text{-aminopyridine})_2]ClO_4$ [185] are low spin, as is the one-dimensional polynuclear $[Fe(acen)(1,1'\text{-tetramethylenediimidazole})]ClO_4$ [180]. Different degrees of gradual spin crossover behaviour have been observed for several members of this family: $[Fe(acen)(\beta\text{-picoline})_2]ClO_4$ ($\mu_{eff}$= 2.51 B.M. (295 K), $\mu_{eff}$=1.93 B.M. (80 K)) [185], $[Fe(acen)(pyridine)_2]BPh_4$ ($\mu_{eff}$=3.31 B.M. (295 K), $\mu_{eff}$=2.30 B.M. (80 K)) [185], $[Fe(acen)(\gamma\text{-picoline})_2]BPh_4$ ($\mu_{eff}$=3.64 B.M. (295 K), $\mu_{eff}$=2.04 B.M. (80 K)) [185], whereas $[Fe(acen)(base)_2]BPh_4$ (base=*N*-methyl-imidazole [176], 1,3-di-4-pyridylpropane [193], 4-methylpyridine [193], 3,4-dimethylpyridine [193]) exhibit fairly complete, gradual spin transitions.

Derivatives of bzacen have been studied to a minor extent: $[Fe(bzacen)(N\text{-methyl-imidazole})_2]ClO_4$ [176] and $[Fe(bzacen)(Him)(CN)]$ [185] are purely low spin, whereas $[Fe(bzacen)(Him)_2]BPh_4$ shows gradual spin crossover [185].

The di-anionic ligands derived from $H_2$salacen and $H_2$hapacen (Fig. 15) may be considered as providing a field strength intermediate between that of salen and acen. The structure of $[Fe(salacen)(Him)_2]PF_6$ has been determined at 293 K, where 83% of the Fe(III) ions are low spin [184]. Both the Fe–O (1.879(6) Å) and the Fe–N (1.912(7) Å) bond distances associated with the salicylideneimine residue are shorter than those associated with the acetylacetonylideneimine residue (1.911(5) Å and 1.936(6) Å, respectively) [184]. $[Fe(salacen)(Him)_2]PF_6$ shows the onset of gradual spin crossover at about 200 K, reaching a magnetic moment of 2.83 B.M. at room temperature. In contrast, the *N*-methyl-imidazole derivative is high spin at room temperature but a gradual transition to the low spin state takes place between 300 and 200 K [184]. Both compounds exhibit striking thermochromism in organic solvents, being purple at room temperature and green at ca. 200 K. The absorption spectrum of $[Fe(salacen)(Him)_2]PF_6$ recorded at 289 K shows a strong band at 525 nm assigned to the high spin state, together with a shoulder at 680 nm attributed to the low spin state. From a study of the temperature dependence of the spectrum it was concluded that the transition occurs to a greater extent in solution than in the solid state [184]. Although EPR data indicate that $[Fe(salacen)(Him)_2]BPh_4{\cdot}CH_3OH$ and $[Fe(hapacen)(Him)_2]BPh_4{\cdot}2CH_3OH$ are essentially low spin in the solid state they exhibit thermochromism similar to that described above and indicative of spin crossover in solution [187].

Solid $[Fe(salacen)(1\text{-methyl-imidazole})_2]ClO_4$ displays a relatively complete, gradual spin crossover [180]. Measurements of both $^{57}$Fe Mössbauer spectra and magnetism indicate that the transition observed in the one-dimensional polymeric system $[Fe(salacen)(1,1'\text{-tetramethylenediimidazole})]ClO_4$ is also gradual but incomplete at both 290 K ($\mu_{eff}$=5.37 B.M.) and 4.2 K ($\mu_{eff}$=3.37 B.M.) [180].

### 3.3
### Complexes of Pentadentate $N_3O_2$-Donating Ligands

In the only instances where spin crossover has been observed for a system involving a pentadentate ligand this has been an $N_3O_2$-donating Schiff base and the sixth coordination site has been occupied by a nitrogen donor, giving rise to an $FeN_4O_2$ coordination core. Most examples involve salten (Fig. 17).

When the sixth coordination site is occupied by an anionic group the derivatives are either purely low spin ([Fe(salten)CN]·1.5$CH_3OH$) or purely high spin ([Fe(salten)Cl]·$CH_3OH$ and [Fe(salten)$N_3$]·0.5$H_2O$) [194]. It was soon discovered that upon using heterocyclic bases as co-ligand solvent-free spin crossover compounds could be prepared [194]. The mononuclear compounds [Fe(salten)(base)]$BPh_4$ (base=pyridine, 3-methyl-pyridine, 4-methyl-pyridine, 3,4-dimethyl-pyridine, 2-methyl-imidazole) exhibit spin crossover behaviour [194, 195], whereas derivatives with base=imidazole and *N*-methyl-imidazole are purely high spin [194]. The spin transitions are gradual, and are accompanied by thermochromism both in (dichloromethane) solution and in the solid state, changing from dark violet to blue-green with decreasing temperature.

The spin state of Fe(III) in this series depends directly on the ligand field strength exerted by the co-ligand X, as given by the spectrochemical series: $CN^-$>pyridine or imidazole derivative >$N_3^-$>$Cl^-$ [194].

The structure of [Fe(salten)(4-methyl-pyridine)]$BPh_4$ has been determined at 293 K [194]. The Fe(III) ion is in a pseudo-octahedral environment in which the basal plane is formed by two salicylideneiminate entities (average Fe–O=1.885 Å, Fe–N=1.987 Å) oriented in *trans* geometry. The two axial positions are occupied by the secondary amine nitrogen atom of the di(3-aminopropyl) moiety of the ligand (Fe–N=2.035(7) Å) and the nitrogen

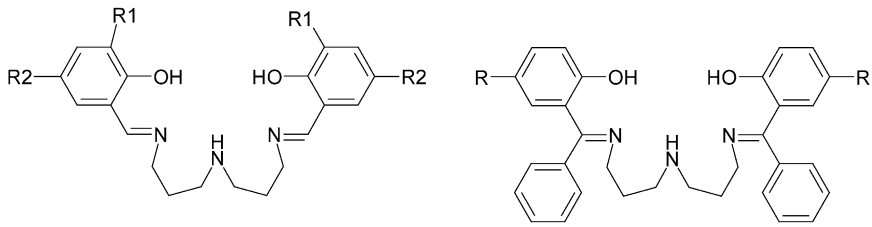


$H_2$salten : R1 = R2 = H
3-OMe-$H_2$salten : R1 = OMe, R2 = H
5-OMe-$H_2$salten : R1 = H, R2 = OMe
5-Cl-$H_2$salten : R1 = H, R2 = Cl

$H_2$bpN : R = H
$H_2$mbpN : R = $CH_3$

**Fig. 17** Pentadentate $N_3O_2$-donating Schiff base ligands

atom of 4-methyl-pyridine (Fe–N=2.010(6) Å). The bond lengths observed are consistent with the magnetic data showing about 26% of high spin Fe(III) ions at 293 K.

More recently, [Fe(salten)(base)]$BPh_4$ compounds containing a potentially photo-isomerisable ligand have been reported [196, 197]. [Fe(salten)(1-(pyridin-4-yl)-2-(*N*-methylpyrrol-2-yl)-ethene)]$BPh_4$ having the nitrogenous base in the *trans* conformation exhibits a gradual Fe(III) spin crossover taking place between 150 and 320 K [196]. In addition, spin transition compounds of both isomers of 4-styrylpyridine could be obtained [197]. The transitions are gradual for [Fe(salten)(*trans*-4-styrylpyridine)]$BPh_4 \cdot (CH_3)_2CO \cdot 0.5H_2O$ and [Fe(salten)(*cis*-4-styrylpyridine)]$BPh_4$; however, the transition temperature for the *trans* derivative is 260 K, whereas it is almost 100 K higher for the *cis* compound. These features open interesting perspectives for testing the possibility of ligand-driven light-induced spin conversion (LD-LISC) for these materials (see below). This topic is treated in detail in Chap. 20. Confirmation of the conformation of the co-ligand has been obtained from crystal structures determined for both materials at 296 K [197].

The use of *N*-(4-picolyl)-aza-15-crown-5-ether as co-ligand enabled the encapsulation of alkali metal ions and the study of their effect on the Fe(III) spin transition within the series [Fe(salten)(base)M]$ClO_4$ (base=*N*-(4-picolyl)-aza-15-crown-5-ether; M=$Li^+$, $Na^+$, $K^+$, $Rb^+$) [198]. The magnetic moments determined for the non-alkali metal-containing [Fe(salten)(base)]$ClO_4$ in the solid state are 4.20 B.M. at 80 K and 4.85 B.M. at 300 K. Incorporation of the monovalent cations resulted in significant changes in the magnetic moment for the lithium derivative (2.29 B.M. at 80 K and 4.00 B.M. at 300 K), whereas only moderate changes were observed for sodium (4.21 B.M. at 80 K and 5.03 B.M. at 300 K), potassium (4.78 B.M. at 80 K and 5.82 B.M. at 300 K) and rubidium (4.52 B.M. at 80 K and 5.68 B.M. at 300 K). Since these compounds are thermochromic, the spin crossover could be monitored by recording the electronic spectra in acetonitrile solutions. Attempts at triggering the spin crossover in [Fe(salten)(base)]$ClO_4$ (base=*N*-(4-picolyl)-aza-15-crown-5-ether) in solution by ion-recognition have met with some success. On the addition of sodium perchlorate to a solution of the complex salt a change in the absorption spectrum was observed, suggesting that the high spin to low spin transition may be induced by the encapsulation of $Na^+$ ions [198].

Attaching the rather bulky methoxy substituent at the 3-position of the salicylaldehyde ring of salten does not appear to preclude formation of Fe(III) spin crossover materials. Using 3-OMe-salten yielded [Fe(3-OMe-salten)(pyridine)]$BPh_4$, which also displays spin crossover both in solution and in the solid state [199, 200]. On the other hand, the 5-Cl substituted salten derivative turns out to be a high spin compound [200].

Dinuclear materials of formula [(salten)Fe(base)Fe(salten)]$(BPh_4)_2$ have been obtained from *N,N′*-bridging heterocyclic ligands. The pyrazine deriva-

tive is low spin, but compounds containing 1,1′-tetramethylenebis(imidazole), 4,4′-bipyridine, 4,4′-ethylenebis(pyridine) or 4,4′-vinylenebis(pyridine) exhibit gradual and incomplete (at 300 K) transitions [201]. These materials are the first reported dinuclear Fe(III) spin crossover compounds. For [(salten)Fe(base)Fe(salten)]$(BPh_4)_2$ (base=azobis(4-pyridine), 4,4′-vinylenebis (pyridine)) in which the bridging system is potentially photo-isomerisable a gradual spin crossover characterised by $\mu_{eff}$=ca. 2.2 B.M. at 200 K and $\mu_{eff}$=4.3 B.M. at 350 K was observed for both systems [202]. The dinuclear nature of these complexes, in which both bridging moieties adopt the *trans* configuration, was confirmed by X-ray structure determinations carried out at 100 and 298 K [189, 203]. Magnetic measurements on single crystals under an external pressure of 8 kbar have revealed a suppression of the spin crossover: under these conditions both compounds are low spin at 350 K [203].

Dinuclear Fe(III) compounds were also obtained using substituted salten derivatives together with 4,4′-bipyridine as bridging ligand [200]. The 3-OMe-salten tetraphenylborate compound seems to show the onset of spin crossover at about 270 K, the 5-OMe-salten material is probably a purely high spin compound, whereas the 5-Cl-salten derivative exhibits gradual spin crossover behaviour.

Heterodinuclear Fe(III)Ni(II) imidazole-bridged compounds have been prepared starting from $[Fe(salten)]^+$ and NiL with L being the $N_3O$ ligand shown in Fig. 16 [191]. Gradual and incomplete spin crossover occurs in the range 80–295 K for [Fe(salten)NiL]$BPh_4$. For the analogous complex containing a methyl group at the central nitrogen atom of the ligand a spin transition was also observed but only below 120 K [191].

The related ligands $H_2$bpN [205] and its 5-methyl-substituted derivative $H_2$mbpN (Fig. 17) [204, 205] have also been investigated. [Fe(bpN)(pyridine)]$BPh_4$ shows gradual and partial spin crossover between 78 and 300 K [205]. [Fe(mbpN)(imidazole)]$BPh_4$ is high spin ($\mu_{eff}$=5.85 B.M. at 298 K), whereas [Fe(mbpN)(3,4-dimethylpyridine)]$BPh_4$ exhibits a gradual spin transition ($\mu_{eff}$=2.64 B.M. at 78 K and 5.40 B.M. at 320 K) [205]. The structure of the latter material determined at 293 K confirmed that it is essentially high spin at this temperature [204].

## 3.4 Complexes of Hexadentate $N_4O_2$-Donating Ligands

### 3.4.1 General Considerations

The $N_4O_2$ ligand systems depicted in Fig. 18 have been shown to generate spin crossover in Fe(III). Two families of Schiff base ligands have been obtained from the 1:2 condensation of triethylenetetramine with derivatives of

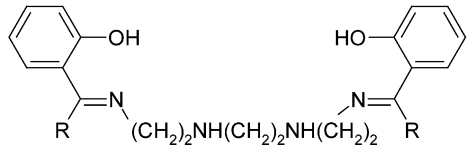


$H_2sal_2trien$ : R = H
$H_2bpk_2trien$ : R = $C_6H_5$

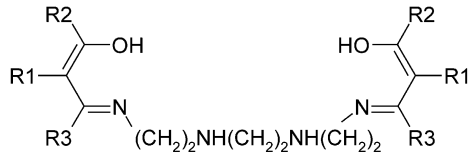


$H_2acac_2trien$ : R1 = H, R2 = R3 = $CH_3$
$H_2acacCl_2trien$ : R1 = Cl, R2 = R3 = $CH_3$
$H_2bzac_2trien$ : R1 = H, R2 = $C_6H_5$, R3 = $CH_3$
$H_2bzacCl_2trien$ : R1 = Cl, R2 = $C_6H_5$, R3 = $CH_3$
$H_2tfac_2trien$ : R1 = H, R2 = $CF_3$, R3 = $CH_3$

**Fig. 18** Hexadentate $N_4O_2$-donating Schiff base ligands

either salicylaldehyde or $\beta$-diketones. In addition, variation of the tetramine has been systematically explored within the salicylaldehyde series [206].

Several common structural features have been observed for iron(III) compounds of di-anionic hexadentate ligands containing a triethylenetetramine (abbreviated as trien) moiety. The stereochemical requirements of these ligands are such that hexadentate coordination towards the Fe(III) ion involves the formation of two six-membered chelate rings using the adjacent outer O and imine N donor atoms, together with three five-membered chelate rings containing the imine and amine N donor atoms of the central ligand moiety. X-ray structures have been determined for several compounds of this type, which revealed an identical general structure with the Fe(III) ion in a distorted octahedral $N_4O_2$ environment [206–209]. In each case the terminal oxygen atoms occupy *cis* positions and the remaining four nitrogen atoms (two *cis* amine and two *trans* imine) complete the coordination sphere.

### 3.4.2 Hexadentate $N_4O_2$-Donating Ligands Derived from Salicylaldehyde Derivatives and Triethylenetetramine

Within the [Fe($sal_2$trien)](anion)·x(solvent) family the magnetic moments determined at room temperature are anion and solvation dependent, span-

ning the range from essentially high spin Fe(III) ($\mu_{eff}$=5.81 B.M.) for anhydrous [Fe(sal$_2$trien)]PF$_6$ to low spin Fe(III) ($\mu_{eff}$=1.94 B.M.) for [Fe(sal$_2$trien)]Cl·2H$_2$O [149]. It seems that the greater the extent of hydration the larger the population of the low spin state at room temperature. This may be illustrated by the following range of magnetic moments: 5.00 B.M for the anhydrous PF$_6^-$ and BPh$_4^-$ salts, about 2.4 B.M. for the mono- and 1.5 hydrated I$^-$ and NO$_3^-$ salts, respectively, and 1.94 B.M. for the dihydrated Cl$^-$ salt [149].

X-Ray structures have been reported for the purely low spin compounds [Fe(sal$_2$trien)]Cl·2H$_2$O [207], [Fe(sal$_2$trien)]NO$_3$·H$_2$O [207] and [Fe(sal$_2$trien)]Br·2H$_2$O [208], as well as for the predominantly high spin material [Fe(sal$_2$trien)]PF$_6$ [208] at room temperature. In addition, structures have been determined for [Fe(sal$_2$trien)]BPh$_4$ [208] and [Fe(sal$_2$trien)]BPh$_4$·acetone [209] at room temperature where significant fractions of both spin states are present. As expected, the average metal-donor atom distances observed for the low spin complexes are shorter by about 0.12–0.13 Å relative to those determined for the (predominantly) high spin materials. However, this difference is not uniform: the Fe–N bonds vary more ($\Delta$r(Fe–N(amine))=$\Delta$r(Fe–N(imine))=0.17 Å) than the Fe–O bonds ($\Delta$r(Fe–O)=0.04 Å). In addition, the 12 angles subtended at the metal ion by adjacent donor atoms lie in the range 75–105° in the predominantly high spin materials, whereas these are closer to regular octahedral values (84–95°) in the low spin forms [208].

The role of the lattice water molecules in stabilising the low spin state for the Fe(III) ion could be clarified by analysis of the structures of the isomorphous low spin [Fe(sal$_2$trien)]X·2H$_2$O (X=Cl$^-$ [207], Br$^-$ [208]) compounds. In these materials, the halogen anion is hydrogen bonded to the two water molecules, one of which is in turn hydrogen bonded to an amine donor atom. This hydrogen bonding network in the solid state is consistent with solution state studies on Fe(III) sal$_2$trien materials (see below) where strong [N–H...solvent] interactions were shown to favour the low spin state. The hydrogen bonding links the anions and cations in a polymeric chain. A similar hydrogen bonding scheme also exists in the low spin compound [Fe(sal$_2$trien)]NO$_3$·H$_2$O [207].

[Fe(sal$_2$trien)]PF$_6$ and [Fe(sal$_2$trien)]BPh$_4$ exhibit gradual spin crossover behaviour, that for the latter being the more gradual and shifted to higher temperature [149, 207, 208]. The structure of [Fe(sal$_2$trien)]BPh$_4$ determined at 293 K shows that the compound is essentially in the high spin state [208]. Interestingly, the asymmetric unit of [Fe(sal$_2$trien)]PF$_6$ (293 K) contains two crystallographically independent and predominantly high spin Fe(III) ions, for which the bond lengths and angles involving the ligand donor atoms differ slightly [208]. The authors have ascribed the unusual variation of the magnetic moment with temperature to the occurrence of two separate and gradual transitions, one occurring at one of these Fe(III) sites between 200

and 100 K, and the other at the second Fe(III) site below 100 K. This hypothesis has not been confirmed by other experimental techniques, however, and it may be more likely that the slight decrease in magnetic moment starting at about 50 K with decreasing temperature is due to zero-field splitting associated with the remaining high spin Fe(III) ions.

Crystals of [Fe(sal$_2$trien)]BPh$_4$·acetone could be obtained in two crystalline forms, i.e. monoclinic and twinned crystals [209]. Both forms have distinctly different X-ray powder patterns. The twinned crystals contain high spin Fe(III) over the temperature range 78–320 K, whereas the monoclinic form exhibits gradual spin crossover. The average Fe–donor atom bond lengths determined for a monoclinic crystal at 290 K (Fe–O=1.875 Å, Fe–N(imine)=1.988 Å, Fe–N(amine)=2.069 Å) are in good agreement with the extent to which the spin transition has proceeded at this temperature (40% high spin). The difference between these two modifications also becomes evident from the EPR spectral data, recorded for the monoclinic compound with decreasing temperature, which show that the low spin signals ($g_1$=2.20, $g_2$=2.194, $g_3$=1.944) increase in intensity at the expense of the high spin signals (g=4 and g=2). These high spin and low spin EPR signals are typical for ferric centres of this type. For the twinned crystals broad signals at g=2.1, 3.7 and 5.3 were observed at 296 K [209].

The $^{57}$Fe Mössbauer spectra collected for the monoclinic form of [Fe(sal$_2$trien)]BPh$_4$·acetone comprise a time-average of contributions from both electronic spin states [209]. The quadrupole splitting values decrease with increasing temperature, i.e. with increasing population of the high spin state. These features indicate that the lifetimes of the low spin and high spin states are as short as or less than the nuclear lifetime $\tau_N$ of $^{57}$Fe ($10^{-7}$ s); this has also been found in a subsequent and more extended study [210]. In contrast, the $^{57}$Fe Mössbauer spectra for [Fe(sal$_2$trien)]BPh$_4$ consist of a superposition of high spin and low spin signals [207] indicating longer lifetimes for the spin states in this instance [207]. In addition, the dynamics of the spin state interconversion of [Fe(sal$_2$trien)](anion)·x(solvent) complexes have also been studied in detail for solutions by laser Raman temperature-jump kinetics [149, 211, 212], and the lifetimes estimated are consistent with the spectral data.

Tweedle and Wilson have carried out extensive studies on Fe(III) compounds of X-substituted sal$_2$trien derivatives in solution [149]. The compounds [Fe(X-sal$_2$trien)]Y (X=H, 3-NO$_2$, 5-NO$_2$, 3-OCH$_3$, 4-OCH$_3$, 5-OCH$_3$; Y=PF$_6^-$, NO$_3^-$, BPh$_4^-$, I$^-$, Cl$^-$) have been found to exhibit variable temperature magnetic susceptibility, $^1$H NMR and electronic spectral properties indicative of spin crossover behaviour. The differences observed in the spin transition characteristics have been related to the hydrogen bonding capability of the particular solvent, the anion associated with the complex, and the nature and position of the substituent in the salten ligand. For the parent [Fe(sal$_2$trien)]Y series, the spin transition appears to be strongly solvent de-

pendent but essentially anion independent. The solvent dependency has been interpreted as arising mainly from a specific $[Fe(sal_2trien)]^+$·solvent hydrogen bonding interaction involving the N–H protons on the trien backbone, where the strongest [N–H...solvent] hydrogen bonding produces the largest population of the low spin isomer. Most elegantly, the N–H stretching frequency in the infrared spectra for the $[Fe(sal_2trien)]PF_6$ parent compound has been measured in a variety of solvents and correlated with the magnetic behaviour of this compound in the same solvents at 295 K. Interestingly, the results indicate a nearly linear relationship between the splitting pattern of the $\nu_{N-H}$ vibration and the measured magnetic moment for a rather diverse series of nitrogen- and oxygen-containing solvents. The effect of substitution in the salicylaldehyde moiety has been studied [149] and at room temperature the measurement of the magnetism of $[Fe(X\text{-}sal_2trien)]PF_6$ in acetone solution indicated that the percentage of high spin isomer depends on the salicylaldimine ring substituent and decreases in the order: 4-$OCH_3$ (97%)>5-$OCH_3$ (85%)>3-$OCH_3$ (73%)>H (68%)>3-$NO_2$ (49%)>5-$NO_2$ (19%). Magnetic data recorded down to 180 K confirm that this order is followed over a wide temperature range. Obviously, the nature of this substituent effect must be electronic in origin since the spatial orientation of the two chelated salicylaldimine rings indicates no specific intramolecular substituent steric interactions. For this X-$sal_2$trien series the more electronegative $NO_2$ groups favour the low spin state while $OCH_3$ favours the high spin form, with the unsubstituted parent compound exhibiting intermediate behaviour. It is of note that a similar substituent effect has also been found for tris(substituted-monothio-$\beta$-diketonato)iron(III) compounds in the solid state, where electronegative $CF_3$ substituents favoured the low spin state relative to the $CH_3$ groups (see above) [84]. For the $[Fe(X\text{-}sal_2trien)]PF_6$ materials the location of the substituent seems to be almost as important as its nature in influencing the spin crossover in solution. In their analysis of the magnetic properties Tweedle and Wilson pointed out that for this range of substituents the different extents to which either spin state is favoured may be explained by the assumption that $\pi$-acceptance by the ligands is more important than the $\sigma$-donor capabilities in stabilising the low spin state [149].

The $sal_2$trien system has also been modified by incorporating a sulfonate group at the 5-position of the salicylaldehyde moiety and spin crossover is observed in the Fe(III) complex [213]. Substitution by phenyl groups at the imine carbon atom of the $sal_2$trien ligand has resulted in the purely high spin $[Fe(bpk_2tet)]ClO_4$·EtOH [206].

In a systematic study of the effects of variation of the tetramine involved in formation of the hexadentate $N_4O_2$ donor Schiff base the linear 3,3,3-, 3,2,3-, 2,3,2- or 2,2,2-tetramines, where the numbers refer to the number of carbon atoms between the amine groups (note 2,2,2-tetramine is synonymous with the nomenclature trien used previously) have been condensed with salicylaldehyde, acetophenone or benzophenone [206]. Crystal struc-

tures have been determined at room temperature for a number of Fe(III) compounds of this series. However, none of these displayed spin crossover behaviour but their spin state seemed to depend on the arrangement of the $N_4O_2$ ligand donor atoms about the Fe(III). When the terminal oxygen atoms occupy *cis* positions the complexes have been found to be purely high spin, whereas when they are in *trans* positions the complexes are low spin.

### 3.4.3 Hexadentate $N_4O_2$-Donating Ligands Derived from $\beta$-Diketones and Triethylenetetramine

Condensation of triethylenetetramine with two equivalents of acetylacetone or its substituted derivatives results in the formation of the second class of hexadentate $N_4O_2$ Schiff base-type ligands (Fig. 18) which can generate spin crossover in iron(III). Only two crystal structures are available for Fe(III) compounds belonging to this series. Those of $[Fe(acac_2trien)]PF_6$ and $[Fe(acacCl_2trien)]PF_6$ have been determined at room temperature where they are high spin [207]. The general structural features are similar to those of the Fe(III) $sal_2trien$ series, involving a distorted octahedral *cis* $FeN_4O_2$ chromophore. The Fe-donor atom bond lengths are typical for high spin Fe(III). The average Fe–O distances are by far the shortest (1.930 Å for the acac derivative and 1.908 Å for the acacCl compound), the Fe–N(amine) distances are relatively long (2.174 Å), whereas the Fe–N(imine) bonds are intermediate (2.097 Å). Typically, the 12 angles subtended at the Fe(III) ion by adjacent donor atoms range from 76.7° to 102.1° implying a significant deviation from perfect octahedral symmetry.

While $[Fe(acac_2trien)]PF_6$ is a purely high spin compound, $[Fe(acacCl_2trien)]PF_6$ displays spin crossover to a moderate extent below 200 K [207]. In contrast, $[Fe(acac_2trien)]BPh_4$ is essentially low spin at 77 K, but appears to show the onset of spin crossover above 200 K [207], its magnetic moment increasing to 3.04 B.M. at room temperature [211]. On the other hand, the trifluoroacetylacetone analogue, $[Fe(tfac_2trien)]PF_6$, is predominantly high spin at room temperature ($\mu_{eff}$=4.91 B.M.) [211]. The $^{57}Fe$ Mössbauer spectra of these spin crossover compounds show separate signals attributable to the high spin and low spin states [207, 211].

Spin crossover for a series of Fe(III) compounds of several $\beta$-ketoimine ligands in solution has been confirmed [211]. The compounds $[Fe(acac_2trien)]Y$ ($Y=PF_6^-$, $BPh_4^-$, $Br^-$, $I^-$) exhibit a striking reversible thermochromism associated with the spin crossover in acetone solutions. The solutions are red at room temperature and change to blue at −80 °C, which parallels the thermochromism displayed by the $[Fe(sal_2trien)]^+$ complexes [149]. The measurement of the temperature dependence of the electronic spectrum, coupled with that of the magnetic moment, has allowed characterisation of the spin crossover for $[Fe(acac_2trien)]PF_6$ in methanol. The higher

energy bands at 520–540 nm were found to decrease steadily in intensity with decreasing temperature and magnetic moment, and thus could be assigned to the high spin form. Conversely, the intensity of lower energy bands at 610–640 nm increased steadily with decreasing temperature and magnetic moment, permitting assignment mainly to the low spin form. Although the spin crossover for the [Fe($acac_2$trien)]Y [211] complexes is more gradual than that for the [Fe($sal_2$trien)]Y series [149], there are strong similarities in the way this behaviour is influenced by solvent, anion and ligand substitution, but the effects are in fact generally more pronounced [149]. Although the influence of the anion seems to be greater for the [Fe($acac_2$trien)]Y series, the same order is found for both series, at least in acetonitrile solution.

The effects of ligand substitution on the Fe(III) spin crossover properties have been examined for [Fe($Z_2$trien)]$PF_6$ (Z=acacCl, bzac, bzacCl, tfac; Fig. 18). Comparisons of the low spin population in the spin crossover systems at a given temperature indicates a systematic effect of the R1, R2 and R3 chelate ring substituents on the Fe(III) spin state. Since the low spin isomer population for a given temperature increases according to the ligand series $acacCl_2$trien>$bzac_2$trien>$acac_2$trien, it appears that electron-withdrawing substituents (assuming $C_6H_5$>$CH_3$) produce the strongest ligand fields and, thus, the largest low spin populations [211]. This general pattern parallels that found for the [Fe($sal_2$trien)]Y complexes where the low spin form is favoured according to X=$NO_2$>H>$OCH_3$ [149].

## 3.5 Iron(III) Spin Crossover Induced by Irradiation

The progress achieved in the detailed understanding of photophysical and photochemical processes that may be induced by light-irradiation in particular spin crossover systems has driven research efforts towards the development of materials that may be used for various technological applications. Only relatively recently, reports have appeared exploring this field for Fe(III) spin crossover materials.

Spin-interconversion by light-irradiation was first observed for Fe(II) spin crossover materials. In some of these Fe(II) compounds in the solid state, the thermally stable low spin state could be converted to a metastable high spin state by light-irradiation (Light-Induced Excited Spin State Trapping (LIESST)) (see Chap. 17). Since thermally-induced spin state relaxation processes may be operative favouring the reverse spin conversion, the lifetime of this metastable high spin form may be rather short and in most instances it may be observed only at very low temperatures. As a first approach it may be assumed that the lifetime increases when the structural differences relative to the initial low spin form become more pronounced. In Fe(II) and Fe(III) spin crossover compounds, major differences are observed between the metal-donor atom bond distances for the low spin and high

spin states. The average change in these bond distances is 0.18 Å for Fe(II), while a significantly smaller change (0.12 Å) is observed for Fe(III). Therefore, it may be presumed that the light-induced high spin form of Fe(III) will have a considerably shorter lifetime than that of the metastable high spin form of Fe(II), or alternatively, the back conversion from the metastable high spin to the low spin state requires a much smaller activation energy for Fe(III) compounds compared to the Fe(II) derivatives. The generation of metastable high spin species by light irradiation of Fe(III) compounds in solution was first reported by Lawthers and McGarvey [214] and later by Schenker and Hauser [215, 216]: irradiation into the spin-allowed ligand-to-metal charge transfer (LMCT) band results in the transient generation of high spin Fe(III) states. It has been estimated that the low-temperature tunnelling rate constant for the high spin to low spin relaxation is about seven orders of magnitude greater for Fe(III) than for Fe(II) compounds in solution [216].

Successful LIESST studies on Fe(III) spin crossover compounds in the solid state have been achieved by preventing the rapid relaxation from the metastable high spin to the low spin state through the introduction of strong intermolecular interactions [137, 138]. It has been proposed that the cooperativity resulting from the intermolecular interaction enhances the activation energy for the relaxation processes, enabling the observation of a relatively long-lived metastable state after irradiation [137]. In fact, strong intermolecular $\pi$-stacking interactions are responsible for the observation of the LIESST effect, as well as for the abrupt transition for $[Fe(pap)_2]ClO_4 \cdot H_2O$ (pap=the deprotonated bis(2-hydroxyphenyl-(2-pyridyl)-methaneimine); $T_{1/2}\uparrow$=180 K, $T_{1/2}\downarrow$=165 K, $\Delta T_{1/2}$=15 K) [137] and the somewhat less abrupt spin transition without thermal hysteresis for $[Fe(pap)_2]PF_6 \cdot MeOH$ ($T_{1/2}$=288 K) [138]. The formation of high spin Fe(III) ions at 5 K upon irradiation ($\lambda$=400–600 nm) into the spin-allowed ligand-to-metal charge transfer (LMCT) band of $[Fe(pap)_2]ClO_4 \cdot H_2O$ has been confirmed by the increase of the magnetic moment, as well as by the $^{57}Fe$ Mössbauer spectra showing two well-separated quadrupole doublets typical for low spin and high spin Fe(III) ions [137]. Relaxation of this metastable high spin state sets in above about 70 K. The LIESST effect has also been observed for $[Fe(pap)_2]PF_6 \cdot MeOH$ at 5 K [138]. The critical temperature of the photo-induced high spin species for this complex ($T_c$(LIESST)=55 K) is lower than that of the perchlorate derivative ($T_c$(LIESST)=105 K), consistent with the lower degree of cooperativity for the transition in the former.

An alternative strategy towards photo-induced spin crossover behaviour was proposed several years ago by Roux et al. [217]. This ligand-driven light-induced spin conversion (LD-LISC) is a very promising process which could also enable photo-induced spin crossover at room temperature. The principle is based on ligands containing potentially photo-isomerisable groups. The first studies have taken advantage of the *cis-trans* photo-iso-

merisation of a C=C entity incorporated in a ligand coordinated to an Fe(II) active spin crossover centre [217–219]. The topic is treated in detail by Boillot, Zarembowitch and Sour in Chap. 20. Recently, this strategy has been applied to mononuclear Fe(III) compounds [196, 197]. For this purpose the Fe(III) $N_4O_2$ environment was provided by the pentadentate salten ligand (see above) together with the potentially photo-isomerisable ligand 1-(pyridin-4-yl)-2-(*N*-methylpyrrol-2-yl)-ethene (abbreviated as Mepepy) [196] or 4-styryl-pyridine [197]. Solid state [Fe(salten)(Mepepy)]$BPh_4$ with Mepepy in *trans* configuration, exhibits a gradual Fe(III) spin crossover taking place between 150 and 320 K. Irradiation experiments have been carried out in acetonitrile solutions with a wavelength of 405±5 nm, at which the *trans* to *cis* isomerisation is expected to take place. The evolution of the magnetic data under irradiation has been followed by the Evans method. In this way, the ligand field strength is varied under the effect of electromagnetic radiation. Since the methylpyrrole moiety of Mepepy is a strong $\pi$-donor group, the *trans* to *cis* isomerisation results in a decrease of the $\pi$-donor character of the ligand and has been found to induce a partial high spin to low spin change even at room temperature [196]. Further experiments have been carried out on [Fe(salten)(*trans*-4-styrylpyridine)]$BPh_4 \cdot (CH_3)_2CO \cdot 0.5H_2O$ and [Fe(salten)(*cis*-4-styrylpyridine)]$BPh_4$, which both display gradual spin crossover behaviour in the solid state with $T_{1/2}$ being 260 K for the former, whereas it is almost 100 K higher for the latter [197]. Although irradiation ($\lambda$=313 nm) of the materials in acetonitrile solutions, as well as in the solid state, brought about changes in the UV spectra, conclusive evidence for an actual change in the spin state of Fe(III) could not be obtained.

The same approach has been applied to dinuclear Fe(III) spin crossover materials. In [(salten)Fe(azobis(4-pyridine))Fe(salten)]$(BPh_4)_2$ the Fe(III) spin crossover centres are connected by the potentially photo-isomerisable azobis(4-pyridine) entity [202]. The solid compound undergoes a gradual temperature-induced spin transition ($\mu_{eff}$=ca. 2.2 B.M. at 200 K and 4.3 B.M. at 350 K). Since the material is thermochromic in acetonitrile solution, it has been possible to monitor the spin transition by recording the electronic spectra. These results could be compared to those obtained from irradiation measurements. Upon the thermal spin transition the absorption at 430 nm increases in intensity, whereas the absorption at 480 nm simultaneously decreases in intensity. The same changes in electronic spectra have been observed upon irradiation with a wavelength of 300 nm at room temperature. The experiments are consistent with a reversible photo-induced Fe(III) spin crossover taking place in solution. Interestingly, irradiation ($\lambda$=300 nm) of a KBr disc containing the complex at room temperature revealed that the *trans* to *cis* photo-isomerisation also occurs in the solid state, although the process is irreversible in this instance [202].

## 3.6 Developments in Materials Science

Several approaches to obtaining Fe(III) spin crossover materials in a form suitable for incorporation in devices for possible practical application have been reported.

Nakano et al. have demonstrated that Fe(III) spin crossover complexes adsorbed on the surface of silicon dioxide retain their spin crossover behaviour [220]. EPR and $^{57}$Fe Mössbauer spectral data indicated that the spin transitions observed are similar to those of the neat solid materials used, i.e. $[Fe(acpa)_2]PF_6$, $[Fe(acpa)_2]BPh_4$ (Hacpa=*N*-(1-acetyl-2-propylidene)(2-pyridylmethyl)amine) and $[Fe(bzpa)_2]PF_6$ (Hbzpa=(1-benzoylpropen-2-yl)(2-pyridylmethyl)amine).

$[Fe(salten)]^+$ entities (salten is a pentadentate Schiff base; see above) have been attached to polymer matrices providing the sixth N-donor atom through their pyridine or imidazole entities [221]. The polymers used are polymeric-4-vinylpyridine, the copolymer of octylmethacrylate and 4-vinylpyridine, and the copolymer of octylmethacrylate and 1-vinylimidazole. The resultant six-coordinate materials show spin crossover, confirmed by measurements of magnetic susceptibility, EPR and $^{57}$Fe Mössbauer spectra, together with thermochromism. An alternative and more direct approach involved modified five-coordinate $[Fe(salten)]^+$ or six-coordinate $[Fe(sal_2trien)]^+$-type entities containing appropriate polymerisable groups attached to the 5-position of the salicylideneimine moiety. These have been polymerised with 4-vinylpyridine to obtain spin crossover polymeric materials by a more direct synthetic route [221]. Despite the polymeric nature of these systems, the transitions are not strongly cooperative.

Recently, the preparation of liquid crystals displaying spin crossover has been achieved [222]. For this purpose the $N_2O$-tridentate Schiff base ligand obtained from the condensation of 4-(dodecyloxybenzoyloxy)-2-hydroxybenzaldehyde and *N*-ethylethylenediamine ($H_2L$) (analogous to those shown in Fig. 12) has been selected. Liquid crystal properties were confirmed for $[FeL_2]PF_6$ in the crystal state and meso phase by polarising optical microscopy, differential scanning calorimetry and X-ray scattering, from which it could be concluded that the compound consists of rod-like molecules; it exhibits the fan-shaped texture usually attributed to the smectic A mesophase in the temperature range 388–419 K [222]. Measurements of magnetism and $^{57}$Fe Mössbauer spectra indicate an almost complete, gradual spin crossover over the range ca. 75 to 200 K.

## 4 Conclusions

The comparison of Fe(III) spin transition systems with those of other metal ions reveals the greater variety of chromophores for which spin crossover is observed in iron(III). This is reflected in a generally more diverse coordination environment as well as a far broader range of donor atom sets. For six-coordinate systems the spin crossover generally involves an S=1/2↔S=5/2 change, whereas for five-coordinate materials an intermediate (quartet) spin state is involved in S=1/2↔S=3/2 transitions. There is just one report of such a transition in a six-coordinate system and that is considerably distorted [126].

The donor atom sets for six-coordinate systems range from $FeS_6$ in the dithiocarbamate and X-xanthate (X=O, S) systems to $FeS_3O_3$ for monothiocarbamates and monothio-$\beta$-diketones, and $FeS_3Se_3$ or $FeSe_6$ for thioseleno- or diselenocarbamates, respectively. In addition, $FeS_2N_2O_2$ and $FeSe_2N_2O_2$ chromophores are formed from the important thiosemicarbazone or selenosemicarbazone-type ligands, respectively. $FeN_3S_3$ chromophores are known but are less common [120, 121, 123]. In addition, spin crossover $FeN_5Cl$ and $FeN_4Br_2$ chromophores have been identified [122, 166]. In contrast to the $FeS_6$ systems which, particularly in the dithiocarbamates, represent the most widely studied group, there is only a single example for an $FeO_6$ spin crossover species [93]. Multidentate Schiff base-type ligands are widely suited to the generation of spin crossover in iron(III) but the range of donor atom sets for these is more limited than for the systems above. Two $N_2O$-donating tridentate ligands or a single hexadentate $N_4O_2$ ligand are remarkably effective in leading to spin transitions in six-coordinate $FeN_4O_2$ chromophores. Several $N_3O_2$- or $N_2O_2$-donating systems are also effective but require one or two appropriate additional N-donating heterocyclic bases to complete the pseudo-octahedral $N_4O_2$ coordination sphere.

The S=1/2↔S=3/2 Fe(III) spin crossover in five-coordinate compounds is also found for a relatively large number of donor atom sets: $FeOS_4$ [124, 125], $FeNS_4$ [125], $FeN_3O_2$ [169–171, 174, 175], $FeN_5$, and $FeN_4X$ ($X=Cl^-$, $Br^-$) [168].

Apart from the wider range of donor atom sets, the transitions in iron(III) are distinguished from those in iron(II) in a number of other ways. Although for both metal ions the change in the total spin for the transitions in six-coordinate systems is $\Delta S=2$, the actual change in bond length (for the same donor atoms) accompanying the transitions is less for iron(III) than for iron(II). This is the origin of many of the important differences encountered in the nature of the spin crossover observed for the two metal ions. Perhaps the two most important characteristics resulting from this are the generally increased rate of inter-conversion of the spin states and the lower degree of cooperativity associated with the transitions in the solid state for iron(III).

The inter-conversion of the spin states in many instances is so rapid that the separate contributions to the $^{57}$Fe Mössbauer spectra are not resolved. Thus this technique, which has proved so diagnostic in iron(II) systems, is frequently less suited to the derivation of spin transition curves for iron(III). A further corollary of the faster spin state inter-conversion is the rarity of the LIESST effect among iron(III) systems, in contrast to its ubiquitous occurrence in iron(II).

The great majority of transitions observed for iron(III) are gradual and the observation of thermal hysteresis associated with them is relatively rare. In the only instances where features indicative of significant cooperativity have been reported, extensive hydrogen-bonding networks (formed in some thiosemicarbazone compounds [111, 115, 118, 119]) or $\pi$-$\pi$ stacking interactions (operative in several compounds of $N_2O$ Schiff base systems [135–138, 164, 165]) have been invoked as the origin of the cooperativity.

Despite these differences, the similarities predominate and virtually all the features noted for spin crossover in iron(II) are also found for iron(III). Because of the great emphasis on the cooperative aspects of the spin crossover phenomenon, iron(II) systems have tended to dominate more recent research. However, there are very striking examples among the iron(III) systems which are of strong relevance to these aspects and there is certainly scope for future work in this area. This is evident in much of the very recent work where it can be seen that specific strategies to increase the cooperativity have been successful and have led, for example, to solid iron(III) systems which display the LIESST effect [137, 138]. The generation of polymeric species as a means of increasing cooperativity, an approach which has been widely adopted for iron(II), has received relatively little attention for iron(III) and this is an area which can be expected to be exploited further.

It is clear that spin crossover occurs widely for iron(III). The treatment given here has been confined in the main to typical synthetic systems but it needs to be stressed that among iron(III) naturally occurring porphyrin-type systems spin crossover is widespread and its presence in them is vital to their roles [223–227].

**Acknowledgement** P.J.v.K. gratefully acknowledges the kind provision of work facilities at the Johannes-Gutenberg-University by Professor Philipp Görlich.

## References

1. Cambi L, Szegö L (1931) Ber 10:2591
2. Cambi L, Szegö L (1933) Ber 66:656
3. Tanabe Y, Sugano S (1954) J Phys Soc Jpn 9:753
4. Albertsson J, Oskarsson Å, Ståhl K, Svensson C, Ymén I (1981) Acta Crystallogr B37:50
5. Albertsson J, Oskarsson Å (1977) Acta Crystallogr B33:1871

6. Leipoldt JG, Coppens P (1973) Inorg Chem 12:2269
7. Ewald AH, Martin RL, Sinn E, White AH (1969) Inorg Chem 8:1837
8. Albertsson J, Oskarsson Å (1979) Acta Crystallogr B35:1473
9. Albertsson J, Oskarsson Å, Ståhl K (1982) Acta Chem Scand A36:783
10. Hoskins BF, Kelly BP (1968) J Chem Soc Chem Commun 1517
11. White AH, Roper R, Kokot E, Waterman H, Martin RL (1964) Aust J Chem 17:294
12. Mitra S, Raston CL, White AH (1976) Aust J Chem 29:1899
13. Terzis A, Filippakis S, Mentzafos D, Petrouleas V, Malliaris A (1984) Inorg Chem 23:334
14. Healy PC, White AH (1972) J Chem Soc Dalton Trans 1163
15. Albertsson J, Elding I, Oskarsson Å (1979) Acta Chem Scand A33:703
16. Mitra S, Raston CL, White AH (1978) Aust J Chem 31:547
17. Sinn E (1976) Inorg Chem 15:369
18. Butcher RJ, Sinn E (1976) J Am Chem Soc 98:5159
19. Healy PC, Sinn E (1975) Inorg Chem 14:109
20. Ståhl K (1983) Acta Crystallogr B39:612
21. Butcher RJ, Sinn E (1976) J Am Chem Soc 98:2441
22. Cukauskas EJ, Deaver BS Jr, Sinn E (1977) J Chem Phys 67:1257
23. Bereman RD, Rowen Churchill M, Nalewajek D (1979) Inorg Chem 18:3112
24. Griffith JS (1961) The theory of transition metal ions. Cambridge University Press
25. Figgis BN (1961) Trans Faraday Soc 57:198
26. Figgis BN (1961) Trans Faraday Soc 57:204
27. McGrath CM, O'Connor CJ, Sangregorio C, Seddon JMW, Sinn E, Sowrey FE, Young NA (1999) Inorg Chem Commun 2:536
28. Eley RR, Duffy NV, Uhrich DL (1972) J Inorg Nucl Chem 34:3681
29. Gregson K, Doddrell DM (1975) Chem Phys Lett 31:125
30. Sorai M (1978) J Inorg Nucl Chem 40:1031
31. Cambi L, Malatesta L (1937) Ber 70:2067
32. Cukauskas EJ, Deaver BS Jr, Sinn E (1977) Inorg Nucl Chem Lett 13:283
33. Figgis BN, Toogood GE (1972) J Chem Soc Dalton Trans 2177
34. Ståhl K, Ymén I (1983) Acta Chem Scand A37:729
35. Merrithew PB, Rasmussen PG (1972) Inorg Chem 11:325
36. Eley RR, Duffy NV, Uhrich DL (1972) J Inorg Nucl Chem 34:3681
37. Golding RM, Whitfield HJ (1966) Trans Faraday Soc 62:1713
38. Frank E, Abeledo CR (1966) Inorg Chem 5:1453
39. Rickards R, Johnson CE, Hill HAO (1968) J Chem Phys 48:5231
40. Rininger D, Zimmerman JB, Duffy NV, Uhrich DL (1980) J Inorg Nucl Chem 42:689
41. Wajda S, Drabent K, Ozarowski A (1980) Inorg Chim Acta 45:L201
42. Eisman GA, Reiff WM, Butcher RJ, Sinn E (1981) Inorg Chem 20:3484
43. Malliaris A, Papaefthimiou (1981) J Chem Phys 74:3626
44. Malliaris A, Papaefthimiou V (1982) Inorg Chem 21:770
45. Drabent K, Wolny J, Janski J, Wajda S (1985) J Radioanal Nucl Chem Lett 95:93
46. Pandeya KB, Singh R, Prakash C, Baijal JS (1987) Solid State Commun 64:801
47. Pandeya KB, Singh R, Prakash C, Baijal JS (1987) Inorg Chem 26:3216
48. Boyd DL, Duffy NV, Felczan A, Gelerinter E, Uhrich DL, Katsoulos GA, Zimmerman JB (1992) Inorg Chim Acta 191:39
49. Manhas BS, Bala S (1988) Polyhedron 7:2465
50. Singhal S, Sharma CL, Garg AN, Chandra K (2002) Polyhedron 21:2489
51. Hall GR, Hendrickson DN (1976) Inorg Chem 15:607
52. Flick C, Gelerinter E (1973) Chem Phys Lett 23:422

53. Gelerinter E, Stefanov ME, Lockhart TE, Rininger DP, Duffy NV (1980) J Inorg Nucl Chem 42:1137
54. Pandeya KB, Singh R (1988) Inorg Chim Acta 147:5
55. Cotton SA (1994) Polyhedron 13:2579
56. Domracheva NE, Luchkina SA, Ovchinnikov IV (1995) Russ J Coord Chem 21:24
57. Hutchinson B, Neill P, Finkelstein A, Takemoto J (1981) Inorg Chem 20:2000
58. Butcher RJ, Ferraro JR, Sinn E (1976) Inorg Chem 15:2077
59. Nakajima H, Takana T, Kobayashi H, Tsuijikawa I (1976) Inorg Nucl Chem Lett 12:689
60. Ahmed J, Ibers JA (1977) Inorg Chem 16:935
61. Kunze KR, Perry DL, Wilson LJ (1977) Inorg Chem 16:594
62. Perry DL, Wilson LJ, Kunze KR, Maleki L, Deplano P, Trogu EF (1981) J Chem Soc Dalton Trans 1294
63. Cervone E, Diomedi Camassei F, Luciani ML, Furlani C (1969) J Inorg Nucl Chem 31:1101
64. Klayman DL, Günther WHH (eds) (1973) Organic selenium compounds. Wiley New York, p 1029
65. De Filippo D, Depalano P, Diaz A, Steffé S, Trogu EF (1977) J Chem Soc Dalton Trans 1566
66. De Filippo D, Deplano P, Diaz A, Trogu EF (1976) Inorg Chim Acta 17:139
67. Aramu F, Maxia V, De Filippo D, Trogu EF (1978) Lett Nuovo Cimento 22:231
68. Dietzsch W, Boyd DL, Uhrich DL, Duffy NV (1986) Inorg Chim Acta 121:19
69. Dietzsch W, Gelerinter E, Duffy NV (1988) Inorg Chim Acta 145:13
70. Dietzsch W, Duffy NV, Gelerinter E, Sinn E (1989) Inorg Chem 28:3079
71. Dietzsch W, Duffy NV, Boyd D, Uhrich DL, Sinn E (1990) Inorg Chim Acta 169:157
72. Gelerinter E, Duffy NV, Dietzsch W, Thanyasiri T, Sinn E (1990) Inorg Chim Acta 177:185
73. Gelerinter E, Duffy NV, Yarish SS, Dietzsch W, Kirmse R (1991) Chem Phys Lett 184:375
74. Wentink T (1958) J Chem Phys 29:188
75. Henriksen L (1985) Synthesis 204
76. Golding RM, Sinn E, Tennant WC (1972) J Chem Phys 56:5296
77. Kirmse R, Wartewig S, Windsch W, Hoyer E (1972) J Chem Phys 56:5273
78. Ewald AH, Martin RL, Ross IG, White AH (1964) Proc R Soc A 280:235
79. Ewald AH, Martin RL, Sinn E, White AH (1969) Inorg Chem 8:1837
80. Ewald AH, Sinn E (1968) Aust J Chem 21:927
81. Lewis DF, Lippard SJ, Zubieta JA (1972) Inorg Chem 11:823
82. Hoskins BF, Kelly BP (1970) J Chem Soc Chem Commun 45
83. Bellitto C, Flamini A, Piovesana O (1979) J Inorg Nucl Chem 41:1677
84. Ho RKY, Livingstone SE (1968) Aust J Chem 21:1987
85. Ho RKY, Livingstone SE (1968) J Chem Soc Chem Commun 217
86. Cox M, Darken J (1971) Coord Chem Rev 7:29
87. Livingstone SE (1971) Coord Chem Rev 7:59
88. Roof RB (1956) Acta Crystallogr 9:781
89. Epstein LM (1962) J Chem Phys 36:2731
90. Wertheim GK, Kingston WR, Herber RH (1962) J Chem Phys 37:687
91. Wignall JWG (1966) J Chem Phys 44:2462
92. Bancroft GM, Maddock AG, Ong WK, Prince RH (1967) J Chem Soc A 1966
93. Adimado AA (1983) Polyhedron 2:1059
94. König E, Lindner E, Ritter G (1970) Z Naturforsch 25b:757

95. Beckett R, Heath GA, Hoskins BF, Kelly BP, Martin RL, Roos IAG, Weickhardt PL (1970) Inorg Nucl Chem Lett 6:257
96. Hoskins BF, Pannan CD (1975) Inorg Nucl Chem Lett 11:409
97. Cox M, Darken J, Fitzsimmons BW, Smith AW, Larkworthy LF, Rogers KA (1970) J Chem Soc Chem Commun 105
98. Cox M, Darken J, Fitzsimmons BW, Smith AW, Larkworthy LF, Rogers KA (1972) J Chem Soc Dalton Trans 1192
99. Das M, Golding RM, Livingstone SE (1978) Trans Met Chem 3:112
100. Padhyé S, Kauffman GB (1985) Coord Chem Rev 63:127
101. Zelentsov VV (1983) Advances in inorganic chemistry. Spitsyn VI (ed). MIR Publishers, p 122
102. Ryabova NA, Ponomarev VI, Zelentsov VV, Shipilov VI, Atovmyan LO (1981) J Struct Chem 22:111
103. Ryabova NA, Ponomarev VI, Atovmyan, Zelentsov VV, Shipilov VI (1978) Koord Khim 4:119
104. Ryabova NA, Ponomarev VI, Zelentsov VV, Atovmyan LO (1982) Sov Phys Crystallogr 27:46
105. Zelentsov VV, Bogdanova LG, Ablov AV, Gerbeleu NV, Dyatlova CV (1973) Russ J Inorg Chem 18:1410
106. Ryabova NA, Ponomarev VI, Zelentsov VV, Atovmyan LO (1981) Kristallografiya 26:101
107. Ivanov EV, Zelentsov VV, Gerbeleu NV, Ablov AV (1970) Dokl Akad Nauk SSSR 191:827
108. Zelentsov VV, Ablov AV, Turta KI, Stukan RA, Gerbeleu NV, Ivanov EV, Bogdanov AP, Barba NA, Bodyu VG (1972) Russ J Inorg Chem 17:1000
109. Ablov AV, Goldanskii VI, Turta KI, Stukan RA, Zelentsov VV, Ivanov EV, Gerbeleu NV (1971) Dokl Akad Nauk SSSR 196:1101
110. Shipilov VI, Zelentsov VV, Zhdanov VM, Turdakin VA (1974) JETP Lett 19:294
111. Floquet S, Boillot M-L, Rivière E, Varret F, Boukheddaden K, Morineau D, Négrier P (2003) New J Chem 27:341
112. Ablov AV, Gerbeleu NV, Romanov AM (1968) Russ J Inorg Chem 11:1558
113. Ablov AV, Gerbeleu NV (1970) Russ J Inorg Chem 15:952
114. Negryatse NY, Ablov AV, Gerbeleu NV (1972) Russ J Inorg Chem 17:65
115. Timken MD, Wilson SR, Hendrickson DN (1985) Inorg Chem 24:3450
116. Mathew M, Palenik GJ (1969) J Am Chem Soc 91:6310
117. Mathew M, Palenik GJ (1971) Inorg Chim Acta 5:349
118. Mohan M, Madhuranath PH, Kumar A, Kumar M, Jha NK (1989) Inorg Chem 28:96
119. Gupta NS, Mohan M, Jha NK, Antholine WE (1991) Inorg Chim Acta 184:13
120. Beissel T, Bürger KS, Voigt G, Wieghardt K, Butzlaff C, Trautwein AX (1993) Inorg Chem 32:124
121. Butzlaff C, Bill E, Meyer W, Winkler H, Trautwein AX, Beissel T, Wieghardt K (1994) Hyperfine Inter 90:453
122. Fallon GD, McLachlan GA, Moubaraki B, Murray KS, O'Brien L, Spiccia L (1997) J Chem Soc Dalton Trans 2765
123. Kersting B, Kolm MJ, Janiak C (1998) Z Anorg Allg Chem 624:775
124. Sutter J-P, Fettouhi M, Li L, Michaut C, Ouahab L, Kahn O (1996) Angew Chem Int Ed Engl 35:2113
125. Fettouhi M, Morsy M, Waheed A, Golhen S, Ouahab L, Sutter J-P, Kahn O, Menendez N, Varret F (1999) Inorg Chem 38:4910

126. Koch WO, Schünemann V, Gerdan M, Trautwein AX, Krüger H-J (1998) Chem Eur J 4:686
127. Timken MD, Strouse CE, Soltis MS, Daverio SA, Hendrickson DN, Abdel-Mawgoud AM, Wilson SR (1986) J Am Chem Soc 108:395
128. Conti AJ, Chadha RK, Sena KM, Rheingold AL, Hendrickson DN (1993) Inorg Chem 32:2670
129. Sim PG, Sinn E, Petty RH, Merrill CL, Wilson LJ (1981) Inorg Chem 20:1231
130. Timken MD, Hendrickson DN, Sinn E (1985) Inorg Chem 24:3947
131. Costes J-P, Dahan F, Laurent J-P (1990) Inorg Chem 29:2448
132. Oshio H, Toriumi K, Maeda Y, Takashima Y (1991) Inorg Chem 30:4252
133. Maeda Y, Oshio H, Takashima Y, Mikuriya M, Hidaka M (1986) Inorg Chem 25:2958
134. Maeda Y, Oshio H, Toriumi K, Takashima Y (1991) J Chem Soc Dalton Trans 1227
135. Hayami S, Gu ZZ, Yoshiki H, Fujishima A, Sato O (2001) J Am Chem Soc 123:11644
136. Hayami S, Kawahara T, Juhasz G, Kawamura K, Uehashi K, Sato O, Maeda Y (2003) J Radioanal Nucl Chem 255:443
137. Hayami S, Gu ZZ, Shiro M, Einaga Y, Fujishima A, Sato O (2000) J Am Chem Soc 122:7126
138. Juhász G, Hayami S, Sato O, Maeda Y (2002) Chem Phys Lett 364:164
139. Federer WD, Hendrickson DN (1984) Inorg Chem 23:3861
140. Federer WD, Hendrickson DN (1984) Inorg Chem 23:3870
141. Timken MD, Abdel-Mawgoud AM, Hendrickson DN (1986) Inorg Chem 25:160
142. Wei-Da Y, Chuan-Liang Y (1989) Acta Chim Sinica 339
143. Conti AJ, Kaji K, Nagano Y, Sena KM, Yumoto Y, Chadha RK, Rheingold AL, Sorai M, Hendrickson DN (1993) Inorg Chem 32:2681
144. Kaji K, Sorai M, Conti AJ, Hendrickson DN (1993) J Phys Chem Solids 54:1621
145. Sorai M, Nagano Y, Conti AJ, Hendrickson DN (1994) J Phys Chem Solids 55:317
146. Maeda Y, Tsutsumi N, Takashima Y (1984) Inorg Chem 23:2440
147. Mohan M, Gupta NS, Chandra L, Jha NK, Prasad RS (1988) Inorg Chim Acta 141:185
148. Petty RH, Dose EV, Tweedle MF, Wilson LJ (1978) Inorg Chem 17:1064
149. Tweedle MF, Wilson LJ (1976) J Am Chem Soc 98:4824
150. Haddad MS, Federer WD, Lynch MW, Hendrickson DN (1981) Inorg Chem 20:123
151. Haddad MS, Federer WD, Lynch MW, Hendrickson DN (1980) J Am Chem Soc 102:1468
152. Haddad MS, Federer WD, Lynch MW, Hendrickson DN (1981) Inorg Chem 20:131
153. Maeda Y, Tsutsumi N, Takashima Y (1985) J Radioanal Nucl Chem Lett 93:253
154. Sasaki N, Kambara T (1987) J Phys Soc Jpn 56:3956
155. Maeda Y, Tsutsumi N, Takashima Y (1984) Inorg Chem 23:2440
156. Maeda Y, Tomokiyo M, Kitazaki K, Takashima Y (1988) Bull Chem Soc Jpn 61:1953
157. Sorai M, Maeda Y, Oshio H (1990) J Phys Chem Solids 51:941
158. Sorai M, Seki S (1972) J Phys Soc Jpn 33:575
159. Sorai M, Seki S (1974) J Phys Chem Solids 35:555
160. Kaji K, Sorai M (1985) Thermochim Acta 88:185
161. Maeda Y, Tsutsumi N, Takashima Y (1982) Chem Phys Lett 88:248
162. Dahl BM, Dahl O (1969) Acta Chem Scand 23:1503
163. Dickinson RC, Baker WA Jr, Collins RL (1977) J Inorg Nucl Chem 39:1531
164. Oshio H, Kitazaki K, Mishiro J, Kato N, Maeda Y, Takashima Y (1987) J Chem Soc Dalton Trans 1341
165. Hayami S, Maeda Y (1997) Inorg Chim Acta 255:181
166. Desideri A, Raynor JB (1977) J Chem Soc Dalton Trans 2051

167. Hodges KD, Wollmann RG, Kessel SL, Hendrickson DN, Van Derveer DG, Barefield EK (1979) J Am Chem Soc 101:906
168. Brewer G, Jasinski J, Mahany W, May L, Prytkov S (1995) Inorg Chim Acta 232:183
169. Wells FV, McCann SW, Wickman HH, Kessel SL, Hendrickson DN, Feltham RD (1982) Inorg Chem 21:2306
170. Earnshaw A, King EA, Larkworthy LF (1965) J Chem Soc Chem Commun 180
171. Earnshaw A, King EA, Larkworthy LF (1969) J Chem Soc A 2459
172. Haller KJ, Johnson PL, Feltham RD, Enemark JH, Ferraro JR, Basile LJ (1979) Inorg Chim Acta 33:119
173. Mosback H, Poulsen KG (1971) Acta Chem Scand 25:2421
174. Fitzsimmons BW, Larkworthy LF, Rogers KA (1980) Inorg Chim Acta 44:L53
175. König E, Ritter G, Waigel J, Larkworthy LF, Thompson RM (1987) Inorg Chem 26:1563
176. Kennedy BJ, McGrath AC, Murray KS, Skelton BW, White AH (1987) Inorg Chem 26:483
177. Milne AM, Maslen EN (1988) Acta Crystallogr B44:254
178. Nishida Y, Kino K, Kida S (1987) J Chem Soc Dalton Trans 1157
179. Brewer CT, Brewer G, Jameson GB, Kamaras P, May L, Rapta M (1995) J Chem Soc Dalton Trans 37
180. Fukuya M, Ohba M, Motoda K-I, Matsumoto N, Okawa H, Maeda Y (1993) J Chem Soc Dalton Trans 3277
181. Bhadbhade MM, Srinivas D (1998) Polyhedron 17:2699
182. Hernández-Molina R, Medero A, Dominguez S, Gili P, Ruiz-Pérez C, Castiñeiras A, Solans X, Lloret F, Real J-A (1998) Inorg Chem 37:5102
183. Maeda Y, Oshio H, Toriumi K, Takashima Y (1991) J Chem Soc Dalton Trans 1227
184. Maeda Y, Takashima Y, Matsumoto N, Ohyoshi A (1986) J Chem Soc Dalton Trans 1115
185. Nishida Y, Oshio S, Kida S (1977) Bull Chem Soc Jpn 50:119
186. Geiger DK, Lee YJ, Scheidt WR (1984) J Am Chem Soc 106:6339
187. Matsumoto N, Kimoto K, Ohyoshi A, Maeda Y (1984) Bull Chem Soc Jpn 57:3307
188. Maeda Y, Tsutsumi N, Takashima Y (1985) J Radioanal Nucl Chem Lett 93:253
189. Hayami S, Inoue K, Maeda Y (1999) Mol Cryst Liq Cryst 335:573
190. Hayami S, Nomiyama S, Hirose S, Yano Y, Osaki S, Maeda Y (1999) J Radioanal Nucl Chem 239:273
191. Brewer CT, Brewer G, May L, Sitar J, Wang R (1993) J Chem Soc Dalton Trans 151
192. Brewer CT, Brewer G, Jameson GB, Kamaras P, May L, Rapta M (1995) J Chem Soc Dalton Trans 37
193. Oshio H, Maeda Y, Takashima Y (1983) Inorg Chem 22:2684
194. Matsumoto N, Ohta S, Yoshimura C, Ohyoshi A, Kohata S, Okawa H, Maeda Y (1985) J Chem Soc Dalton Trans 2575
195. Maeda Y, Noda Y, Oshio H, Takashima Y, Matsumoto N (1994) Hyperfine Inter 84:471
196. Sour A, Boillot M-L, Rivière E, Lesot P (1999) Eur J Inorg Chem 2117
197. Hirose S, Hayami S, Maeda Y (2000) Bull Chem Soc Japan 73:2059
198. Maeda Y, Suzuki M, Hirose S, Hayami S, Oniki T, Sugihara A (1998) Bull Chem Soc Jpn 71:2837
199. Ohyoshi A, Honbo J, Matsumoto N, Ohta S, Sakamoto S (1986) Bull Chem Soc Jpn 59:1611
200. Boca R, Fukuda Y, Gembický M, Herchel R, Jarošciak R, Linert W, Renz F, Yuzurihara J (2000) Chem Phys Lett 325:411

201. Ohta S, Yoshimura C, Matsumoto N, Okawa H, Ohyoshi A (1986) Bull Chem Soc Jpn 59:155
202. Hayami S, Inoue K, Osaki S, Maeda Y (1998) Chem Lett 987
203. Hayami S, Hosokoshi Y, Inoue K, Einaga Y, Sato O, Maeda Y (2001) Bull Chem Soc Jpn 74:2361
204. Maeda Y, Noda Y, Oshio H, Takashima Y (1992) Bull Chem Soc Jpn 65:1825
205. Maeda Y, Noda Y, Oshio H, Takashima Y, Matsumoto N (1994) Hyperfine Inter 84:471
206. Hayami S, Matoba T, Nomiyama S, Kojima T, Osaki S, Maeda Y (1997) Bull Chem Soc Jpn 70:3001
207. Sinn E, Sim G, Dose EV, Tweedle MF, Wilson LJ (1978) J Am Chem Soc 100:3375
208. Nishida Y, Kino K, Kida S (1987) J Chem Soc Dalton Trans 1957
209. Maeda Y, Oshio H, Tanigawa Y, Oniki T, Takashima Y (1991) Bull Chem Soc Jpn 64:1522
210. Maeda Y, Oshio H, Tanigawa Y, Oniki T, Takashima Y (1991) Hyperfine Inter 68:157
211. Dose EV, Murphy KMM, Wilson LJ (1976) Inorg Chem 15:2622
212. Dose EV, Hoselton MA, Sutin N, Tweedle MF, Wilson LJ (1978) J Am Chem Soc 100:1141
213. Evans DF, Jakubovic DA (1988) J Chem Soc Dalton Trans 2927
214. Lawthers I, McGarvey JJ (1984) J Am Chem Soc 106:4280
215. Schenker S, Hauser A (1994) J Am Chem Soc 116:5497
216. Schenker S, Hauser A, Dyson RM (1996) Inorg Chem 35:4676
217. Roux C, Zarembowitch J, Gallois B, Granier T, Claude R (1994) Inorg Chem 33:2273
218. Boillot M-L, Roux C, Audière J-P, Dausse A, Zarembowitch J (1996) Inorg Chem 35:3975
219. Boillot M-L, Chantraine S, Zarembowitch J, Lallemand J-Y, Prunet J (1999) New J Chem 179
220. Nakano M, Okuno S, Matsubayashi G-E, Mori W, Katada M (1996) Mol Cryst Liq Cryst 286:83
221. Maeda Y, Miyamoto M, Takashima Y, Oshio H (1993) Inorg Chim Acta 204:231
222. Galyametdinov Y, Ksenofontov V, Prosvirin A, Ovchinnikov I, Ivanova G, Gütlich P, Haase W (2001) Angew Chem Int Ed Engl 113:4399
223. Messana S, Cerdonio M, Shenkin P, Noble RW, Fermi G, Perutz RW, Perutz MF (1978) Biochemistry 17:3652
224. Lange R, Bonfils C, Debye P (1977) Eur J Biochem 79:623
225. Iizuka T, Kotani M, Yonetani M (1971) J Biol Chem 246:4731
226. Noble RW, DeYoung A, Rousseau DL (1989) Biochemistry 28:5293
227. Scheidt WR, Reed CA (1981) Chem Rev 81:543